

ENHANCED PASSIVE BALANCING APPROACH FOR  
BATTERY MANAGEMENT SYSTEMS USING MACHINE  
LEARNING

BY

MUHAMAD AQIL MUQRI BIN MUHAMAD FAHMI

A thesis submitted in fulfilment of the requirements for the  
degree of Master of Science in Engineering

Kulliyyah of Engineering  
International Islamic University Malaysia

DECEMBER 2025

## ABSTRACT

Passive cell-balancing remains attractive for cost-sensitive battery management systems (BMS), but its fixed-threshold control wastes energy and accelerates component ageing. Many cost-sensitive applications rely on passive shunt-resistor balancing for lithium-ion battery packs because it is simple, reliable and low-cost, which typically uses open circuit voltage (OCV) as a proxy of state of charge (SOC), and this does not provide enough accuracy, mainly in lithium-ion cells where the voltage remains nearly the same for a wide range of SOC levels. In these aspects, despite large differences in SOC, the voltage variations may be too small for the BMS to measure accurately. For those reasons, the cells may remain persistently imbalanced during the balancing process, which can result in them not being fully used, a higher risk of overcharging and faster wear from heat produced. This study aims to investigate recent advancements in passive balancing and machine learning for SOC estimation, develop an enhanced passive balancing BMS architecture that integrates machine learning, and evaluate the proposed system against conventional OCV-based approaches in terms of accuracy, efficiency, and performance. An enhanced passive balancing architecture has been developed that couples a low-cost switched-shunt network with a long-short-term-memory (LSTM) SOC estimator trained on multi-temperature public datasets. The data-driven predictor supplies real-time SOC values to a hysteresis controller, enabling balancing decisions that are informed by cell dynamics rather than voltage alone. A three-cell lithium-ion in 3S1P arrangement was modelled in MATLAB/Simulink and validated against a hardware prototype configured for conventional OCV-based estimation that was used for the balancing process. Performance metrics such as balancing time, switching frequency, power dissipation and thermal rise were recorded for both strategies, and such findings were discovered in this study. The ML-assisted approach reduced balancing time to 80% SOC by 29% (2.88 hours vs. 4.05 hours), decreased average switching frequency by 97% (10.2 mHz vs. 333.8 mHz), and lowered total power dissipation by 81% (0.422 W vs. 2.22 W). The LSTM-based SOC estimator maintained high predictive accuracy across a temperature range of  $-10^{\circ}\text{C}$  to  $25^{\circ}\text{C}$  with a root mean square error (RMSE) of 0.025, ensuring reliable SOC guidance under typical operating conditions. Thermal analysis revealed minimal temperature rise, with cell temperatures remaining within  $0.3\text{--}0.5^{\circ}\text{C}$  of ambient during the final charging phase. These results show that machine learning enables passive balancing circuits to match the efficiency of much more expensive active balancers, while maintaining simplicity, low cost, and safety of the battery cell. The proposed framework extends battery life, reduces thermal management costs, lowers total power loss, and increases efficiency.

## ملخص البحث

لا تزال موازنة الخلايا السلبية (Passive cell-balancing) خياراً جذاباً لأنظمة إدارة البطاريات (BMS) الحساسة للتكلفة، ولكن أسلوب التحكم ذي العتبة الثابتة (fixed-threshold control) يهدر الطاقة ويسرع من شيخوخة المكونات. تعتمد العديد من التطبيقات الحساسة للتكلفة على الموازنة السلبية عبر مقاومة التحويل (shunt-resistor) لحزم بطاريات الليثيوم-أيون نظراً لبساطتها وموثوقيتها وتكلفتها المنخفضة، والتي تستخدم عادةً جهد الدائرة المفتوحة (OCV) كمؤشر تقريبي لحالة الشحن (SOC)، وهذا لا يوفر دقة كافية، خاصة في خلايا الليثيوم-أيون حيث يظل الجهد ثابتاً تقريباً ضمن نطاق واسع من مستويات حالة الشحن. في هذه الجوانب، وعلى الرغم من الفروقات الكبيرة في حالة الشحن، قد تكون تقلبات الجهد صغيرة جداً بحيث لا يتمكن نظام إدارة البطارية من قياسها بدقة. لهذه الأسباب، قد تظل الخلايا غير متوازنة بشكل مستمر أثناء عملية الموازنة، مما قد يؤدي إلى عدم استخدامها بالكامل، وزيادة خطر الشحن الزائد، وتآكل أسرع بسبب الحرارة المتولدة. تهدف هذه الدراسة إلى استقصاء التطورات الحديثة في الموازنة السلبية وتعلم الآلة (Machine Learning) لتقدير حالة الشحن، وتطوير بنية مُحسَّنة لنظام إدارة البطاريات للموازنة السلبية يدمج تعلم الآلة، وتقييم النظام المقترح مقارنة بالأساليب التقليدية القائمة على جهد الدائرة المفتوحة من حيث الدقة والكفاءة والأداء. تم تطوير بنية مُحسَّنة للموازنة السلبية تجمع

بين شبكة تحويل مُبدّلة (switched-shunt) منخفضة التكلفة ومُقدّر لحالة الشحن (SOC) يعتمد على الذاكرة طويلة قصيرة المدى (LSTM)، والذي تم تدريبه على مجموعات بيانات عامة متعددة درجات الحرارة. يزود المتنبئ القائم على البيانات (data-driven predictor) وحدة تحكم بالتلاكؤ (hysteresis controller) بقيم حالة الشحن في الوقت الفعلي، مما يتيح اتخاذ قرارات موازنة مستتيرة بناءً على ديناميكيات الخلية بدلاً من الجهد وحده. تم نمذجة ثلاث خلايا ليثيوم-أيون بتكوين (3S1P) في برنامج MATLAB/Simulink وتم التحقق من صحتها بمقارنتها بنموذج أولي مادي (hardware prototype) مُهيأاً للتقدير التقليدي القائم على جهد الدائرة المفتوحة والذي استُخدم لعملية الموازنة. تم تسجيل مقاييس الأداء مثل زمن الموازنة، وتردد التبديل، وتبديد الطاقة، والارتفاع الحراري لكلا الاستراتيجيتين، وتم اكتشاف هذه النتائج في الدراسة. أدى النهج المعزز بتعلم الآلة (ML-assisted) إلى تقليل زمن الموازنة للوصول إلى 80% من حالة الشحن بنسبة 29% (2.88 ساعة مقابل 4.05 ساعة)، وخفض متوسط تردد التبديل بنسبة 97% (10.2 ملي هرتز مقابل 333.8 ملي هرتز)، وخفض إجمالي تبديد الطاقة بنسبة 81% (0.422 واط مقابل 2.22 واط).

حافظ مُقدّر حالة الشحن القائم على (LSTM) على دقة تنبؤية عالية عبر نطاق درجات حرارة من -10° مئوية إلى 25° مئوية مع جذر متوسط مربع الخطأ (RMSE) يبلغ 0.025، مما يضمن توجيهها موثقاً لحالة الشحن في ظل ظروف التشغيل النموذجية. كشف التحليل الحراري عن ارتفاع ضئيل في درجة الحرارة، حيث ظلت درجات حرارة الخلايا ضمن 0.3-0.5° مئوية من درجة الحرارة

المحيطة خلال مرحلة الشحن النهائية. تُظهر هذه النتائج أن تعلم الآلة يُمكن دوائر الموازنة السلبية من مضاهاة كفاءة الموازونات النشطة (active balancers) الأكثر تكلفة، مع الحفاظ على البساطة، والتكلفة المنخفضة، وسلامة خلية البطارية. الإطار المقترح يطيل عمر البطارية، ويقلل من تكاليف الإدارة الحرارية، ويخفض إجمالي فقدان الطاقة، ويزيد من الكفاءة.



## APPROVAL PAGE

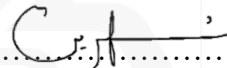
I certify that I have supervised and read this study and that in my opinion, it conforms to acceptable standards of scholarly presentation and is fully adequate, in scope and quality, as a thesis for the degree of Master of Science in Engineering.



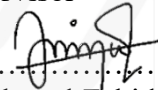
.....  
Siti Hajar Yusoff  
Supervisor



.....  
Teddy Surya Gunawan  
Co-Supervisor



.....  
Mohd Shahrin Abu Hanifah  
Co-Supervisor



.....  
Suriza Ahmad Zabidi  
Co-Supervisor

I certify that I have read this study and that in my opinion it conforms to acceptable standards of scholarly presentation and is fully adequate, in scope and quality, as a thesis for the degree of Master of Science in Engineering.



.....  
Noor Hazrin Hany Mohamad Hanif



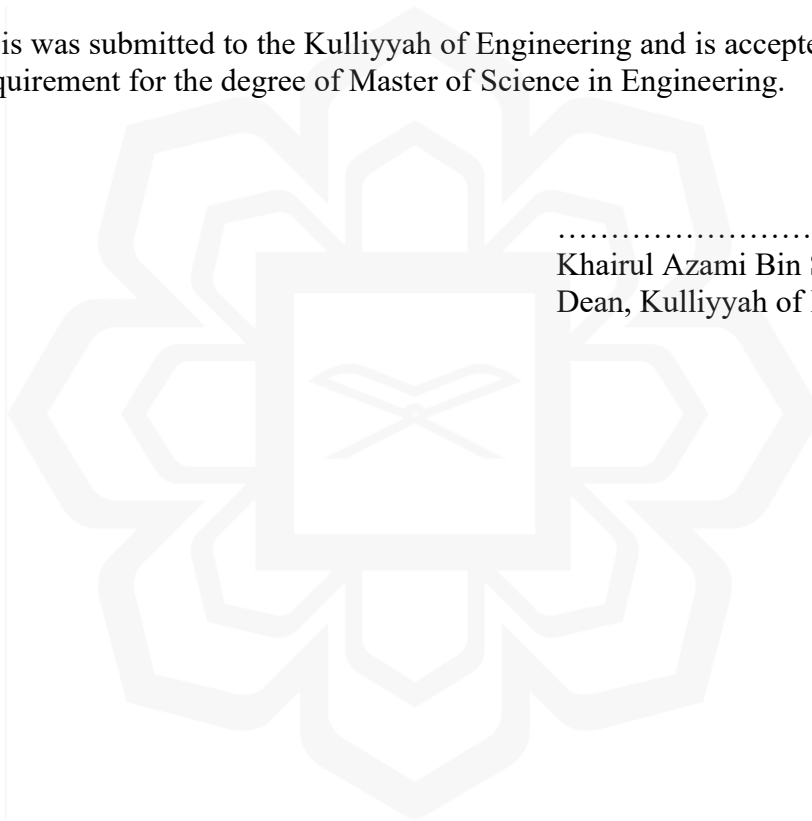
.....  
Mohd Azlishah Bin Othman

This thesis was submitted to the Department of Electrical and Computer Engineering and is accepted as a fulfilment of the requirement for the degree of Master of Science in Engineering.

.....  
Othman Omran Khalifa  
Head, Department of Electrical and  
Computer Engineering

This thesis was submitted to the Kulliyah of Engineering and is accepted as a fulfillment of the requirement for the degree of Master of Science in Engineering.

.....  
Khairul Azami Bin Sidek  
Dean, Kulliyah of Engineering



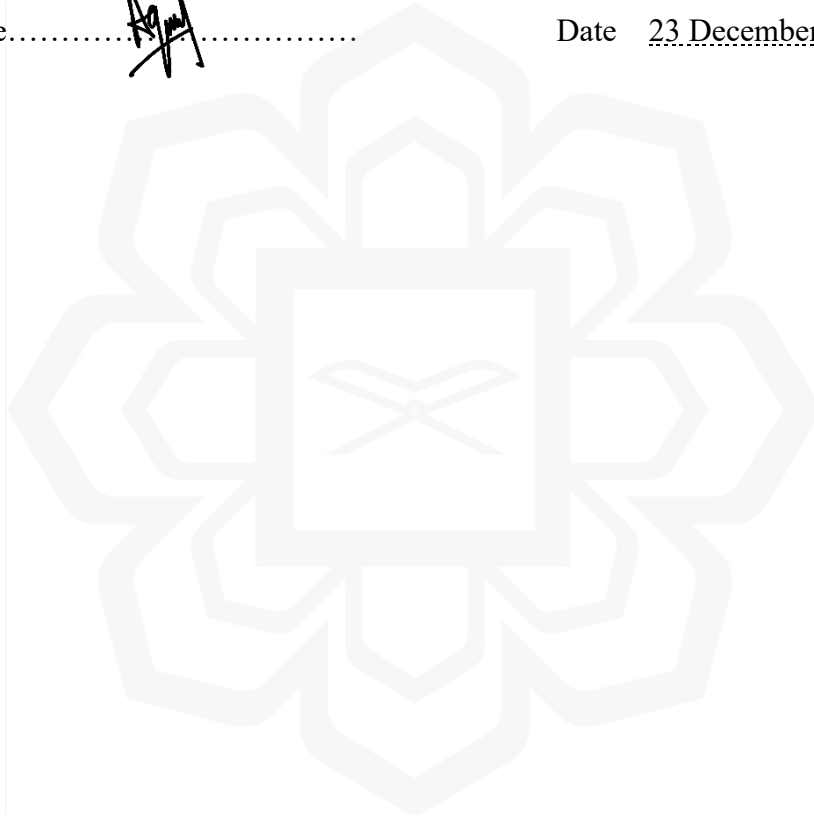
## DECLARATION

I hereby declare that this thesis is the result of my own investigations, except where otherwise stated. I also declare that it has not been previously or concurrently submitted as a whole for any other degrees at IIUM or other institutions.

Muhamad Aqil Muqri Bin Muhamad Fahmi

Signature.....

Date 23 December 2025



**INTERNATIONAL ISLAMIC UNIVERSITY MALAYSIA**  
**DECLARATION OF COPYRIGHT AND AFFIRMATION OF**  
**FAIR USE OF UNPUBLISHED RESEARCH**

**ENHANCED PASSIVE BALANCING APPROACH FOR**  
**BATTERY MANAGEMENT SYSTEMS USING MACHINE**  
**LEARNING**

I declare that the copyright holder of this thesis is International Islamic University Malaysia.

Copyright © 2025 International Islamic University Malaysia. All rights reserved.

No part of this unpublished research may be reproduced, stored in a retrieval system, or transmitted, in any form or by any means, electronic, mechanical, photocopying, recording or otherwise without prior written permission of the copyright holder except as provided below

1. Any material contained in or derived from this unpublished research may only be used by others in their writing with due acknowledgement.
2. IIUM or its library will have the right to make and transmit copies (print or electronic) for institutional and academic purpose.
3. The IIUM library will have the right to make, store in a retrieval system and supply copies of this unpublished research if requested by other universities and research libraries.


By signing this form, I acknowledged that I have read and understand the IIUM Intellectual Property Right and Commercialization policy.

Affirmed by Muhamad Aqil Muqri Bin Muhamad Fahmi

  
.....  
Signature

23 December 2025

Date



*This thesis is born of perseverance, shaped by struggle, and completed through the  
grace of those who believed in me when I no longer did.*

## ACKNOWLEDGEMENTS

*“In the name of Allah, the Most Gracious and the Most Merciful”*

All praise and gratitude are due to Allah, the Most Merciful and Compassionate, and He guided me throughout my thesis journey. Although there were difficulties, His blessings made it easier and helped me get to this important milestone.

I sincerely thank Assoc Prof. Ts. Dr. Siti Hajar Yusoff for her continuous help, kindness and support, which played a major role in finishing this work. I am very grateful for her precise input, helpful recommendations and insightful questions, which have improved this thesis. Her knowledge of what this research involves has allowed her to make significant contributions that have greatly improved the study. She has always managed to give her time and advice, even with everything else she has to do. What she has said to me about being a writer has fueled me every time I sat down to write.

I would like to thank Prof. Ts. Dr. Teddy Surya Gunawan, Dr. Shahrin Abu Hanifah, and Assoc. Prof. Dr. Suriza Ahmad Zabidi for their guidance and time spent with me during my master’s research. I am truly grateful to my friends and peers for their continuous support, motivation, and knowledge, which have helped me during all parts of this research. All our perspectives and experiences together have added great value to this work.

I also take this opportunity to say a big thank you to my parents, Muhamad Fahmi Bin Abu Hasan and Roziana Binti Rusdi, as well as my siblings, for always praying and helping me complete my master’s degree. May Allah reward all of them with the good in this Dunya and the Hereafter for their uncountable kindness and moral support.

Once again, I offer my utmost gratitude to Allah for His infinite mercy, which has enabled me to successfully complete this thesis. Alhamdulillah.

# TABLE OF CONTENTS

Abstract .....	ii
ملخص البحث.....	iii
Approval Page.....	vi
Acknowledgements.....	xi
Table Of Contents .....	xii
List Of Tables .....	xv
List Of Figures .....	xvi
<b>CHAPTER ONE: INTRODUCTION .....</b>	<b>1</b>
1.1 Background .....	1
1.2 Problem Statement .....	3
1.3 Research Objectives.....	6
1.4 Research Methodology .....	6
1.5 Research Scope .....	7
1.6 Thesis Organisation .....	8
<b>CHAPTER TWO: LITERATURE REVIEW .....</b>	<b>1</b>
2.1 Introduction.....	1
2.2 Battery Management System (BMS).....	1
2.2.1 Monitoring .....	3
2.2.2 Balancing .....	3
2.2.3 Cell Balancing Topologies.....	4
A. Passive Cell Balancing Method.....	5
i. Fixed Shunt Resistor.....	6
ii. Switched Shunt Resistor.....	6
B. Active Cell Balancing Method.....	7
2.2.4 Protection .....	8
2.3 Battery Management System Standard.....	9
2.3.1 Overview of relevant BMS standards.....	9
2.3.2 BMS standards for its functionality, testing, and development.....	10
2.4 Types Of Batteries .....	10
2.4.1 Lead Acid Battery .....	13
2.4.2 Lithium-Ion .....	14
2.4.3 Supercapacitor.....	15
2.5 Battery Management System Topologies .....	16
2.5.1 Centralized BMS.....	16
2.5.2 Distributed BMS .....	17
2.5.3 Semi-Distributed BMS.....	17
2.6 Cell Balancing Approach .....	17
2.6.1 SOC Estimation Based Balancing Method .....	18
A. Direct Method of SOC Estimation.....	20

B. Indirect Method of SOC Estimation.....	24
i. Electrochemical Mechanism-Based Model.....	29
ii. Electrical Equivalent Circuit Model.....	30
iii. Data Driven Approach.....	31
2.6.2 Voltage Dependent Balancing Method.....	34
2.6.3 SOC – Voltage Balancing Method .....	36
2.7 Summary.....	38
<b>CHAPTER THREE: METHODOLOGY.....</b>	<b>40</b>
3.1 Overview.....	40
3.2 Research Methodology .....	41
3.3 Simulation of Passive Balancing Method Using MATLAB.....	43
3.3.1 Battery Cell Modeling.....	43
3.3.2 Proposed Design BMS Simulation Setup .....	44
3.3.3 The Balancing Algorithm .....	45
3.3.4 Evaluation Metrics .....	48
3.4 Validation of Prototype Development .....	49
3.4.1 Prototype Setup.....	50
A. Block Diagram of the Proposed System .....	50
B. Algorithm Schema of the BMS.....	51
3.4.2 Proposed BMS Working Principle.....	52
A. Monitoring.....	53
B. Balancing.....	54
C. Protection .....	55
3.4.3 BMS Prototype Hardware Design .....	55
3.5 The Integration Of Machine Learning Soc Estimation.....	58
3.5.1 Machine Learning Model Training Workflow.....	58
3.5.2 Defining Model Requirements and Data Preparation.....	59
3.5.3 Model Training and Model Testing .....	62
3.5.4 Model Tuning and Integration into MATLAB Simulink .....	71
<b>CHAPTER FOUR: RESULTS AND DISCUSSION.....</b>	<b>74</b>
4.1 Overview.....	74
4.2 Simulation Results .....	75
4.2.1 Charging Simulation Results .....	75
A. OCV Results.....	75
B. Prototype Results.....	85
C. ML – SOC Estimation Results.....	88
4.2.2 Discharging Results .....	100
A. Simulation Results.....	100
B. Experimental Prototype Results.....	103
4.3 Summary.....	107

**CHAPTER FIVE: CONCLUSION AND FUTURE WORKS.....109**  
5.1 Conclusion ..... 109  
5.2 Future Works ..... 110  
    5.2.1 Real-Time Hardware Implementation and Embedded ML Deployment  
        111

**REFERENCES.....113**  
**LIST OF PUBLICATIONS .....126**



## LIST OF TABLES

Table 2.1 Active Cell Balancing Topologies using Capacitor (Paudyal et al., 2019)	8
Table 2.2 Active Cell Balancing Topologies using Converters (Paudyal et al., 2019)	8
Table 2.3 Comparison Between Passive and Active Balancing Methods	8
Table 2.4 International Standards for Battery System	9
Table 2.5 Summary of Direct SOC Estimation Method	22
Table 2.6 Summary of Indirect Method of SOC Estimation	24
Table 3.1 Battery Parameters Used in MATLAB Simulation	44
Table 3.2 Description for Figure 3.10	57
Table 4.1 Total Average Power Loss During OCV Charging	84
Table 4.2 Total Average Power Loss During ML-SOC Charging	99
Table 4.3 Summary of OVC SOC Estimation and ML SOC Estimation Results	107

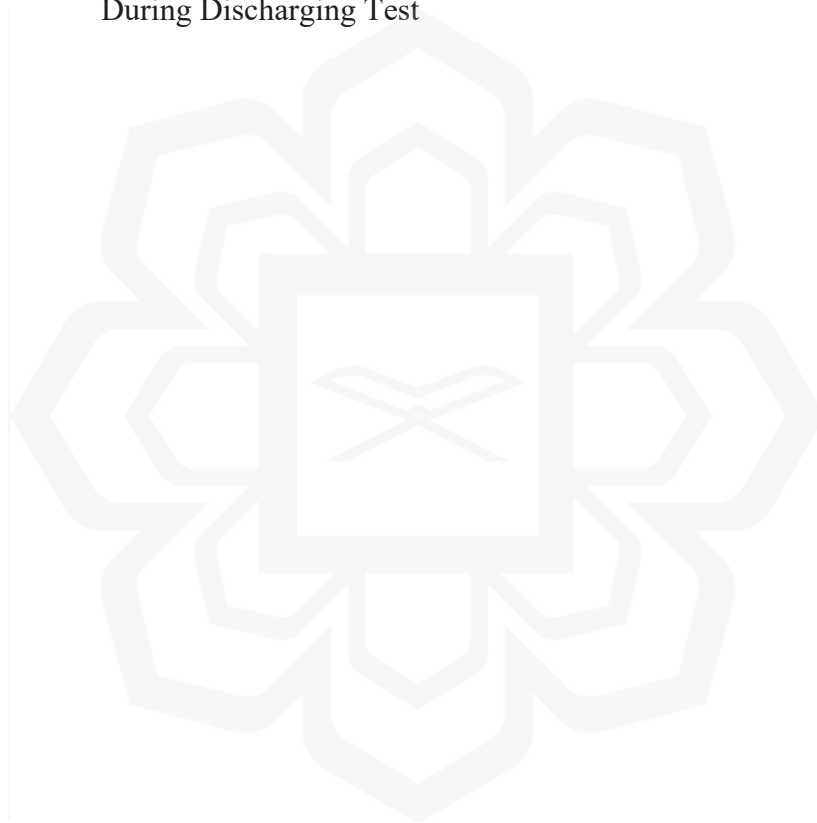
## LIST OF FIGURES

Figure 1.1	General Flowchart for The Research	7
Figure 2.1	Overview of A Sample BMS Design (Hariprasad et al., 2020)	2
Figure 2.2	BMS Functionalities	2
Figure 2.3	Battery Balancing Methods	4
Figure 2.4	Active and Passive Cell Balancing Technique (Paudyal et al., 2019)	5
Figure 2.5	Switched Shunt Resistor Topology of Passive Cell balancing (Paudyal et al., 2019)	7
Figure 2.6	Ragone Plots for An Array of Energy Storage	11
Figure 2.7	Ragone plot showing the typical values of energy and power of different energy storage devices (Castro-Gutiérrez et al., 2020)	12
Figure 2.8	Comparison of Energy Density in Battery Cells (NASA)	12
Figure 2.9	Cut-away cell lead acid battery showing details of construction (Garche, 2025)	13
Figure 2.10	Overview of a Lithium-Ion Battery (Garche, 2025)	14
Figure 2.11	Mechanism of formation of the electrostatic double-layer (EDL) in a Supercapacitor (Castro-Gutiérrez et al., 2020)	15
Figure 2.12	BMS Topologies (BMS and KEMET METCOM Inductors)	16
Figure 2.13	Battery Responding Variables	19
Figure 2.14	SOC Estimation Methods	19
Figure 3.1	Overall Research Methodology Flowchart	42
Figure 3.2	MATLAB Simscape Battery (Table-Based) block used for lithium-ion cell modeling. Adapted from MathWorks, 2024.	43
Figure 3.3	BMS Simulation Design in MATLAB Simulink	45
Figure 3.4	Balancing Algorithm for OCV Simulation	48
Figure 3.5	Block diagram of the BMS design	51
Figure 3.6	The BMS balancing algorithm	52

Figure 3.7	Monitoring Portion of the BMS	53
Figure 3.8	Balancing Portion of the BMS	54
Figure 3.9	Prototype BMS Schematic Diagram	56
Figure 3.10	Prototype of The BMS Design	57
Figure 3.11	ML Training Workflow	59
Figure 3.12	Non-Normalized Battery Data for Model Training	60
Figure 3.13	SOC (%) Data for Model Training	61
Figure 3.14	Normalized Battery Data for Model Training	61
Figure 3.15	One Observation of One Dataset Chunk	62
Figure 3.16	Illustration of The Model Network Architecture	64
Figure 3.17	MATLAB Model Training Progress Window	65
Figure 3.18	RMSE Values at Each Ambient Temperature Condition	67
Figure 3.19	Plot of The Predicted and The Target SOC for Each Temperature Condition	68
Figure 3.20	View of One Noisy Observation For The Battery Dataset	70
Figure 3.21	Confusion Matrix of Discriminator Accuracy	70
Figure 3.22	Exported SOC Estimation Model	72
Figure 3.23	Subsystem of The Model Network	72
Figure 3.24	Plot of Predicted and True SOC Values at 10°C	73
Figure 3.25	BMS Simulation Design in MATLAB Simulink With SOC Estimation Model	73
Figure 4.1	Cell Voltage During OCV Charging Simulation	76
Figure 4.2	Voltage Fluctuation of Each Cell During Balancing Process	77
Figure 4.3	Close-up of Voltage Cell 3 During Balancing Process	77
Figure 4.4	Cell Current During OCV Charging Simulation	78
Figure 4.5	Close-up on Cell 3 Current During Balancing Process	78
Figure 4.6	SOC of Each Cell for OCV Charging Simulation	79
Figure 4.7	Close-up SOC of Each Cell During Charging	80
Figure 4.8	Measurement of Switching Frequency During OCV Balancing Process	80
Figure 4.9	Switching State During Balancing Process	81

Figure 4.10	Close-up of Switch 3 Switching State During Balancing Process	82
Figure 4.11	Power Dissipation of Balancing Resistors During Charging	83
Figure 4.12	Close-up of Power Dissipation of Balancing Resistors During Charging	83
Figure 4.13	Temperature of Cell During OCV Charging	85
Figure 4.14	Monitoring of Cells Voltage During BMS Charging Test	86
Figure 4.15	Close-up of Cell Voltage 1 During BMS Charging Test	87
Figure 4.16	Protection Monitoring of Balancer Condition During Charging	87
Figure 4.17	BMS Prototype Balancer Light Activate During Charge Balancing Process	88
Figure 4.18	Cell Voltage During Charging for ML-SOC Simulation	89
Figure 4.19	Close-up of Cell Voltage During Charging for ML-SOC Simulation	90
Figure 4.20	Cell Current During ML-SOC Charging	90
Figure 4.21	Close-up of Cell Current During ML-SOC Charging	91
Figure 4.22	SOC of Each Cell During ML-SOC Charging	92
Figure 4.23	Close-up of SOC of Each Cell During ML-SOC Charging	93
Figure 4.24	Measurement of Switching Frequency During ML-SOC Balancing Process	93
Figure 4.25	Comparison of Time Needed to Fully Charge the Battery Cells	94
Figure 4.26	Frequency Comparison Between the OCV vs ML-SOC During Charging Simulation	95
Figure 4.27	Switching State During Balancing Process of ML-SOC Simulation	96
Figure 4.28	Close-up of Switching State During Balancing Process of ML-SOC Simulation	96
Figure 4.29	Power Dissipation of Balancing Resistors During ML-SOC Charging	97
Figure 4.30	Close-up of Power Dissipation of Balancing Resistors During ML-SOC Charging	98
Figure 4.31	Cell Temperature During Charging	100

Figure 4.32	Cell Voltage During Discharging Simulation	101
Figure 4.33	Cell Current During Discharging Simulation	102
Figure 4.34	SOC of Each Cell During Discharging Simulation	102
Figure 4.35	Cells Voltage During Experimental BMS Discharging Test	103
Figure 4.36	Close-up of Cell Voltage During BMS Discharging Test	104
Figure 4.37	BMS Monitoring of Current and Power Used During BMS Discharging Test	105
Figure 4.38	Cell Voltages and Discharge MOSFET Gate Signal Status During Discharging Test	106



# CHAPTER ONE

## INTRODUCTION

### 1.1 BACKGROUND

Rechargeable battery packs are widely used in modern applications due to their high energy density and long cycle life. However, cell-to-cell variations can lead to poor performance and safety hazards. Variations in battery state of charge (SOC) and cell chemistry arise from manufacturing tolerances and uneven operating conditions. These variations can cause overcharging or deep discharging, which reduce runtime, accelerate degradation, and increase the risk of cell damage (Ganapati Chikkalkar et al., 2022; Hosseinzadeh et al., 2021; Imran et al., 2024; H. Li, Zhuo, et al., 2024; Sabarimuthu et al., 2023). To overcome these challenges, advanced battery management systems (BMS) using enhanced cell balancing techniques have been studied to employ both passive and active approaches to regulate SOC levels across different cells (Imran et al., 2024). Furthermore, the distributed methods for SOC estimation increase the reliability because each cell's SOC estimation is used to determine the SOC of the entire battery pack in which if some cells are failing, the pack will still operate correctly (H. Li, Zhuo, et al., 2024). Also, the current split strategies and model-driven manufacturing approaches are under consideration to improve the energy distribution and manufacturing yield of the Li-ion battery systems (Maddireddy, 2024; Maksimovna Vakhrusheva & Xu, 2024). These improvements are collectively planned to increase the durability and reliability of the battery packs in different applications, from consumer electronics to grid storage systems (Anapolsky et al., 2024).

To address these challenges, battery management systems (BMS) play a critical role in ensuring the safety and efficiency of lithium-ion batteries, particularly in electric vehicles. Conventional BMS primarily focus on monitoring voltage and temperature while performing cell balancing to minimize imbalances between cells. Passive balancing is

commonly used because of its simple implementation and low cost. However, this approach dissipates excess energy as heat, leading to energy waste and potential overcharging or over-discharging issues (Anurudha Gedam et al., 2024; Ashraf et al., 2024). While passive balancing remains dominant in cost-sensitive applications, advanced BMS implementations increasingly adopt active balancing approaches. Active balancing methods redistribute energy between cells using DC-DC converters, achieving better efficiency and faster SOC equalization, albeit at significantly higher cost and complexity (Anurudha Gedam et al., 2024; M et al., 2024). The choice between passive and active balancing depends largely on application requirements, with passive methods preferred for cost-sensitive applications and active methods suited for high-performance environments such as electric vehicles (Grebtsov et al., 2024; Mirela et al., 2024).

Recent developments in artificial intelligence and data analytics have provided an alternative approach to improving BMS performance without the cost penalties of active balancing hardware. The integration of machine learning (ML) into BMS revolutionizes battery control by enabling real-time monitoring and predictive maintenance, thereby optimizing accuracy and maintaining efficiency. By processing multiple datasets that include voltage, current, and temperature metrics that enable the ML models to forecast potential cell imbalances and degradation with high precision. This capability allows proactive balancing interventions and tailored optimization of charge/discharge cycles at the individual cell level (Ahwiadi & Wang, 2025; Hussain et al., 2025). Such a data-driven strategy not only mitigates energy waste in passive balancing circuits but also extends battery lifespan and reduces the risk of unexpected failures (B. et al., 2024; Malik & Saini, 2025). For example, adaptive deep neural networks have proven effective in prolonging battery longevity by dynamically regulating thermal stress during charging processes (Malik & Saini, 2025). Beyond standalone ML applications, hybrid frameworks that integrate physics-informed models with machine learning algorithms demonstrate superior predictive performance. These integrative approaches enhance state-of-health estimation and operational reliability, particularly in electric vehicles, encouraging smarter energy management and sustainable battery usage (B. et al., 2024; Qin et al., 2025).

Combining ML with passive balancing in BMS enhances the efficiency and effectiveness of battery performance, particularly in electric vehicles (EVs). Passive cell balancing, which dissipates excess energy from higher voltage cells, is cost-effective and straightforward but can be optimized through ML algorithms to improve balancing time and minimize power loss (Aswini et al., 2024a; Chandana & Chavan, 2024; Duraisamy & Kaliyaperumal, 2021). For instance, the integration of Proportional-Integral (PI) and Artificial Neural Network (ANN) controllers has demonstrated significant improvements in SOC balancing, reducing average power and heat dissipation, thereby enhancing battery lifespan (Karmakar, Bera, et al., 2023; Karmakar, Bohre, et al., 2023). Additionally, ML models can predict the remaining useful life (RUL) of batteries, allowing for proactive balancing strategies that enable the maintenance of SOC levels, ultimately increasing overall battery health and performance (Sultan et al., 2025). This synergistic approach not only extends battery life but also enhances the efficiency of modern EVs (Karmakar, Bera, et al., 2023; Karmakar, Bohre, et al., 2023; Singh & Agnihotri, 2022; Sultan et al., 2025; Weng & Ababei, 2024).

This research focuses on how combining ML algorithms to estimate SOC levels with passive balancing can enhance even basic resistor-based circuits through data-driven optimization, which bridges the gap between traditional passive systems that often struggle with energy inefficiency. With the growing complexity of modern battery usage, solution by integrating the BMS with a better algorithm that can better detect imbalance trends, proactively tackle immediate risk, and ultimately deliver a more reliable and cost-effective way to manage rechargeable battery packs across all sorts of electronics application.

## **1.2 PROBLEM STATEMENT**

Passive balancing methods in traditional BMS maintain simple designs but show poor performance in precision and adaptability, as well as delayed responsiveness. The resulting constraints produce unwanted energy losses as well as slow cell balancing, inaccurate SOC

evaluation, and insufficient battery protection that shortens the lifespan of the entire battery pack system. Heat dissipation through resistors during passive balancing of battery cells at higher voltages creates substantial energy waste, with research demonstrating that passive systems can dissipate 10-30% of energy during charge cycles, while active balancing methods save an additional 4.15% additional energy savings compared to passive methods (Kumar et al., 2023). This energy efficiency decrease becomes more problematic in large-scale battery energy storage systems (BESS), where cumulative passive balancing losses can result in total energy retention as low as 1.53% during the entire balancing process (Kumar et al., 2023; Lee Pan, 2025; Omi & Hatakeyama, 2024). The energy efficiency decreases while thermal maintenance grows as a challenge, and safety risks increase since the weakest cell determines the overall battery pack performance (Bashir et al., 2022). The conventional implementation of passive balancing techniques encounters three main challenges, which include slow balancing response time and imprecise SOC measurements alongside insufficient protection mechanisms. The limitations become worse because of inherent cell-to-cell variations that come from manufacturing imperfections, temperature changes, and self-discharge rate differences. These factors lead to unbalanced cell conditions, which may shorten battery life and raise the probability of battery failures (Aswini et al., 2024b; Itagi et al., 2024). The wide adoption of passive balancing techniques requires improvement with advanced technologies together with modern SOC estimation methods utilizing a state-of-the-art machine learning approach (Bashir et al., 2022; Itagi et al., 2024). Improved battery performance and operational safety, together with longer duration, would result from these advancements, which are particularly beneficial in power storage applications that are always under intensified demand.

The SOC levels of rechargeable battery cells with flat open-circuit voltage (OCV) characteristics present a significant challenge for precise measurement because of their inherent cell properties. The flat OCV-SOC relationship curve makes it difficult for even minor measurement errors to lead to substantial estimation mistakes in SOC. For lithium iron phosphate (LiFePO<sub>4</sub>) batteries, the flat OCV-SOC relationship means that minor OCV measurement errors can result in SOC estimation uncertainties where the signal-to-noise ratio drops to as low as -25 dB in critical SOC ranges (0.4-0.6 and 0.8-0.9) (Gao et al.,

2024). These estimation inaccuracies directly impact balancing decisions, as voltage-based passive balancing methods can exhibit up to 9.8% lower energy accumulation efficiency compared to advanced state-of-charge-based approaches (A. K. Sharma et al., 2025). The errors produce complications in the balancing process, which leads to uneven distribution of charge and unbalanced operational performance between the connected cells in the battery pack (Yi et al., 2024). These mismatches between cells become more severe because they have unique internal resistances from differences in manufacturing and aging processes that cause notable current variations (Hosseinzadeh et al., 2019). The occurrence of challenging OCV profiles both elevates battery degradation risks and intensifies thermal runaway events because of their impact on SOC estimation accuracy. Thus, better SOC measurement methods are crucial in these situations.

Furthermore, significant motivation for this research stems from the observed gap in current literature: despite the growing interest in intelligent BMS technologies, limited studies have conducted rigorous comparative evaluations between conventional OCV-based SOC estimation and modern machine learning-based SOC estimation methods. The absence of direct evaluation eliminates essential information regarding both advantages and disadvantages related to switching from standard estimation models to data-driven methods. This research studies the gap to deliver both improved SOC accuracy and balancing control while providing empirical evidence about strategic BMS design methods for future energy storage applications.

To address the limitation of the conventional approach of passive balancing techniques, this research proposed utilizing advanced ML algorithms in passive balancing techniques because they offer precise and continuous SOC estimation of individual cells found within a battery pack. Real-time estimation of battery imbalances combined with continuous essential parameter monitoring enables the enhanced BMS system developed in this research to adapt efficiently in balancing each of the battery cells according to the appropriate limit. The proposed system targets substantial enhancements in balancing precision while simultaneously decreasing energy consumption, minimizing balancing time, and protecting cells in achieving extended battery lifespan.

### **1.3 RESEARCH OBJECTIVES**

The objectives of this research are listed below:

1. To investigate recent advancements in battery management systems (BMS), focusing explicitly on innovations in passive balancing techniques and the integration of machine learning algorithms in state of charge (SOC) estimation.
2. To develop a BMS that integrates enhanced passive balancing techniques assisted by machine learning estimation methods.
3. To evaluate the performance of ML-based passive balancing versus conventional OCV estimation in terms of accuracy, efficiency, and balancing performance.

### **1.4 RESEARCH METHODOLOGY**

The whole research flow can be depicted in a flow diagram, as shown in Figure 1.1 below. This project was started by acquiring and gathering knowledge on the topic from the literature review of other previous research papers and projects. Next, problem identification can be made from all the knowledge gained. Then, the implementation of the project can be started after a complete understanding of the project's needs. Following that, the development project needs to be tested to ensure a good functioning project. The final step of the project is to analyze the results obtained from the test to complete the project.

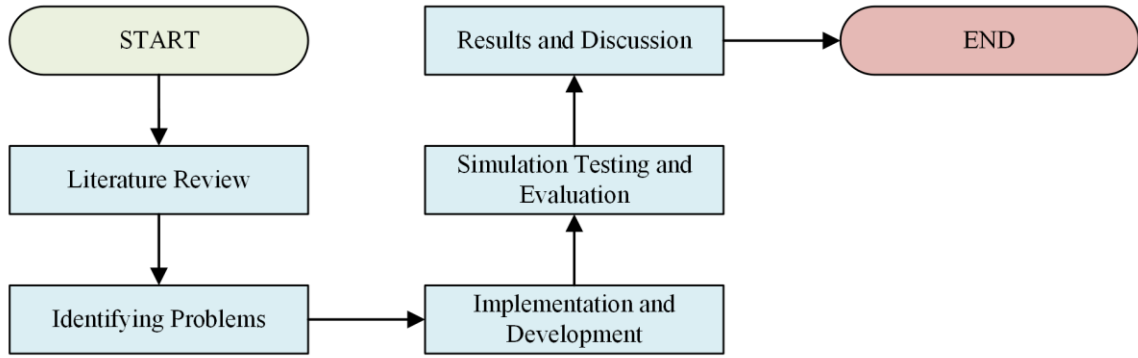


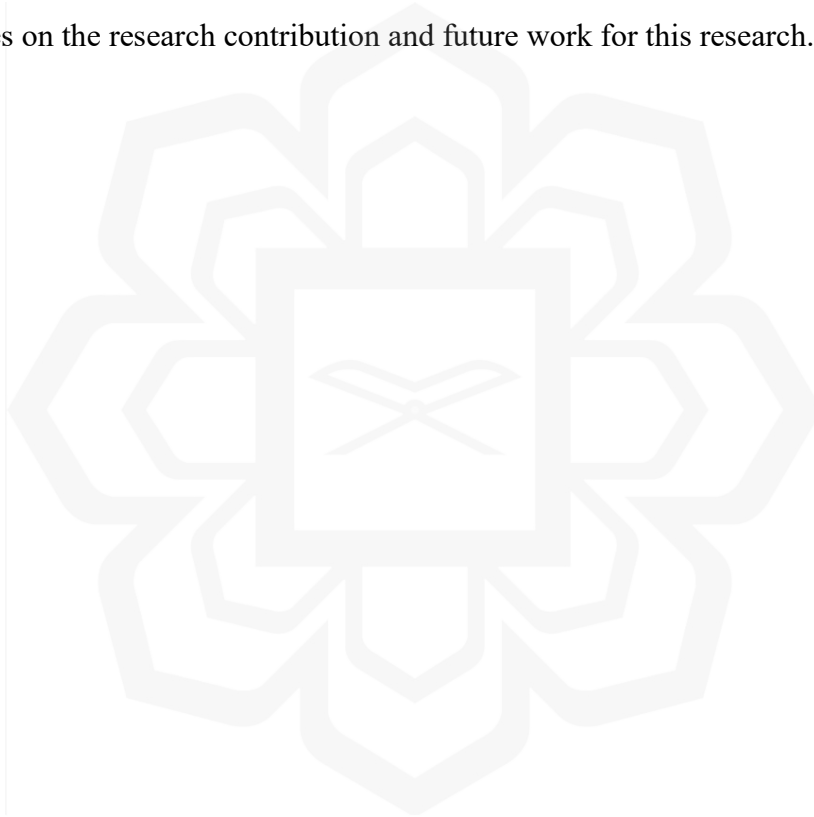
Figure 1.1 General Flowchart for The Research

## 1.5 RESEARCH SCOPE

The research examines how standard OCV-based SOC estimation performs against ML-based estimation when used in passive balancing BMS systems for lithium-ion batteries in which the research goal evaluates the accuracy together with responsiveness of SOC estimation techniques for passive balancing BMS regarding energy efficiency, battery cell protection, and lifespan protection. A simulated environment functions with the exact operating conditions while using established battery configurations and load patterns in a simulation environment. Resistive energy dissipation serves as the passive balancing strategy during the assessment of both SOC estimation methods. A simulated ML-based SOC estimation method operated against an OCV-based method that received independent prototype system validation. The prototype evaluation of the OCV method's performance behavior in real-life scenarios. This research also aims to compare different SOC estimation methods on balancing dynamics and energy efficiency, as well as cell protection and total battery pack lifetime. The simulation platform integrates a resistor-based passive balancing design by implementing both estimation approaches under equivalent battery setups and charging patterns. Ultimately, this research investigates the need for future BMS to use advanced SOC estimation methods because of their performance advantages, even when passive balancing remains economical.

## **1.6 THESIS ORGANISATION**

This thesis is organized into five chapters. Chapter One elaborates on the introduction of this research. The introduction discusses the background, problem statement, research objectives, and research scopes. Chapter Two describes the literature review on the BMS approach, especially on the passive balancing technique using machine learning. Chapter Three explains the research methodology. Meanwhile, Chapter Four demonstrates the results and the discussion. Finally, this thesis is concluded in Chapter Five in which it elaborates on the research contribution and future work for this research.



# CHAPTER TWO

## LITERATURE REVIEW

### 2.1 INTRODUCTION

This chapter reviews existing research on battery management systems (BMS), focusing on passive balancing methods and the emerging role of machine learning (ML) in battery control. Early studies addressed voltage and state-of-charge (SOC) imbalances using simple resistor-based circuits for cell equalization. Although these passive systems proved cost-effective and straightforward to implement, they struggled to adapt to varying load conditions and environmental factors. As the field evolved, researchers explored advancements including active balancing hardware and data-driven approaches designed to predict and address imbalances proactively. The rise of ML-based models, capable of processing vast amounts of operational data, represents a paradigm shift in balancing optimization strategies. By analyzing both foundational and state-of-the-art research, this review situates the proposed study within the broader research landscape, emphasizing the current state of passive balancing, the potential of machine learning, and the challenges of integrating these technologies.

### 2.2 BATTERY MANAGEMENT SYSTEM (BMS)

Battery management systems coordinate three interrelated functions: battery management, power management, and energy management. Battery management encompasses operations that optimize energy utilization in portable devices. Power management regulates power distribution across system components, while energy management ensures

efficient and feasible energy conversion processes. Energy management also encompasses energy storage optimization within the system. These three management concepts are integrated within a BMS, whose primary task is to ensure optimal energy utilization while minimizing the risk of battery damage. Electric vehicles depend on BMS to prevent overcharging and excessive discharging while maximizing usable stored energy for optimal vehicle operation (Hariprasad et al., 2020). Figure 2.1 and Figure 2.2 illustrate an overview of BMS design and functionalities, respectively. Key BMS functionalities include capability estimation of the state of charge (SOC), state of health (SOH) monitoring, thermal management, and cell balancing. As seen in Figure 2.2, illustrate an overview of BMS design and functionalities, respectively. Key BMS functionalities include capability estimation, state of charge (SOC) assessment, state of health (SOH) monitoring, thermal management, and cell balancing.

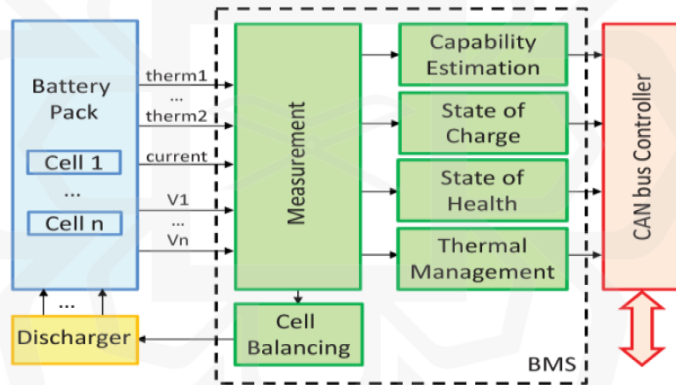


Figure 2.1 Overview of A Sample BMS Design (Hariprasad et al., 2020)

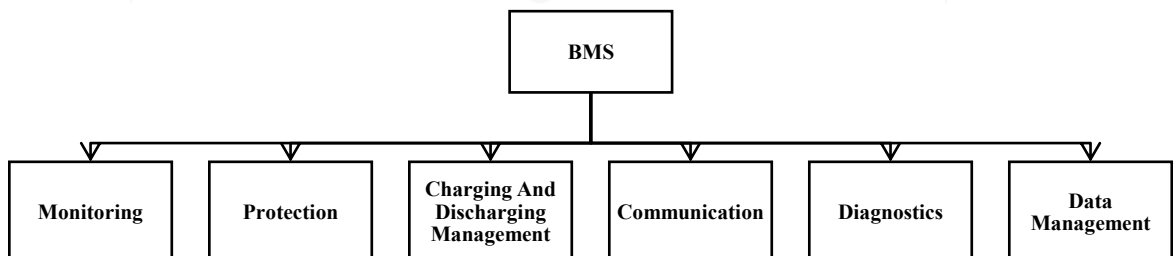


Figure 2.2 BMS Functionalities

### **2.2.1 Monitoring**

A well-designed BMS monitors vital battery parameters including voltage, current, temperature, SOC, SOH, and power capacity through a dedicated subcomponent called the cell monitoring unit (CMU). This real-time monitoring system regulates a variety of BMS tasks to guarantee the safe operation of the battery's stored energy. This real-time monitoring system regulates various BMS functions to ensure safe battery operation. An effective cell monitoring system prevents critical faults including overcharging and over-discharging. Overvoltage and overcurrent conditions can permanently damage the battery system and cascade into secondary failures. Overcharging may cause battery swelling or cell venting, both of which pose severe safety hazards. Swollen batteries can unpredictably release flammable gases, creating critical risks for users. (Gabbar et al., 2021).

Similarly, undervoltage and undercurrent conditions significantly degrade overall battery efficiency. Furthermore, cell temperature substantially affects component operation and can progressively reduce power delivery capacity. Therefore, temperature monitoring is a critical BMS responsibility, as elevated temperatures can cause thermal runaway and other abnormalities that damage the battery system (Lee et al., 2019).

### **2.2.2 Balancing**

Cell balancing equalizes voltages and charge capacities across series-connected battery cells. In multicell battery packs, variations in nominal cell voltage or capacity result in suboptimal energy output. Manufacturing tolerances cause cell-to-cell variations that accumulate with each charge cycle, progressively degrading pack performance. Additionally, self-discharge depletes battery capacity over time. Cell balancing methods mitigate these issues, extending both battery lifespan and usable capacity. Cell balancing methods can be categorized as illustrated in Figure 2.3.

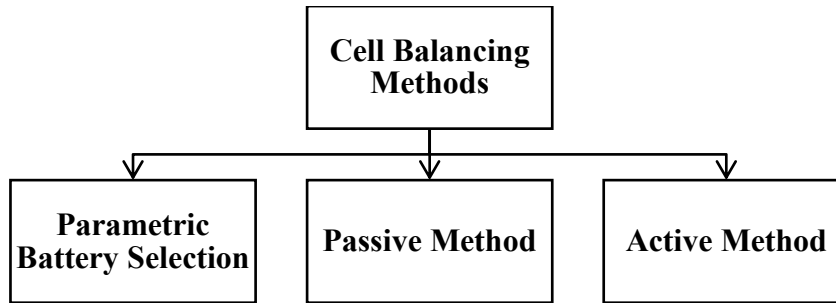


Figure 2.3 Battery Balancing Methods

Based on Figure 2.3, parametric selection involves choosing cells with closely matched electrochemical properties, a costly approach. Moreover, this method cannot guarantee that batteries will maintain their matched characteristics during operational aging. Therefore, passive balancing represents the most common approach, as it is more practical and cost-effective than rigorous cell selection. This method dissipates excess energy as heat through shunt resistors. Alternatively, active balancing redistributes energy among cells using external control circuitry (Kurpiel et al., 2021). Alternatively, active balancing redistributes energy among cells using external control circuitry. Further explanation can be seen in the next section on passive and active cell balancing mechanisms.

### 2.2.3 Cell Balancing Topologies

In Figure 2.4, various cell-balancing topologies that have been studied in research are discussed below:

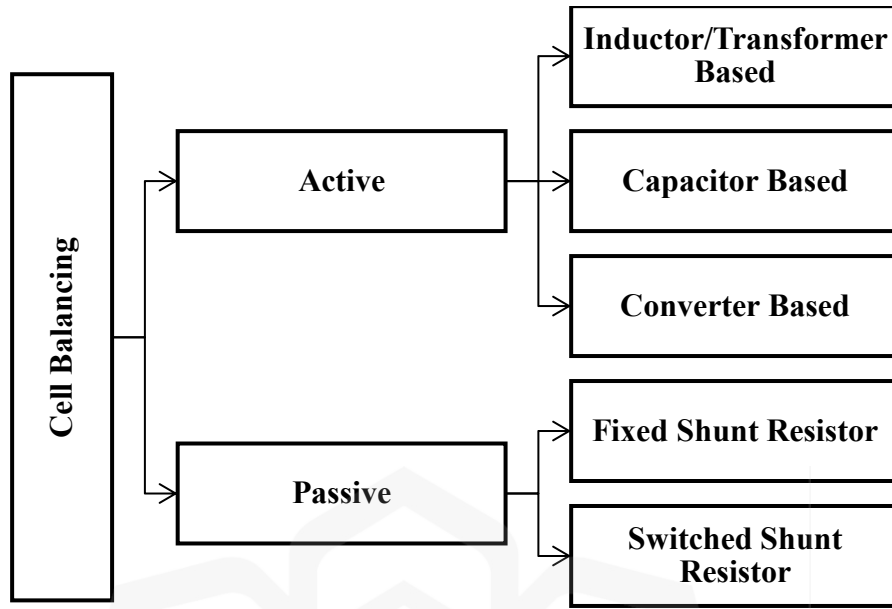


Figure 2.4 Active and Passive Cell Balancing Technique (Paudyal et al., 2019)

Based on Figure 2.4, the report will focus more on the passive cell balancing technique that will briefly be explained in the following segments of this subchapter, such as the fixed shunt resistor and switched shunt resistor method. The next section also gives a general description of the active balancing method.

### ***A. Passive Cell Balancing Method***

Excess energy from high-charged cells is released as heat by a shunt resistor in passive cell balancing which equalizes the battery pack's voltage levels (Turksoy et al., 2020a). This approach is favored for its simplicity, minimal circuitry requirements, and low cost. Passive balancing employs either fixed shunt resistors or switched shunt resistors, both discussed in subsequent subsections.

*i. Fixed Shunt Resistor*

In a battery pack of multiple cells, a fixed shunt resistor is used in cell balancing to equalize the voltage across each cell. This helps ensure that all the cells in the battery pack are charged and drained at the same rate. This makes the battery pack work better and last longer overall.

*ii. Switched Shunt Resistor*

In a switched shunt resistor configuration, each cell connects in parallel with a controllable resistor via a switching element (typically a MOSFET). During charging, the control unit selectively activates resistors on higher-voltage cells to dissipate excess energy, equalizing cell voltages across the pack. During charging, the control unit selectively activates resistors on higher-voltage cells to dissipate excess energy, equalizing cell voltages across the pack. Figure 2.5 illustrates a centralized controller managing the switching process to maintain balance.

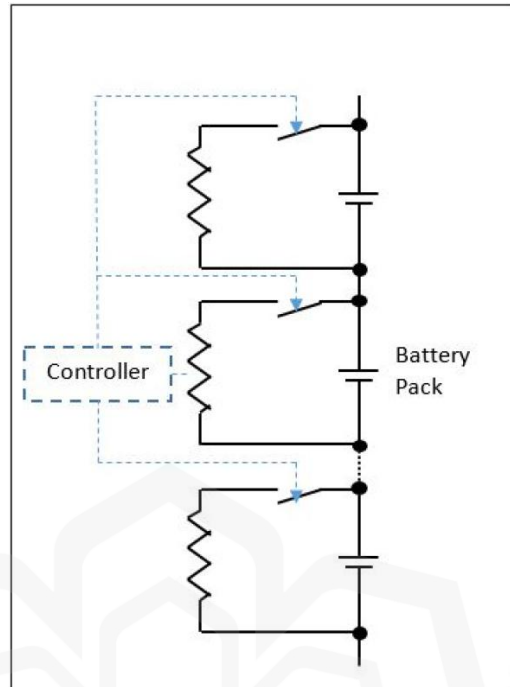


Figure 2.5 Switched Shunt Resistor Topology of Passive Cell balancing (Paudyal et al., 2019)

### ***B. Active Cell Balancing Method***

Active balancing employs dedicated electronic components for each cell, enabling precise control of current flow into and out of individual cells. Active balancing systems continuously monitor cell voltages during charge and discharge cycles, dynamically adjusting current distribution to maintain voltage equilibrium across the pack. This ensures uniform charge and discharge rates across all cells, improving battery efficiency and extending operational lifespan. While active balancing requires more complex circuitry and incurs higher costs, it achieves substantially greater energy efficiency than passive balancing. Various active balancing techniques are available, using capacitive, inductive or power converter methods, as shown in Table 2.1 and Table 2.2. Furthermore, Table 2.3 illustrates the summary and comparison between passive and active balancing techniques.

Table 2.1 Active Cell Balancing Topologies using Capacitor (Paudyal et al., 2019)

<b>Capacitive Based Active Cell Balancing</b>	Switched Capacitor
	Single Switched Capacitor
	Double Tiered Switched Capacitor

Table 2.2 Active Cell Balancing Topologies using Converters (Paudyal et al., 2019)

<b>Converter Based Active Cell Balancing</b>	Cük Converter
	Buck/Boost Converter
	Flyback Converter
	Ramp Converter
	Full-bridge Converter
	Quasi-resonant Converter

Table 2.3 Comparison Between Passive and Active Balancing Methods

<b>Comparison Metric</b>	<b>Passive Balancing</b>	<b>Active Balancing</b>
Fundamental Principle	Energy Dissipation	Energy Redistribution
Circuit Architecture	Simple	Complex
Energy Efficiency	Low	High
Thermal Management	High Thermal Stress	Low Thermal Stress
Balancing Speed	Slow	Fast
Implementation Cost	Low	High

#### 2.2.4 Protection

Protection functions safeguard batteries against excessive currents and extreme temperature fluctuations, extending battery life. These protections prevent damage from

faults including short circuits, overload conditions, overcharging, over-discharging, and thermal events. The BMS measures individual cell voltages and verifies that each cell operates within its safe voltage range, neither exceeding the maximum voltage limit nor falling below the minimum voltage threshold.

## 2.3 BATTERY MANAGEMENT SYSTEM STANDARD

The International Organization for Standardization (ISO) explains that a standard is a formal document that lists the requirements needed to help materials, products, processes and services fulfill their functions every time. They unite technical requirements, increase efficiency in industry and help improve society by bringing standards together. When this happens, it improves the way companies work and also helps lower the difficulties of trading internationally.

### 2.3.1 Overview of relevant BMS standards

Some of the standardization relating to battery systems, in general, can be seen with the International Electrotechnical Commission (IEC), and other international standards organizations can be seen in

Table 2.4.

Table 2.4 International Standards for Battery System

IEC 61508	This standard defines the design and safety requirements that must be considered while designing a programmable electric and electronic system for safe operation (International Electrotechnical Commission, 2010)
-----------	---

IEC 60068-2	This standard defines a set of functional and safety tests to study the influence of operating environmental conditions, like humidity, temperature, vibration, shock, etc., on the behavior of electronic equipment.
EN 62485	This standard defines a set of tests to validate the safe operation of battery systems, safety precautions, and facilities to be present in the installations of the battery system application.

### **2.3.2 BMS standards for its functionality, testing, and development**

A BMS must follow specific criteria to perform in optimal and safe conditions. Electrical management, safety management, and communication are the keys to improving a BMS's effectiveness and efficiency during its lifetime. As an example of a BMS from an electric vehicle (EV), subcomponents such as the Cell Monitoring Unit (CMU), Module Management Unit (MMU), and Pack Management Unit (PMU) correspond to each other. The CMU will monitor and balance each cell. At the same time, the MMU can manage a group of CMUs or a group of cells, and then the PMU can work with the MMUs simultaneously to enable communication with the external systems. These standards have been sought to ensure the end user's safe use of high-voltage batteries.

## **2.4 TYPES OF BATTERIES**

With the fossil fuel supplies decreasing, more industries are concerned about climate change and there is a greater focus on energy security, in which the industry must look for and use other energy sources. Most experts now agree that using energy-saving and renewable energy systems is necessary, not just an option. Using electric vehicles that are as strong as their internal combustion engine counterparts while reducing carbon emissions and generating and storing electricity for later use in stationary systems, are both important for the transition. Managing these variable sources of energy requires storing energy in

systems that are both efficient and reliable. Batteries and supercapacitors help keep energy on hand and distribute it when it is required. Lead-Acid, Nickel-Metal Hydride (Ni-MH) and Lithium-Ion (Li-Ion) batteries are shown in Figure 2.7 and each has a specific energy capacity suitable for different energy storage uses.

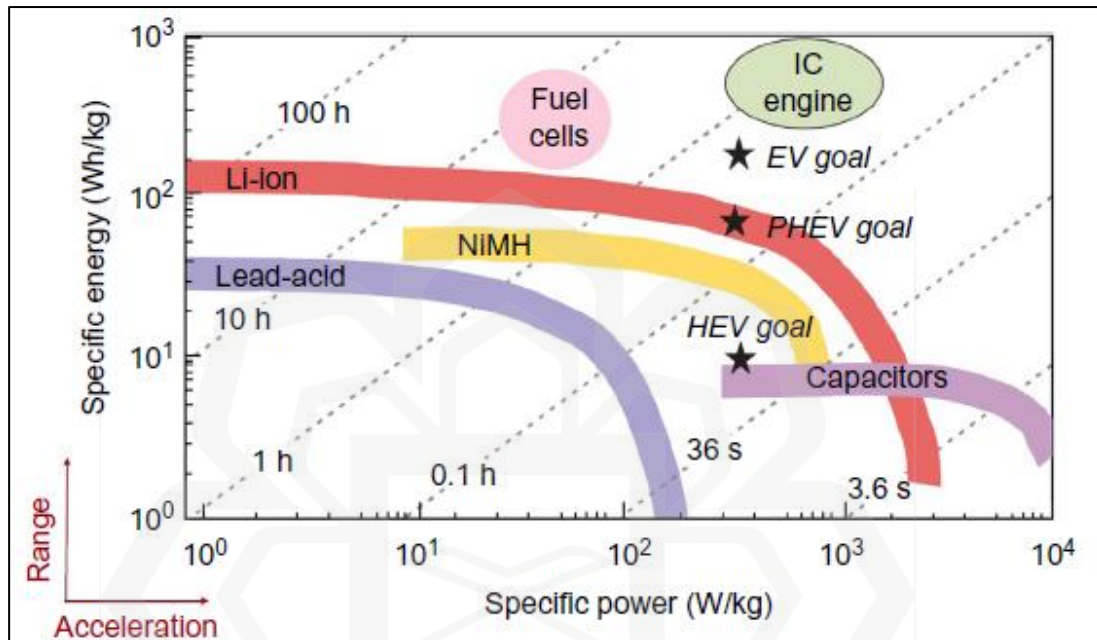


Figure 2.6 Ragone Plots for An Array of Energy Storage

Figure 2.7 and Figure 2.8 shows the plot of the energy density comparison in battery cells, and these plots help to analyze and understand each battery technology's capabilities in every field it can be used for.

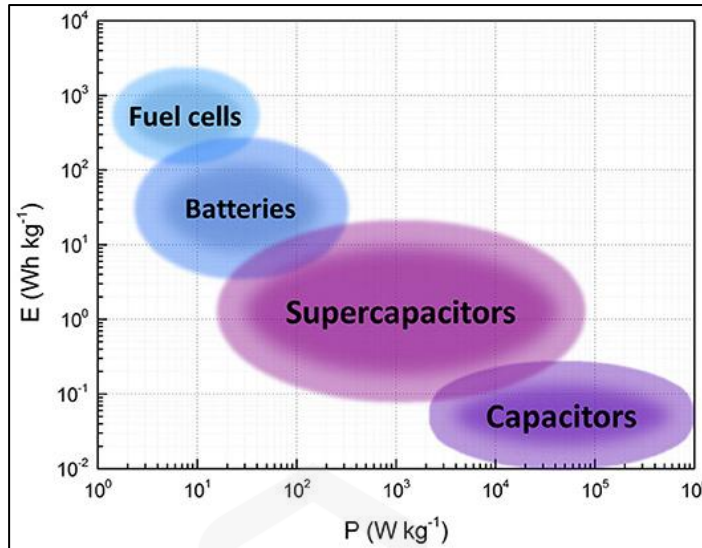


Figure 2.7 Ragone plot showing the typical values of energy and power of different energy storage devices (Castro-Gutiérrez et al., 2020)

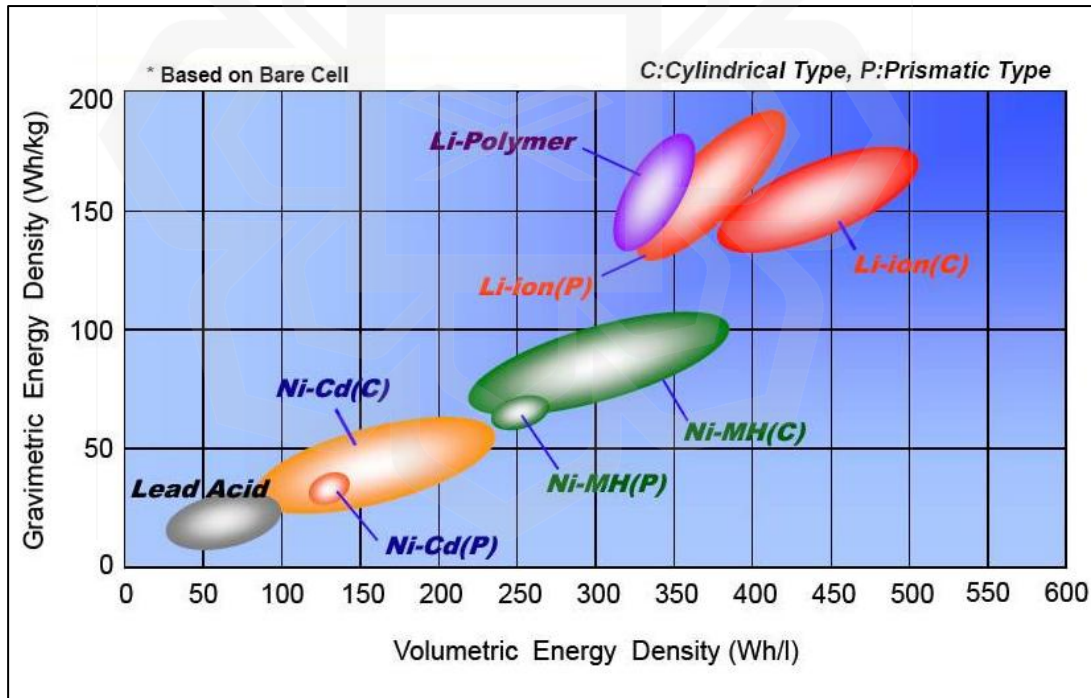


Figure 2.8 Comparison of Energy Density in Battery Cells (NASA)

Further in this section, three generally common batteries such as lead acid, lithium-ion, and supercapacitor, will be explained further in the following sections.

## 2.4.1 Lead Acid Battery

The earliest form of rechargeable battery is lead-acid batteries. Dr Plante, a French scientist, proposed it as a means of energy storage in 1860. Lead-acid batteries continue to dominate the marketplace, particularly for wheeled mobility and stationary applications. The lead-acid battery combines lead, lead dioxide, and an electrolyte composed of sulfuric acid and water. One of the most commonly found types of lead-acid batteries is the flooded type, which is known for its low cost and frequent use in the automotive and industrial sectors. Another type of lead-acid battery, the sealed or valve-regulated lead-acid (VRLA) variety, has also gained popularity in a range of applications, including power supplies and standalone power sources for remote locations. Lead-acid batteries have a shorter lifespan than lithium-ion and nickel-metal hydride batteries. Their power capacity decreases when they are discharged with high power levels, as illustrated in Figure 2.6, Figure 2.7, and Figure 2.8.

Lead-acid batteries have significantly lower specific energy compared to Li-ion batteries, with only a quarter of their energy density. As a result, these batteries are expected to be gradually replaced by Li-ion and Ni-MH batteries due to concerns about their environmental impact. Figure 2.9 depicts a cross-section of a lead acid battery, revealing its construction, which includes a grid, a positive and negative plate, and numerous other components that comprise a lead acid battery.

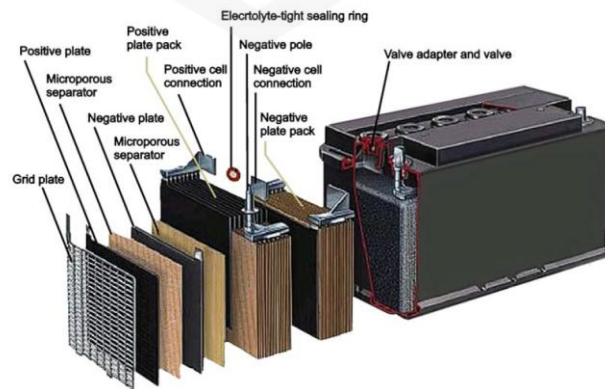


Figure 2.9 Cut-away cell lead acid battery showing details of construction (Garche, 2025)

## 2.4.2 Lithium-Ion

Lithium-ion batteries (LIBs), which power millions of mobile phones, laptops, and other compact devices worldwide, are a growing force in energy storage. Metal with the most significant electrochemical potential is lithium, which is also the lightest. Because of these characteristics, LIBs have been found to have a high energy and power density, which makes them less sensitive to memory effects than other types of batteries. In addition, LIBs are attracting significant interest such as viable energy storage technology because of their low self-discharge, practically zero-memory effect, high open-circuit voltage, and extended lifespan (Kim et al., 2019). As shown in

Figure 2.6, Figure 2.7, and Figure 2.8, these traits make LIBs the most appropriate candidates for achieving sustainability in the vehicle and electronics industries. Figure 2.10 shows an overview of a lithium-ion cell commonly used in today's industries, such as power storage devices and electric vehicles. The combination of transition metal oxide (cathode), in this case, lithium metal layered with graphite (anode), makes the battery.

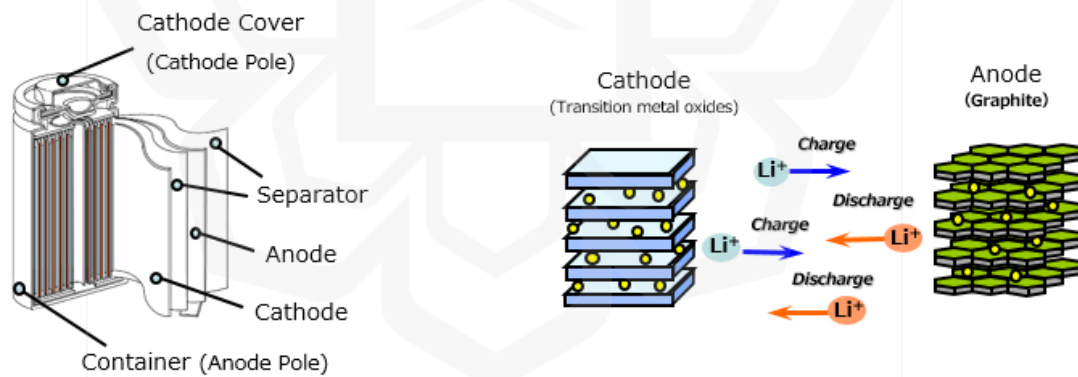


Figure 2.10 Overview of a Lithium-Ion Battery (Garche, 2025)

### 2.4.3 Supercapacitor

Supercapacitors (SC) have drawn significant interest because of their remarkable characteristics, such as high energy output, extended lifespan, and eco-friendliness. Unlike batteries, which store energy through chemical processes of electrode materials, capacitors store energy by the separation of charge. Despite this, supercapacitors have yet to reach the same level of popularity as rechargeable batteries. The life cycle of a storage battery is usually limited and varies with the battery type. In contrast, capacitor energy storage only requires a surplus and deficiency of electron charges on the capacitor plates during charging and discharging, respectively, without the need for any chemical reactions. This makes capacitors very efficient at storing energy, but their energy storage capacity is limited. This indicates that supercapacitors have superior acceleration but an inferior range, contrary to common batteries. Thus, it limits the practicality of using it in a mainstream environment. Figure 2.11 shows the primary mechanism of an electrostatic double-layer (EDL) SC made of two electrodes that act as the anode and cathode, separated by a separator and its electrolyte. The left illustration shows a discharged SC and, on the right, illustrates a charged SC full of separate charges.

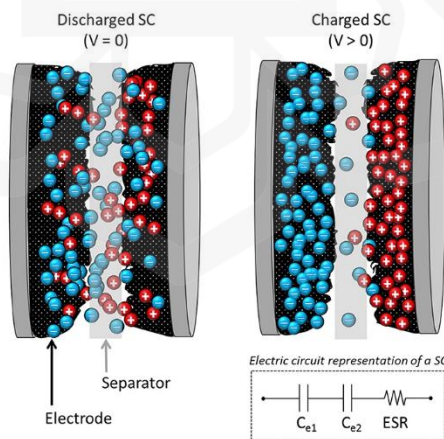


Figure 2.11 Mechanism of formation of the electrostatic double-layer (EDL) in a Supercapacitor (Castro-Gutiérrez et al., 2020)

## 2.5 BATTERY MANAGEMENT SYSTEM TOPOLOGIES

A BMS is a crucial component in any device or system that relies on a battery for power. It monitors, controls, and protects the battery to ensure its safe and efficient operation. In Figure 2.12 several different BMS topologies depend on the number of battery cells used, the output voltage, and the battery density. These factors are the main reasons topology needs to be used for the most efficient BMS and cost-effectiveness.

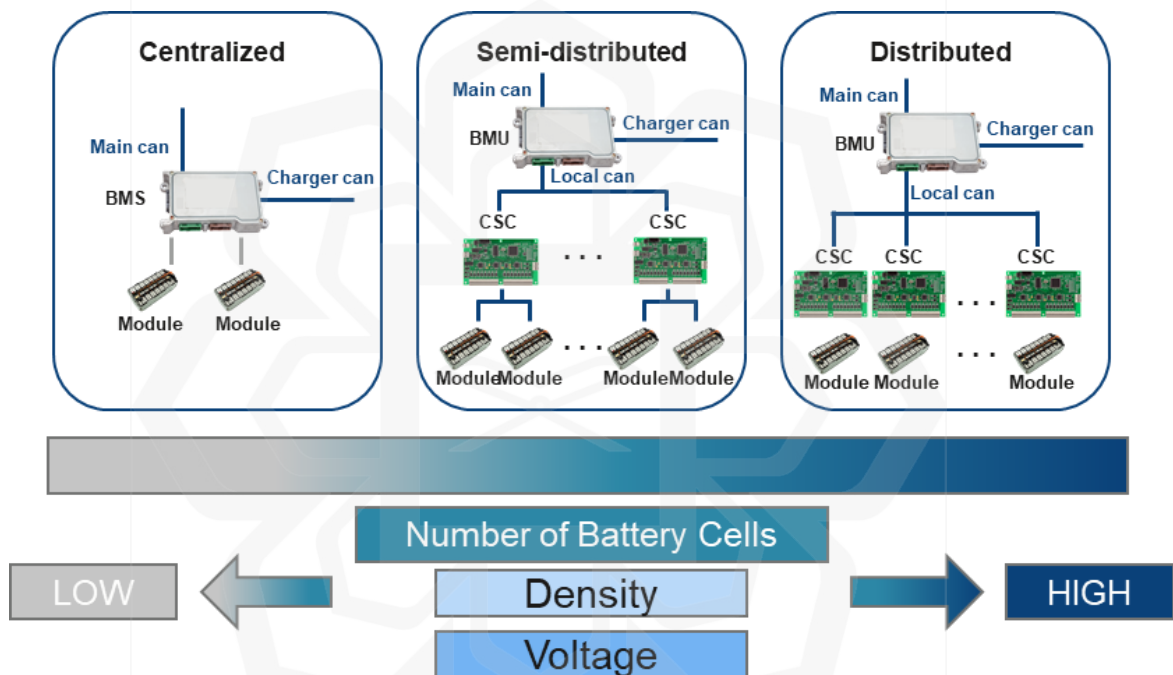


Figure 2.12 BMS Topologies (BMS and KEMET METCOM Inductors)

### 2.5.1 Centralized BMS

In a centralized topology, a single control unit oversees and manages all cells in the battery pack. This type of BMS is relatively simple and inexpensive. Still, it can be less reliable than other topologies because the failure of the central control unit can cause the entire battery pack to fail.

### **2.5.2 Distributed BMS**

Distributed topology, in which each cell in the battery pack has its own dedicated monitoring and control unit, such as the Battery Management Unit (BMU) and Cell Supervisory Circuit (CSC). This type of BMS is more complex and expensive, but it is also more robust and reliable because the failure of one cell will not affect the others, as seen in Figure 2.12.

### **2.5.3 Semi-Distributed BMS**

A Semi-Distributed topology includes aspects of both centralized and distributed systems. A central control unit, or BMU, monitors the battery pack's overall performance. Still, each cell also has a separate monitoring and control unit or CSC. This kind of BMS combines the simplicity and cost-effectiveness of a centralized system with the robustness and dependability of a distributed solution to deliver the best of both worlds.

## **2.6 CELL BALANCING APPROACH**

Balancing methods differ in their energy transfer mechanisms, enabling either unidirectional or bidirectional energy flow between cells. (Cao et al., 2021). While passive balancing faces the challenge of minimizing energy dissipation, active balancing confronts distinct issues including voltage sensing inaccuracies, slow response times, high voltage stress, and increased costs—factors that significantly influence method selection. Each balancing method requires tailored control algorithms to address method-specific challenges (Yildirim et al., 2019). These algorithms determine when and how balancing is triggered, maintaining pack equilibrium by monitoring control parameters that reflect cell-to-cell disparities (Turksoy et al., 2020b). Key measurable variables include terminal pack voltage, individual cell voltages, open-circuit voltage (OCV), state of charge (SOC), charge capacities, and multi-objective control factors. The choice of control variables critically

affects balancing accuracy, with algorithms adapting their strategies based on selected parameters (Cao et al., 2021; Turksoy et al., 2020b). The choice of control variables plays an important role in the accuracy of balancing methods, with different algorithms adapting their approach based on the selected parameters.

### **2.6.1 SOC Estimation Based Balancing Method**

SOC-based control mitigates the limitations of voltage-level cell balancing. This approach is more practical because SOC directly reflects energy state; when cells achieve SOC equilibrium, their voltages naturally align. SOC-based cell balancing adjusts charge distribution among cells according to their SOC levels. Continuous SOC measurement enables the balancing algorithm to detect SOC differences and activate energy transfer from high-SOC cells to low-SOC cells (in active balancing systems) or selective dissipation (in passive systems) (Dai et al., 2021). This maintains optimal balance during both charging and discharging cycles. SOC-based balancing simultaneously improves battery performance, extends lifespan, and mitigates safety hazards. However, accurate SOC estimation is computationally intensive and algorithmically complex. Figure 2.14 illustrates various approaches for achieving sufficiently accurate SOC estimation in cell balancing applications. Accurate SOC estimation is critical for determining both the timing and extent of balancing required to maintain cell uniformity. By precisely assessing battery SOC levels, these methods optimize balancing decisions and enhance overall battery performance.

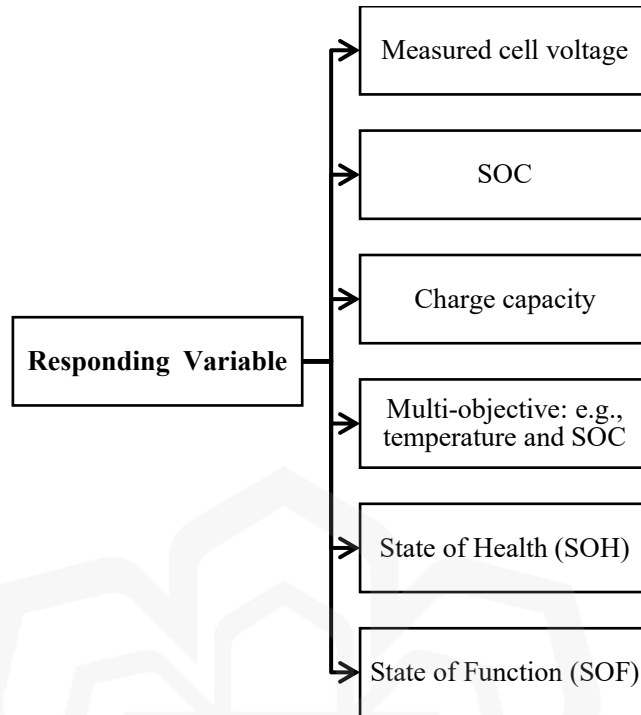


Figure 2.13 Battery Responding Variables

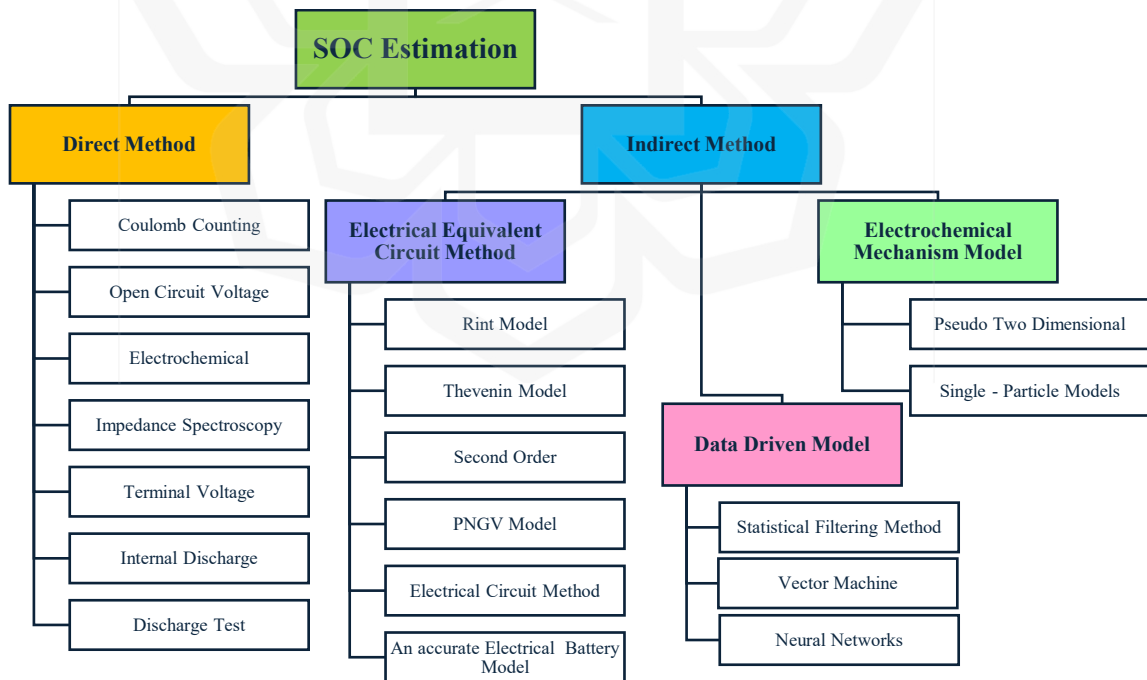


Figure 2.14 SOC Estimation Methods

BMS performance depends critically on selecting appropriate control variables. As illustrated in Figure 2.13, using OCV as a control variable eliminates state estimation errors and balancing inaccuracies associated with total charge capacity variations. However, OCV-based methods cannot effectively balance cells within the flat OCV region (typically 20-80% SOC for lithium-ion batteries) (Turksoy et al., 2020b). While direct voltage measurement eliminates SOC estimation errors, it introduces new errors from internal resistance variations and charge capacity disparities, while failing to balance cells in flat voltage regions. SOC-based control compensates for internal resistance variations, enables balancing within flat OCV regions, and accounts for temperature effects on cell characteristics (Lim et al., 2024). However, SOC-based methods remain susceptible to state estimation inaccuracies and errors from uncorrected charge capacity variations among cells. Using charge capacity as a control parameter offers similar advantages to SOC-based control, including internal resistance compensation, effectiveness in flat OCV regions, temperature sensitivity handling, and energy-based balancing. Nevertheless, this approach suffers from SOC estimation errors and measurement inaccuracies. Multi-objective approaches simultaneously evaluating multiple battery characteristics (SOC, temperature, voltage) enable comprehensive resistance compensation while addressing flat OCV curves and temperature dependencies. However, these methods remain vulnerable to cumulative errors from SOC measurement inaccuracies and charge capacity estimation uncertainties. The consideration of SOH can also address battery capacity variations due to aging yet presents operational challenges because direct SOH measurement by conventional sensors remains difficult during online assessment. Lastly, the State of Function (SOF) presents comprehensive battery output capacity data while dealing with unclear estimations which can reduce its effectiveness during practical applications.

### ***A. Direct Method of SOC Estimation***

The direct SOC estimation method works independently from battery models through the direct measurement of voltage, its internal resistance, current, impedance and several other measurable characteristics that align with the battery's SOC. A summary of the direct

approach in SOC estimation can be shown in Table 2.5. These available parameters in real world scenarios enable easy measurement processes in which this approach provides flexibility through its design because measurements can be taken at any time when the battery is connected to the certain measuring sensors (Sharma & Geda, 2021).

Accurate SOC estimation is essential for BMS to ensure optimal battery performance and longevity. Direct SOC estimation methods rely on measurable electrical properties including coulomb counting, open-circuit voltage (OCV) measurement, terminal voltage analysis, Electrochemical Impedance Spectroscopy (EIS), and internal resistance measurement. Coulomb counting (ampere-hour integration) estimates SOC by measuring total charge flow into and out of the battery. While initially accurate, this method accumulates errors over time due to sensor drift, temperature variations, and initial SOC measurement uncertainties. The OCV method requires a well-characterized voltage-SOC relationship and necessitates battery rest periods, rendering it unsuitable for real-time monitoring during active charge-discharge cycles. Terminal voltage methods estimate SOC by analyzing the relationship between battery terminal voltage and electromotive force (EMF). While functional across various discharge rates, accuracy degrades significantly during end-of-discharge periods when voltage exhibits highly nonlinear behavior. Electrochemical Impedance Spectroscopy (EIS) employs multi-frequency analysis to measure battery impedance and extract electrochemical parameters. While highly accurate, traditional EIS systems are bulky, expensive, and unsuitable for real-time embedded applications. Internal resistance methods exploit the relationship between internal resistance and SOC to achieve straightforward estimation. However, this technique exhibits limited accuracy due to sensitivity to temperature, aging effects, and initial resistance variations.

Table 2.5 Summary of Direct SOC Estimation Method

Method	Summary
Terminal Voltage	<p>When a battery is being discharged, its terminal voltage goes down as a result of internal resistance. As the SOC of a battery and its electromotive force (EMF) are closely linked and terminal voltage tends to match the EMF, a link between terminal voltage and SOC can often be seen. As a result, the terminal voltage can be used as a rough guide to SOC in various situations and under different temperatures. Even so, the accuracy of this method gets worse as the battery nears complete discharge, because the terminal voltage may drop rapidly and affect the accuracy of estimating the remaining charge.</p>
Open Circuit Voltage (OCV)	<p>Using the relationship between a battery's open-circuit voltage (OCV) and SOC, it is possible to estimate the battery's charge level. This relation can be established using either ways of curve fitting or tables that have been set up ahead of time. Even though it's simple to carry out, the accuracy of the method relies on the battery's OCV-SOC profile which can easily change with changes in temperature and the rate at which the battery is discharged. Also, for reliable results, the device needs extended pauses before and after charging or discharging, so monitoring and quick changes are not possible in real time.</p>
Internal resistance method	<p>Calculation of the battery's SOC using internal resistance, as long as having a reliable measurement of the resistance and the SOC trend is usually the same in which it is a simple method that often provides accurate outcomes. Even so, there are problems the necessary instruments are usually pricey and because the resistance only varies a little, it is very sensitive to temperature</p>

	and battery changes. They may reduce the effectiveness of the method in real-world, changing situations.
Electrochemical Impedance Spectroscopy (EIS)	Electrochemical Impedance Spectroscopy (EIS) is used to analyze the impedance of electrochemical systems, for example, batteries, at a wide range of frequencies. The process uncovers electrical and electrochemical features such as the kinetics of reactions and different components in the internal resistance. If performed without the battery connected, EIS gives accurate impedance results and may be used for online monitoring by applying galvanostatic or potentiostatic excitation during the battery's operation. Even though conventional EIS instruments are powerful for diagnosis, their size and cost make it hard to use them in electric vehicles until they are redesigned as onboard systems.
Coulomb Counting or Ah integration method	Coulomb counting measures the charge state of a battery by watching the current moving in and out and adding up the changes which tells on how much charge is left. Since this approach is simple, straightforward and uses little computing and hardware, it supports the development of various advanced SOC estimation strategies. Still, the system's performance is affected by how accurate the current measurements are and this can be reduced by sensor noise, fluctuations in temperature and other external disturbances. Additionally, it does not have a built-in way to correct its beginning errors which makes the model's accuracy very dependent on the initial SOC assumption and can drift with extended operation.

## ***B. Indirect Method of SOC Estimation***

The representation of complex battery physicochemical processes through mathematical equations makes up indirect battery modelling approaches (Mostafa et al., 2023). Such models effectively represent the essential battery phenomena of diffusion intercalation and electrochemical kinetics that explain charge movement, reaction events and SOC development throughout time. Battery modelling plays an essential role for determining battery performance along with optimizing energy control procedures and maintaining energy storage system reliability mainly in electric vehicle (EV) technology and microgrid deployment.

Table 2.6 Summary of Indirect Method of SOC Estimation

Method	Research Work	Contributions	Limitations
Electrochemical Mechanism-Based Model	Mathematical Modeling and Analysis of Electric Vehicle Battery (Bairwa & R, 2024)	The research adds value to SOC estimation through its fundamental Coulomb counting technique combined with thermal and electrochemical modeling which provides a simple yet organized method to predict EV battery SOC changes.	Real-time estimation techniques together with aging effects analysis and experimental validations remain essential for practical battery management systems but are absent from this approach.

	<p>A tracking problem for the state of charge in an electrochemical Li-ion battery model (Hernández et al., 2022)</p>	<p>The research provides a thorough framework which proves the implementation of SOC tracking for Li-ion batteries through a Single Particle Model by utilizing boundary ion concentration measurements.</p>	<p>The model utilizes ideal information about electrochemical parameters together with an ideal control application, yet these assumptions prevent this system from being able to use in real world applications.</p>
	<p>Reduced-order electrochemical model for lithium-ion battery with domain decomposition and polynomial approximation methods (C. Li et al., 2021)</p>	<p>The paper develops an electrochemical model with a reduced order of complexity (ROEM) that adds SOC to states which maintains high accuracy (below a 36.2mv terminal RMSE) while delivering more than 600 times increase in computational speed when compared to the complete P2D model.</p>	<p>The model lacks flexibility when used in real-world conditions because it assumes constant temperature along with constant parameters but does not account for temperature changes and battery aging.</p>

Electrical Equivalent Circuit Model	<p>Physics-Based Equivalent Circuit Model Motivated by the Doyle–Fuller–Newman Model (Bihn et al., 2024)</p>	<p>The equivalent circuit model derived from Doyle–Fuller–Newman framework enables detailed modeling through impedance parameters which maintain validity at wide temperature and SOC conditions resulting in simulation-based SOC voltage responses with &lt;10 mV RMSE.</p>	<p>The exclusion of hysteresis along with aging and current-dependent nonlinearities in the model reduces its accuracy during operating conditions with high C-rates</p>
	<p>Simplified Equivalent Circuit Model for Battery Energy Storage System Used for Grid Frequency Response (Sitompul et al., 2024)</p>	<p>The reduced battery model combining Thevenin’s theorem with a single voltage source and resistor allows current integration to estimate SOC with minimal annual error (0.011%) while cutting simulation time by 99%</p>	<p>The model deals with limited accuracy during short-term changes and neglects essential electrochemical processes resulting in reduced accuracy when measuring SOC under quick or non-linear power usage.</p>

	A Novel Technique for Battery Parameter Estimation Using Equivalent Circuit Models (Rahnama et al., 2024)	<i>First-</i> and second-order ECM parameter estimations through voltage response filtering which leads to highly accurate state of charge measurement exceeding 98.7% across all SOC levels.	The technique requires steady-state conditions for parameter identification while it does not measure SOC directly and depends on high-frequency signal injection
Data Driven Approach	Data-Driven Approaches for State-of-Charge Estimation in Battery Electric Vehicles Using Machine and Deep Learning Techniques (El-Sayed et al., 2024)	Data-driven approach to BEV SOC estimation through ten machine and deep learning models which uses simulated multi-drive cycle data from a high-fidelity BEV model that made accurate predictions by applying optimized model parameters from genetic algorithms.	The approach relies too much on simulated data with fixed battery chemistries, and it functions under constant ambient temperature thus its applicability toward real-world situations is restricted.

	<p>An Ensemble Learning Method for SOC Estimation of Lithium-Ion Batteries Using Machine Learning (Eyasu Tenawerk et al., 2024a)</p>	<p>The paper develops an ensemble learning framework which utilizes RF, Gradient Boosting along with LR to predict SOC based on NASA Battery Cycle data obtaining exceptional accuracy levels (<math>R^2 = 0.9999995</math> and MAPE = 0.0054 and 100% within <math>\pm 5\%</math> tolerance) beyond Coulomb counting and Kalman filter methods.</p>	<p>The current models exist as single-dataset systems which operate under restricted conditions while failing to validate their performance in real-time assessment.</p>
	<p>SOC Estimation of a Li-ion Battery using Deep Learning Method: A comparative Study of LSTM and GRU Architecture (Gole et al., 2023a)</p>	<p>The research implements LSTM and GRU deep learning networks to estimate SOC resulting that GRU delivers better results with 0.0155 RMSE and 0.01221 MAE at 25°C while being more efficient than LSTM.</p>	<p>Database limitations which restricts examination to consistent battery standards under controlled conditions while data verification during deployment testing was inadequate and resistance tests were excluded.</p>

*i. Electrochemical Mechanism-Based Model*

The electrochemical mechanism model represents a complex analytical system which generates mathematical equations to explain lithium-ion battery electrochemical power production and transmission. The thermodynamic and transport principles serve as base foundations for this model which brings better comprehension of the chemical activities inside battery cells. The model uses mathematical expressions to depict electrochemical internal activities which establish specific protocols for battery performance investigation (Bairwa & R, 2024). The electrochemical mechanism model focuses on three main internal processes which include solid-phase diffusion and both polarization effects and electrochemical reaction kinetics. The battery charge and discharge speed along with its operational efficiency depends on the movement of lithium ions through electrode materials known as solid-phase diffusion. The terminal voltage of the battery depends on polarization effects that develop because of resistive losses and reaction kinetics. The model's capability to simulate steady-state and transient battery operations becomes possible through its inclusion of these phenomena.

The model analyzes both physical characteristics of electrode materials and electrolyte features together with internal diffusion behavior. The model delivers complete information about battery internal processes together with its external electrical response. The model uses appropriate mathematical simplifications which transform complex multidimensional configurations into differential equations needed for solution while preserving its accuracy. The battery characteristics derived from the electrochemical mechanism model face high computational challenges during the resolution of intricate partial differential equations (PDEs) that describe charge transport and reaction kinetics. The complexity of the model prompts researchers to use simplified versions such as Pseudo-Two-Dimensional (P2D) model and Single-Particle (SP) model which allow practical simulations (Zhou et al., 2021). When delivering high-level modeling accuracy, the P2D model demands considerable computational resources to operate effectively (C. Li et al., 2021). The SP model reduces the P2D control equations to achieve faster simulation times although it delivers diminished accuracy in the results (Hernández et al., 2022;

Olugbade & Park, 2024). The electrochemical mechanism model functions as a fundamental assessment tool for lithium-ion battery operation analysis. The model describes complex electrochemical and transport phenomena which prove essential for battery research through optimization processes. The model requires specific trade-offs between performance and precision because of its high computational requirements.

## *ii. Electrical Equivalent Circuit Model*

Electrical Equivalent Circuit Models (ECMs) serve as standard tools for battery research to investigate electrical properties, SOC and energy capacity. The battery ECMs reveal essential information about battery electrical properties together with charging patterns and capacity performance (Q. Wang et al., 2022). A key function of BMS is to monitor the condition and state of the battery pack, particularly SOC and SOH (Kallimani et al., 2024). Since these parameters cannot be directly measured by sensors, model-dependent algorithms are often used for estimation. System performance and efficiency require accurate battery models to understand how batteries behave dynamically during operation (Thakkar et al., 2020). The use of accurate circuit designs and battery models allows designers to enhance both system runtime duration and circuit operational efficiency (Zhou et al., 2021). The implementation of models requires careful consideration of accuracy levels in addition to maintaining practical implementation standards.

Through some recent advancements in ECMs for lead-acid batteries incorporate resistance, capacitance, and SOC characteristics, allowing for highly accurate battery simulations during charging and discharging cycles, with cell-level mean bias errors below 90 mV (Koriker et al., 2024). Furthermore, lithium-ion battery electrochemical processes can be effectively modeled through ECMs which deliver root mean square errors (RMSE) below 10 mV during different operational conditions (Bihn et al., 2024). The Randles circuit stands out among simplified ECMs because it provides both high accuracy and efficient computation leading to a yearly SOC error measurement of 0.011% (Sitompul et al., 2024). The functionality of ECMs receives enhanced performance by modern parameter

estimation methods which deliver 99% accuracy without demanding time-consuming setup steps that reduce operational efficiency (Rahnama et al., 2024). The models serve as critical components for improving SOC performance and voltage reading precision because they enable robust operation of BMS systems in electric vehicles and renewable energy solutions (Y. Li et al., 2024).

### *iii. Data Driven Approach*

Data-driven approaches in machine learning have become a big matter in enhancing BMS for applications such as electric vehicles and renewable energy storage. These approaches primarily focus on estimating the SOC and SOH of batteries, which are important for optimizing performance such as the machine and deep learning techniques, such as linear regression, support vector regressors, random forests (RF), and neural networks (NN), have been employed to improve SOC estimation in battery electric vehicles, with the aim of mitigating battery aging and enhancing operational safety (El-Sayed et al., 2024b). In the context of BMS, such data-driven methods would enhance battery performance and longevity, particularly for small electronics consumer products up to electric vehicles (EVs). Gaining real-time analytics on key parameters such as SOC, temperature, and voltages of each cell enables machine learning to facilitate predictive maintenance and adaptive control by the BMS (Lakshmi et al., 2024). Researchers have successfully employed some ML driven techniques such as support vector regressors, artificial neural networks (ANN), and long short-term memory (LSTM) networks to improve SOC estimation and predict RUL with a high level of accuracy (El-Sayed et al., 2024a; Krishna et al., 2024). Furthermore, the integration of Internet of Things (IoT) technologies and advanced connectivity (e.g., 5G) enables real-time data collection and anomaly detection, driving battery systems toward higher efficiency and safety of consumers (Krishna et al., 2024; Paraschiv et al., 2024). Overall, these methodologies not only extend battery life and reduce costs but also contribute to broader sustainable energy solutions in diverse applications (Lakshmi et al., 2024; Paraschiv et al., 2024).

Optimizing SOC and SOH estimation for lithium-ion batteries has increasingly leveraged machine learning and deep learning techniques in which some research suggests that ensemble methods combining RF, gradient boosting, and linear regression significantly improve SOC prediction accuracy compared to traditional approaches like coulomb counting (Eyasu Tenawerk et al., 2024a). Some studies employing deep learning architectures like LSTM and Gated Recurrent Units (GRU) have shown much more performance in attaining low root mean squared errors (RMSE) under diverse operating conditions that they have tested (Rehman, 2024). Furthermore, hyperparameter optimization techniques such as the Tree Parzen Estimator, have refined deep learning models to deliver highly efficient SOC estimations with minimal computational costs (How et al., 2022a). These innovations are encouraging more precise and reliable BMS which are essential for applications in electric vehicles and renewable energy storage (Gole et al., 2023a; How et al., 2022b).

In a study on SOH prediction, gated recurrent neural networks (GRNN) have been utilized to predict the future health of lithium-ion batteries, focusing on the importance of data availability and accuracy in forecasting battery lifespan (Eyasu Tenawerk et al., 2024a). Additionally, some machine learning frameworks incorporating real battery cycle data have been developed to enhance battery health in which they focus on optimizing battery management techniques to extend lifespan and improve battery reliability (Pujari et al., 2024). Researchers focus intensely on predicting lithium-ion battery SOH through neural networks because this technology stands essential for battery optimization and safety applications in electric vehicles and energy storage systems. Development of multiple advanced techniques exists to enhance SOH estimation. The usage of DeepAR forecasting models from (Liang & Cheng, 2024) with residual connections and adaptive dropout reaches extraordinary accuracy levels through maximum RMSE values under 0.01%. The combination of artificial neural networks (ANNs) which receive training from real and synthetic data provides reliable SOH estimates under various operational conditions according to research findings found in (Cabrera García et al., 2024). LSTM networks in deep learning have enhanced prediction accuracy through their application which resulted in maximum errors reaching 2.8% (Shakir et al., 2024). Adding to that, the combination of

variational mode decomposition with temporal convolutional networks (TCN) helps achieve better accuracy levels when handling non-stationary data according to research conducted in (Fu et al., 2024). Advanced techniques like convolutional neural networks (CNNs), especially when optimized with particle swarm optimization (PSO), have shown significant improvements in battery health assessment, outperforming traditional methods like logistic regression in both accuracy and error reduction in which one of the studies using CNNs have proven to be highly effective for SOH estimation, demonstrating greater precision and stability compared to other algorithms such as AdaBoost and Gaussian Processes (Alwabli, 2024; Balaji et al., 2024).

Despite the promising results demonstrated by data-driven ML approaches, several critical limitations warrant careful consideration before widespread adoption in real-world BMS applications. A primary challenge is the dependency of ML models on the quality and diversity of training datasets; models trained on specific battery chemistries, ambient temperature ranges, or driving cycles often exhibit significant accuracy degradation when applied to different operational conditions or cell types not represented in the training data (El-Sayed et al., 2024c; Gole et al., 2023b). Additionally, most current ML-based SOC estimation studies suffer from limited real-time validation and domain generalization capabilities, with many implementations restricted to laboratory environments with controlled temperature profiles and standardized charge/discharge patterns (Eyasu Tenawerk et al., 2024b; How et al., 2022c). Furthermore, the absence of explainability in deep learning models (such as LSTM and GRU networks) presents a significant challenge for safety-critical BMS applications, as these black-box approaches cannot provide transparent reasoning for their SOC predictions under fault conditions or extreme operational scenarios. Consequently, practical BMS implementation requires hybrid approaches that combine data-driven insights with physics-based constraints and extensive real-world validation across diverse operational contexts.

## 2.6.2 Voltage Dependent Balancing Method

A series-connected battery pack shows voltage imbalance between individual cells throughout operation because different characteristics such as capacity, self-discharge rates, capacitance and internal impedance may produce variations (Zilberman et al., 2020). The cell balancing mechanism operates through the voltage dependent method by activating upon detecting substantial voltage differences between individual cells and the average pack voltage. The initiation of this process starts through voltage comparisons against pre-defined thresholds between individual cells. The implementation of this method remains easy because it depends on straightforward voltage measurements that BMSs provide directly. Resistive (passive) balancing methods are commonly used to discharge cells with high voltage values to match them with cells of lower voltage. However, the assessment of a battery's true characteristics cannot be achieved by measuring voltage alone (Lu et al., 2020). Temperature variations and cell resistance may affect the measurement of voltage which can produce inaccurate balancing results. Li-ion batteries demonstrate its most effective balancing operation when conditions of low and high SOC, where the OCV exhibits steep gradients between its relationship with SOC levels. The exact nature of voltage-based balancing becomes more precise due to substantial voltage changes that occur from slight SOC variations. The terminal voltage remains inconsistent even though SOC levels remain equal because the cells exhibit varying internal resistances in which even the cells maintain similar voltage levels during testing, yet their usable energy capacity might differ (Turksoy et al., 2020b).

A BMS contains power electronics together with electronic circuits and integrated chips as well as additional hardware requirements. Systems that employ microcontrollers in their development encounter hardware restrictions and maximum allowable current levels in which the implementation of separate controllers for each battery pack makes these difficulties more complex to deal with. A study in (Yağcı & Orbeyi, 2024) demonstrates how a Programmable Logic Controller (PLC) implements Switched Resistor Passive Balancing (SRPB) as a method to overcome the restrictions of conventional microcontroller-based BMSs. The research developed an algorithm which applied two

separate balancing methods at once to deliver protection and control throughout the cell balancing process. It is essential to resolve all technical problems with passive cell equalization methods because they cause slow balancing and waste of energy. The authors from (Erdoğan et al., 2021) produced a control algorithm that allows large-scale batteries in commercial electric vehicles to reach balance swiftly and with little energy loss. This method makes it possible for multiple charges to switch and for 176 individual cells and their groups to be managed separately. All of the sub-modules contain a switch matrix and a DC-DC converter which helps provide balanced energy to the whole battery pack. The system connects to a bus that have the additional sub-modules. Voltage measurement of individual cells initiates the process that identifies the most and least voltage cells in each sub-module by calculating the minimum, maximum and average voltages. Then the algorithm first arranges cells with minimum voltages according to ascending order and simultaneously arranges the cells with maximum voltages according to descending order. The algorithm matches the arranged cells according to its specifications in which the algorithm evaluates the voltage differences between neighboring cells during its assessment. The algorithm will stop after finding deviations that measure less than or equal to 1 mV. However, the algorithm will use the average voltage measurement when the cell-to-cell voltage difference exceeds 1 mV.

The authors in (X. Yang et al., 2020) proposed a new way to equalize voltage by putting together a boost full-bridge input stage with a Symmetrical Voltage Multiplier (Sy-VM). Because of this design, battery cells with different initial voltages can be balanced, as the target voltage for each cell is the same. The system runs with a bipolar square wave signal from the inverter which has adjustable amplitude and is used by the voltage multiplier to generate the same output voltage several times. The equalizer is built to be simple and small, not using all the switches and inductors that large, traditional circuits might require. Selecting the best settings for the system is possible using an analytical framework which boosts how well it works. The equalizer operates on its own to ensure all cells charge evenly and with few losses. Experiments prove that the method can control cell voltage deviations so that they are only a few millivolts apart.

### 2.6.3 SOC – Voltage Balancing Method

The SOC – voltage based cell balancing method stands as the most common choice because it detects SOC differences between cells by tracking terminal voltages along with monitoring battery SOC. The method detects specific cells that require balancing by monitoring terminal voltages and aggregated SOC of the battery pack to determine individual variations (T. Wu et al., 2019). The fundamental principle of this technique utilizes ampere-hour counting for accurate balancing interval determination without independent SOC measurement of individual cells. The system requires active prevention of imbalances to assist efficient battery pack balancing through voltage difference monitoring. Researchers are enhancing battery balancing techniques to solve the energy imbalance problems in battery systems in which some traditional passive balancing technique that employs resistors shows lower performance because it wastes battery energy instead of transferring it between cells (J. Wang et al., 2024). However, a buck-boost converter alongside other active balancing system transfers power between cells depending on their SOC to achieve optimal operational efficiency (Nam et al., 2023). The technique provides valuable benefits for electric vehicle BMS. Modern BMS systems possess the capability to modify their output voltage automatically for achieving balanced SOC conditions between all battery modules (Xiong et al., 2025). The practice of zero-sequence voltage injection techniques demonstrates success in managing SOC balance for high-voltage cascaded systems (H. Li, Li, et al., 2024). Real-time SOC estimation methods together with advanced control algorithms need integration into battery storage systems to improve both reliability and performance (Nam et al., 2023; R. Yang & Yang, 2024).

Recent research has focused on data-driven algorithms that learn voltage-SOC relationships from operational data. Studies reveal limitations in applying these methods to single-cell-to-single-cell, battery-pack-to-single-cell, and adjacent-cell-group equalization topologies, often requiring extended balancing times and offering limited routing flexibility. Conventional approaches usually have to balance for a long time and provide fewer routing options. As a result, the authors in (H. Wu et al., 2024) came up with a modular design that includes buck-boost converters which makes it possible to use multi-

cell-to-any-cell, any-cell-to-any-cell and multi-cell-to-multi-cell balancing modes. The control system changes dynamically by linking how far the voltage differs from the setpoint to its switching actions. Even though battery cells are made in the same way, their characteristics can differ over time because of differences in self-discharge and state of charge which usually forming normal patterns. Noticing and using these patterns helps in making better balancing decisions. Large differences in SOC among cells can seriously harm both the function and security of lithium-ion batteries.

The authors in (Xia et al., 2024) developed double layer single structured balancing algorithm as a fast and flexible technique to address this problem. The study focuses on the improved version of a proposed topology which unites single-layered and double-layered buck boost balancing topologies. The topology incorporates model predictive control (MPC) equalization strategy which improves speed and reduces losses during equalization process (Schwenzer et al., 2021). The proposed system design operates through three distinct phases in which the first section of the process determines predicted sequence patterns for system operation. The proposed model uses a double-layer single-ring topology as its central design. At the modeling stage, all system constraints are clearly set and then an objective function is designed that fits the desired output sequence. The result of solving this function is a control sequence and the initial control input is given directly to the system. The improved configuration results in a 38.15% faster balancing time and a 27.25% better energy transfer when compared to a single-layer buck-boost converter-based equalizer (BBE) that uses the mean difference approach. The system's operation is validated by the authors for continuous charging and discharging with the same current.

The slow process of cell balancing along with inefficient performance in which serial multi-cell connected batteries are known. A paper in (Devi B & N, 2021) introduced an automatic switching capacitor-based system for balancing 16 cells connected in series to solve this problem. The authors designed a modular balancing architecture through MATLAB/Simulink for 4, 8 and 16 cell configurations because balancing speed remains mostly independent of initial cell voltages and their differences of the series string cell count. The proposed circuit topology connects each cell to two MOSFET switches along

with one capacitor that links to adjacent cells and with two additional capacitors that allow the system to direct energy transfers between cells. More capacitors are connected during the switching phase of charge and discharge cycle operations. This modularized method applies four cells per module which requires different switching capacitors to maintain voltage stability. An hour is all it takes to balance Li-ion batteries with 3.7V nominal voltage and 1200mAh rated capacity regardless of the cells starting conditions.

## 2.7 SUMMARY

This chapter presented a review of battery management systems with the focus on to passive battery balancing methods and machine learning-based state of charge estimation. Basic BMS functions monitoring, protection and balancing in which comparing passive and active methods of cell-balancing and their trade-offs were analyzed. Active balancing is more energy efficient, but passive balancing is the most cost effective as it is simple and cost effective and can be used in cost sensitive applications. The review analyzed the characteristics of lithium-ion batteries, BMS topologies, and different SOC estimation approaches and found that estimation accuracy is a key factor in balancing performance. Conventional voltage-dependent techniques are not suitable with lithium-ion batteries, where flat OCV curves with 20-80% SOC grids give  $\pm 4-5\%$  errors in the estimation of voltage changes by published literature. Recent machine learning methods, especially LSTM networks, show better accuracy (about 0.025 RMSE was reported in literature) by learning the time series patterns in the cell voltage, current and temperature data. Nevertheless, a critical gap in the literature is that there is no research that critically assesses whether passive balancing systems can be enhanced by adding ML-based SOC estimation to gain performance advantages close to those of an active-balancing system and still benefit its cost performance as passive-balancing. Despite the fact that passive balancing optimization and ML-based SOC estimation have been studied in depth, their integration has never been explored. Literature lacks in considering whether intelligent algorithmic optimization can offset passive balancing, which is simple to implement in hardware, and can potentially allow significant increases in switching frequency, power dissipation, and

thermal management. This identified gap acts as motivation behind the current research which is aimed at developing a better passive balancing approach using ML-based SOC estimation using LSTM instead of the conventional voltage-based methods. The goal is to examine whether this integration can span the efficiency gap between passive and active balancing systems that are expensive and low-cost. In the next chapter, the approach to filling this research gap by means of thorough simulation and experimental analysis is introduced.



## CHAPTER THREE

### METHODOLOGY

#### 3.1 OVERVIEW

This chapter gives the methodology used to assess passive balancing strategies combined with machine learning-based SOC estimation within a battery management system (BMS). The methodology consists of three main steps: the development of MATLAB/Simulink simulation, the hardware prototype validation, and the integration of the machine learning model. The evaluation uses dual validation which is the combination of the MATLAB/Simulink simulation for controlled algorithm testing and the hardware prototype experimentation for the performance check under real world conditions. MATLAB simulation with table-based battery models to reproduce the behavior of lithium-ion cells, and the hardware prototype with conventional OCV-based balancing for baseline comparison with the results from ML-enhanced simulation. Hardware testing captures all parameters of design, component specifications and circuit schematics and allows a strict comparison between predicted results through simulation and experimental results to determine the accuracy of a model.

From the thorough and comprehensive literature review, the decided approach is comparing both open circuit voltage (OCV) SOC estimation to the data driven machine learning (ML) based SOC estimation. Moreover, this study investigates the involvement of techniques to enhance SOC estimation in which it directly influences balancing efficiency in which based on previous study the utilization of ML-based SOC estimation resulting in better accuracy than the other methods. The data set originates from public experimental results with a thorough training and validation process before it is being used for the simulation. A quantitative evaluation of ML-based SOC estimation methods against conventional OCV based approaches takes place during the battery cell balancing process by the BMS. Comparison between these well-known conventional methods have not been

studied based on previous research conducted. The research also follows the foundational techniques that enhance battery balancing effectiveness in modern BMS systems.

### **3.2 RESEARCH METHODOLOGY**

The flowchart diagram shown in Figure 3.1 can be used as an overall guide to help plan and organize the research and development process for this research that utilizes a passive control BMS utilizing ML for SOC estimation. The research methodology follows the color-coded flowchart presented in Figure 3.1 and divides into three main stages. Both processes which appear at the beginning of the flowchart serve as preparatory steps alongside defining project scope and identifying key challenges. These guiding steps shape the research direction but do not fall within the formal three stages of the study.

The first stage of research involves developing and optimizing BMS simulation based on MATLAB. The use of MATLAB's table-based battery model to simulate lithium-ion cell properties which include voltage behavior capacity and internal resistance. A passive balancing algorithm implementation was used in the simulation environment following the objectives of the research. The control logic defines how the algorithm manages cell voltages by dissipating excess charge from higher-voltage cells through dissipation using OCV or similar voltage thresholds as its basis. Simulation output serves as a verification tool to demonstrate if the chosen balancing method satisfies initial design criteria especially concerning balancing efficiency together with current limits and speed of balancing process.

Following successful simulation validation, the system is implemented as a physical hardware prototype comprising voltage sensing circuits (ADS1115 ADCs), MOSFET switching networks, balancing resistors (10 $\Omega$ , 5W), and protection circuits guarding against overvoltage and overcurrent conditions. The prototype undergoes controlled charging and discharging experiments to collect real-world voltage, current, and temperature data.

Performance validation compares experimental measurements against simulation predictions to verify model accuracy and assess protection functionality.

The final stage integrates an LSTM-based machine learning model to improve SOC estimation accuracy beyond conventional OCV methods. The ML model is trained on synthetic battery operational data generated through MATLAB/Simulink simulation, capturing voltage, current, and temperature patterns across diverse operating conditions (-10°C to 25°C ambient temperatures). The trained model replaces voltage-based SOC estimation in the simulation framework, enabling performance comparison between OCV-based and ML-based passive balancing approaches across key metrics: balancing time, switching frequency, power dissipation, and thermal behavior. The evaluation of ML-based predictions was evaluated on the relevant performance metrics. The trained ML-based SOC estimation will be implemented into the simulation platform from Stage 1 to test how improved SOC predictions affect balancing performance and voltage and SOC deviation compared to OCV-based methods. The final methodology validates the system through simulation, then prototype testing and advanced SOC estimation to ensure both technical correctness and operational adaptability of the BMS design.

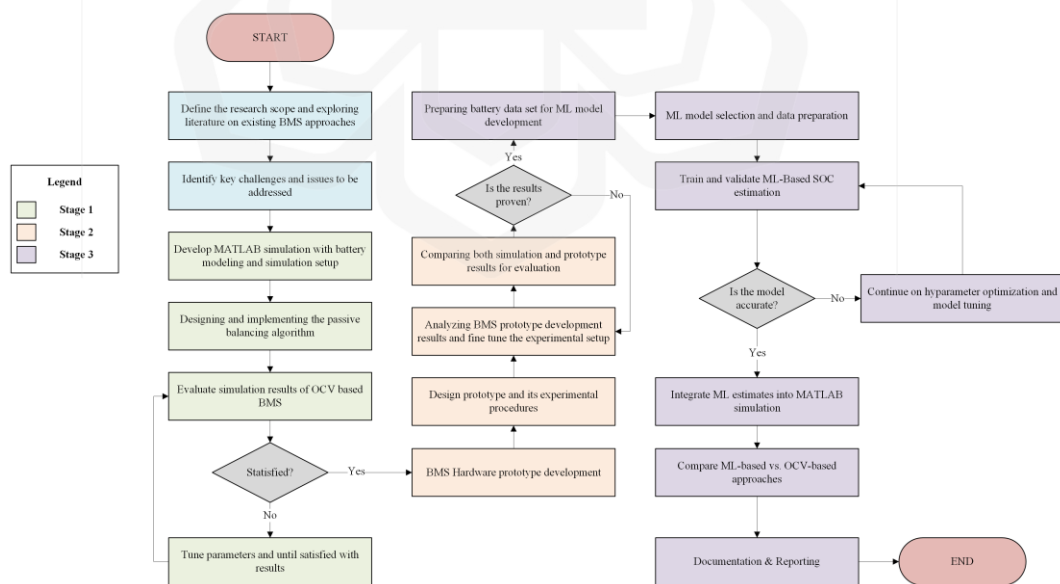


Figure 3.1 Overall Research Methodology Flowchart

### 3.3 SIMULATION OF PASSIVE BALANCING METHOD USING MATLAB

#### 3.3.1 Battery Cell Modeling

In this study, the MATLAB Battery (Table-Based) model from the Simscape Battery package is used to model the passive balancing of battery cells. The model has been set up to represent a Panasonic 18650 lithium-ion cell, with a nominal capacity of 2900 mAh and a nominal voltage of 3.7 V. Table 3.1 presents the specific parameters of the table-based model which include both theoretical features and practical results. More information and reasons for choosing these parameters are explained in the following sections.

The battery (Table-Based) block from Simscape Battery implements a high-fidelity data-driven model which represents how open-circuit voltage (OCV) behaves as a function of charge level (SOC) and optional temperature through lookup tables. Experimental or manufacturer data input enables the block to produce precise non-linear battery simulations across various operating ranges in which the block can be depicted in Figure 3.2. Scientists have multiple modeling choices for the block which enables them to include capacity fade and internal resistance changes and temperature effects while tailoring the block to match particular cell characteristics or application needs.



Figure 3.2 MATLAB Simscape Battery (Table-Based) block used for lithium-ion cell modeling. Adapted from MathWorks, 2024.

Table 3.1 Battery Parameters Used in MATLAB Simulation

<b>Manufacturer</b>	Panasonic
<b>Part Number</b>	UR18650ZTA
<b>Battery Type</b>	Lithium-ion
<b>Capacity (mA *hr)</b>	2900
<b>Nominal Voltage (V)</b>	3.70
<b>Weight (g)</b>	49.0
<b>Geometry</b>	Cylindrical
<b>Diameter (mm)</b>	18.24
<b>Height (mm)</b>	65.10

### 3.3.2 Proposed Design BMS Simulation Setup

MATLAB Simulink have been chosen for the simulation environment because of its vast functionality in modeling battery dynamics and also provide smooth integration with many available parameterizations from common battery manufacturers. This streamline the simulation work in just using necessary addon packages within MATLAB Simulink itself. As stated before, Simulink Simscape Battery was used in this study. The proposed design using 3S1P battery configurations for the BMS in which it will give a good insight into each of the batteries' performance without compromising performance.

Figure 3.3 below shows the configuration and Simulink design that were used in each of the battery simulations. It is simple and also its resemblance to a lot of conventional BMS that are in the market right now. The Simulink model consist of batteries, bleed resistors, and MOSFET to control the flow of current during balancing that were controlled by the balancing algorithm function block. All the other necessary components such as diode, temperature/heat transfer mechanism were also implemented. A battery CC – CV block were used in this simulation to enable charging and discharging process in one

continues simulation. OCV of the battery was tested first as stated in the flowchart in Figure 3.1 and later then evaluated with a hardware prototype finishing with a simulation utilizing ML-based SOC estimation for comparison in this study.

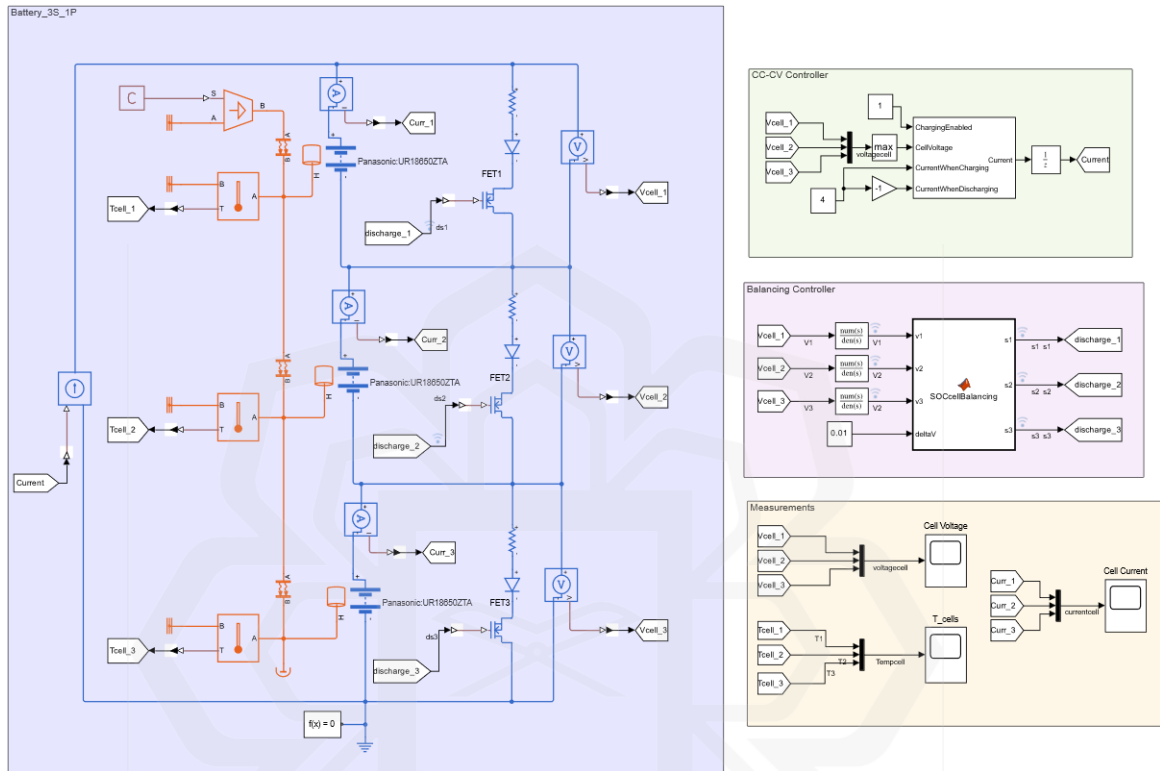


Figure 3.3 BMS Simulation Design in MATLAB Simulink

### 3.3.3 The Balancing Algorithm

The OCV based balancing algorithm works in the form of a continuous control mechanism monitoring the cell voltages and operates balancing resistor if the voltage imbalances are above a predefined threshold. The algorithm employs a simple logic sequence that is repeated for each simulation time step and makes balancing decisions in real time based on measured terminal voltages on three series connected cells. This section explains the complete working of the algorithm beginning from initialization till decision making and implementation of the balancing actions.

In the beginning of each control cycle, the algorithm is setting all switching signals (s1, s2 and s3) to zero, which means that all the switching transistors (MOSFET) controlling the balancing resistors are in the OFF position. This initialization step is critical as it prevents any unintended discharge of the cells as well as having a known baseline state before the algorithm evaluates the current cell conditions. After initialization the terminal voltage of each cell in the battery pack is read by the algorithm, which is V1, V2, and V3. From these three measurements, the algorithm calculates the cell that has the highest voltage ( $V_{\max}$ ) and the cell with the lowest voltage ( $V_{\min}$ ). These identifications are critical because they define which cells need balancing intervention and which cell need to be protected from further discharge.

Once the highest and lowest voltages are identified, the algorithm calculates the absolute voltage difference between them:  $\Delta V = V_{\max} - V_{\min}$ . This calculated difference represents the magnitude of the current imbalance within the pack. The algorithm then compares this voltage difference against a predefined threshold value of 0.1 V. This threshold was selected as a practical compromise that is large enough to ignore measurement noise and sensor resolution limitations (typically  $\pm 10$ -20 mV), yet small enough to maintain effective cell equalization and prevent operating the cells outside acceptable voltage bounds. The comparison result determines whether the pack requires balancing or whether the current imbalance is within acceptable limits.

If the voltage difference is greater than 0.1 V ( $\Delta V > 0.1$  V) the algorithm will conclude that the pack is unbalanced enough to take corrective action. In this case the algorithm finds out which cell is having the minimum voltage and purposely keeps its switch in the OFF state, thus saving this cell from being discharged through the balancing resistor. Simultaneously, the algorithm works to turn on (i.e. set to 1) the switches of all those cells that have a higher voltage, in order for their balancing resistors to carry a current through them, so as to dissipate the excess charge, in the form of heat. This targeted approach means that only energy is pulled from those cells that are already charged so that

the cells are brought down towards the voltage level of the weakest cell, thus reducing the imbalance across the pack as a whole. The balancing process is repeated in subsequent control cycles as long as the voltage difference is greater than the 0.1 V threshold.

The algorithm repeats this entire sequence of decisions and control over regular time intervals during the course of the simulation (in particular, every time step - in this case, every one second). This cyclic operation enables the algorithm to continuously adapt to the changing pack conditions as the battery charges or discharges or as it has variations in cell characteristics due to manufacturing tolerances or operational factors. The process by which the volts are constantly evaluated and reacted to allows any imbalances that may arise to be detected and corrected quickly, as cell voltages can become very consistent, without any of the individual cells becoming overly charged or discharged. The protection of lowest voltage cell is especially important since actively balancing a cell that is already the most depleted would make the pack imbalance worse, not better, therefore the algorithm intelligently protects this cell while draining the higher voltage cells to achieve equilibrium of the pack.

Although the OCV-based algorithm is simple and reliable, with little computational overhead that is suitable for implementation on embedded microcontrollers, it has one inherent limitation, which is that it makes balancing decisions based on terminal voltage, rather than the true state of charge. In the case of lithium-ion batteries the relationship between voltage and SoC is nonlinear, with flat voltage curves being particularly flat between 20-80% SoC, i.e. large changes in actual state of charge can correspond to small changes in voltage. This voltage-based limitation can cause either delay in the balancing initiation or unnecessary switching in areas where the voltage precision is naturally poor. To overcome this drawback the research combines the decision variable of SOC estimation, based on machine learning in which the estimated state of charge replaces the voltage measurements resulting in more efficient and responsive balancing control based on the actual energy state of the cells rather than the proxy voltage measurements. The overall operational sequence of actions for the algorithm is illustrated in Figure 3.4 which is a visual

display of the control flow from initialization, through decision logic to balancing execution of the actions.

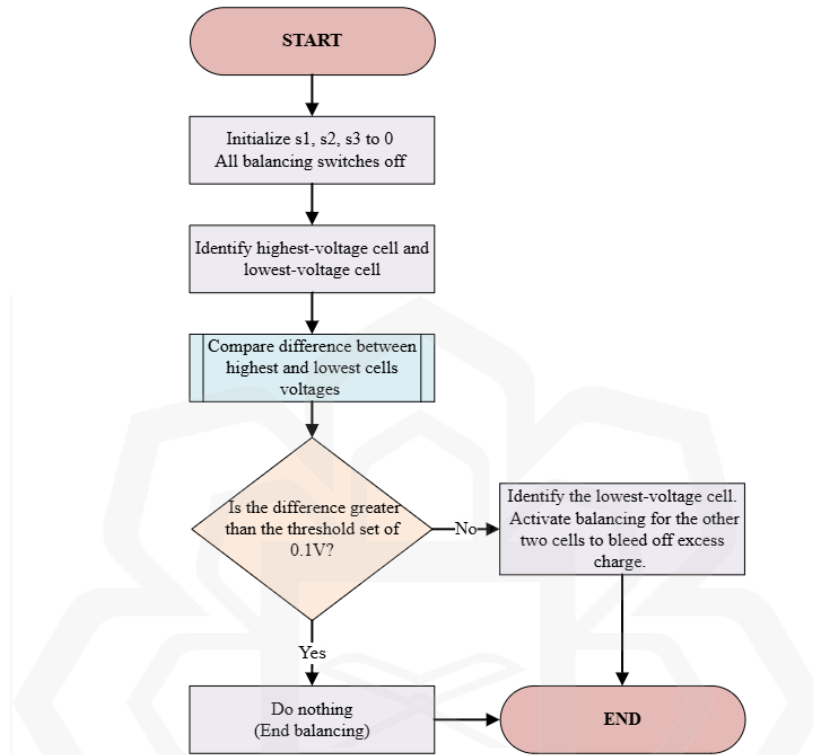


Figure 3.4 Balancing Algorithm for OCV Simulation

### 3.3.4 Evaluation Metrics

The performance evaluation of the passive balancing scheme depends on analyzing multiple essential metrics. First, the voltage and current profiles of individual cells are monitored to verify the convergence of the balancing algorithm and to ensure that current fluctuations remain within safe operational limits. Verification operational safety by monitoring cells through time-based profiling during different load scenarios and charge-discharge rates in which this can be evaluated during experimental prototype testing. The duration of the balancing process extends when resistors have improper sizes in which the value of resistors have been chosen to be a good tradeoff between its balancing capacity

and power loss. Balancing time is another crucial metric; it is assessed by measuring the duration required to equalize the State of Charge (SOC) across the battery pack. A shorter balancing time with appropriately sized resistors indicates a more efficient system. When balancing strategy leads to reduced SOC deviation, it will achieve better total battery performance and efficiency.

Furthermore, power dissipation and thermal behavior are evaluated. The heat generated by the bleeding resistors and switching MOSFETs must be managed to prevent component degradation. The evaluation of system long-term robustness depends heavily on temperature measurements performed on cells and important balancing components that can be important during a real-world application. However, it is out of scope of this research. Lastly, the switching frequency of the MOSFETs is recorded to assess the stress on the switching components. Therefore, by examining these metrics collectively, one obtains a comprehensive picture of how well the passive balancing method reconciles efficiency, reliability, and performance.

### **3.4 VALIDATION OF PROTOTYPE DEVELOPMENT**

The development of the BMS prototype undergoes validation through hardware implementation along with experimental testing of its functional capabilities. The hardware design overview starts with details about the essential components within the prototype including the microcontroller alongside sensors, switches and passive balancing circuitry. The following section details experimental testing of the system through an open-circuit voltage (OCV) based passive balancing method. The prototype undergoes systematic evaluation during controlled charge-discharge testing to measure its operational stability and balancing performance.

### 3.4.1 Prototype Setup

A thorough analysis of the proposed BMS prototype follows through the presentation of its architectural design together with its hardware configuration. The system architecture receives a systematic representation through both a block diagram and a control algorithm functional schema. The visual and descriptive elements serve as essential tools to understand how hardware and software elements function together in the BMS.

#### *A. Block Diagram of the Proposed System*

The block diagram in Figure 3.5 shows the hierarchical architecture of the proposed BMS with four main functional blocks. The cell monitoring portion (left side) includes several sensor subsystems:

1. The circuit of voltage sensors, utilizing ADS1115 16-bit analog-to-digital converters and resistance voltage dividers so that particular voltages of various cells could be measured with high accuracy
2. The INA219 current sensing unit, dedicated to real-time monitoring of current and calculation of power

The MCU performs the balancing algorithm in real-time, reads and processes all the sensor data, performs SOC estimation (either OCV-based or ML-based based on the working mode) and generates all the control signals upon set thresholds. The balancing portion of the BMS consists of N-channel MOSFET transistors, which work as electronically controlled switches driven by the ESP32 GPIO lines. These gating elements are used to activate or deactivate the state of the passive balancing resistors, with the form of a MOSFET. Display interface (OLED) offers real-time visualization of the important parameters such as individual cell voltages, pack current, state-of-charge measurements, and system status measurements allowing the operators to check whether

BMS is operating correctly or not at any given time during the discharging and charging processes.

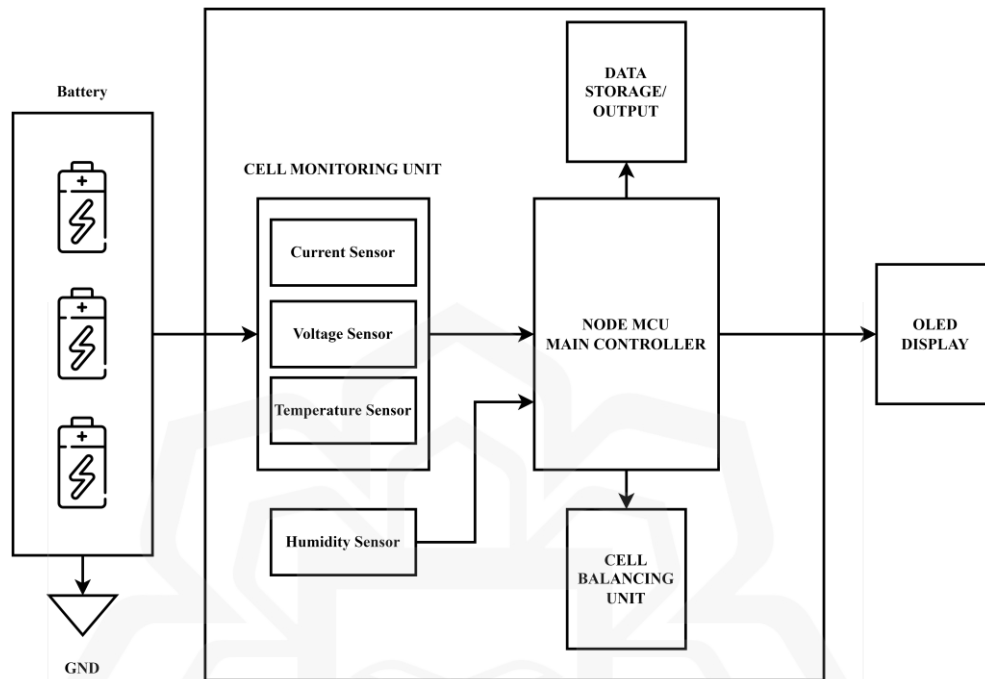


Figure 3.5 Block diagram of the BMS design

### ***B. Algorithm Schema of the BMS***

As depicted in Figure 3.6, an algorithm schema is designed to efficiently monitor and control the performance and lifespan of rechargeable batteries. Initializing the system is the first step, and then the voltage, temperature, and load current of the cells are measured and identified. After processing the input and determining the batteries' voltage level, the algorithm moves on to charging and balancing the appropriate cells when the cell voltage  $\geq 4.0V$ . The algorithm stops balancing and charging if all of the cells' voltages are higher than the maximum allowable voltage. With the help of this algorithm, a BMS will balance the required cell that needs to be balanced, guaranteeing that the batteries are always in the best possible condition and that their life is maximized. Furthermore, when the algorithm goes into a discharging mode, the cell monitoring algorithm will check the cell voltage

level during discharging so that when the voltage level drops below 2.8V, the cutoff mechanism will activate, thus protecting the battery from over-discharge.

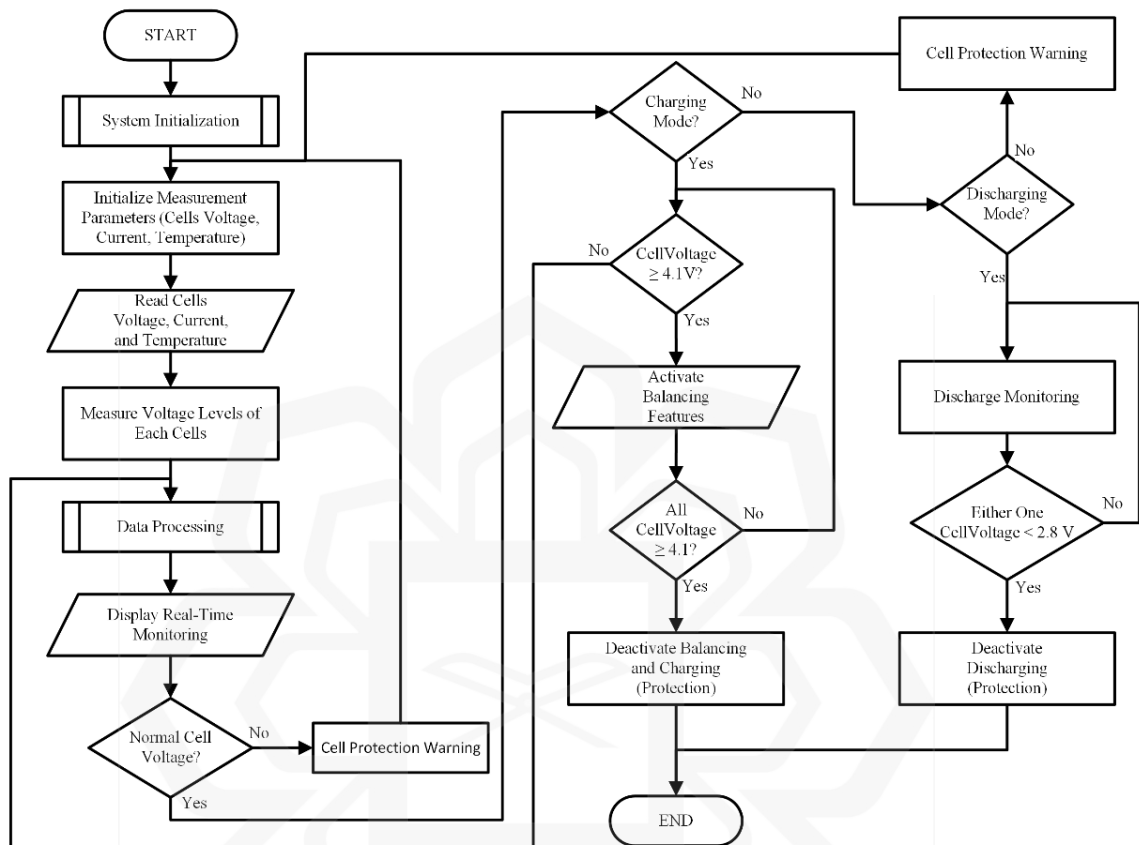


Figure 3.6 The BMS balancing algorithm

### 3.4.2 Proposed BMS Working Principle

The operational functions of the proposed Battery Management System (BMS) cover three main tasks: monitoring, balancing and protection. Each function supports the battery system working properly and the details will be covered in the upcoming subsections.

## A. Monitoring

The BMS system is responsible for measuring and supervising different aspects of the battery's performance. Voltage, current, temperature, and SOC are some of the parameters used in these systems. The BMS uses precise sensors and monitoring circuits to keep an eye on these parameters at all times and transmit the data in real-time. Figure 3.7 gives a simple overview of the ESP32 gathering the needed information to check each cell's behavior and check the humidity and temperature of the environment using the DH11 sensor. A voltage divider circuit is used to check the voltage of every cell in the battery. The voltage divider uses two resistors connected to the positive and negative ends of the cell. Because of the voltage division, the voltage measured is always within the ADC's range, which can handle up to 16 bits of resolution. The ADC is tasked with converting the voltage readings from the voltage divider into digital information that the ESP32 can use. The ESP32 is connected to ADC and gets the voltage values from all the cells at the same time. After processing, the readings are presented at the same time on the OLED screen, making it easy for the user to keep an eye on the battery status.

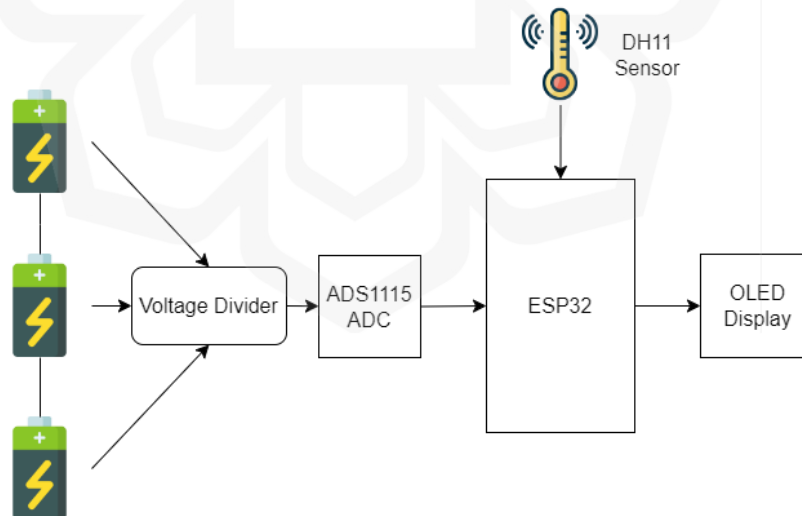


Figure 3.7 Monitoring Portion of the BMS

## B. Balancing

It is a simple way to balance the BMS by allowing extra energy to flow from the batteries into the shunt resistor while charging, heating it up in the process. It can be seen in Figure 3.8 that the batteries are joined in parallel, and every battery is connected to a bleeding resistor. When the voltage in the battery reaches a certain point, this configuration helps to dissipate any excess energy which have been set by the ESP32 microcontroller. The bleeding resistor allows the extra energy to be dissipated through the bleeding resistors, helping to keep the batteries from overcharging. The ESP32 is designed to stop charging once each battery voltage reaches 4.1V in which is the set upper limit for balancing. When the threshold battery voltage is hit, the ESP32 switches on an N-channel Metal-Oxide-Semiconductor (NMOS) transistor. The NMOS transistor acts as a low resistance path for the surplus energy to go through, bypassing the battery that is already charged. While the battery is charging, some energy is bled off to ensure the voltage stays under the upper limit, so the battery does not get overcharged. This way, every battery in the system gets the same amount of charge, as any extra energy is sent away instead of building up in single cells.

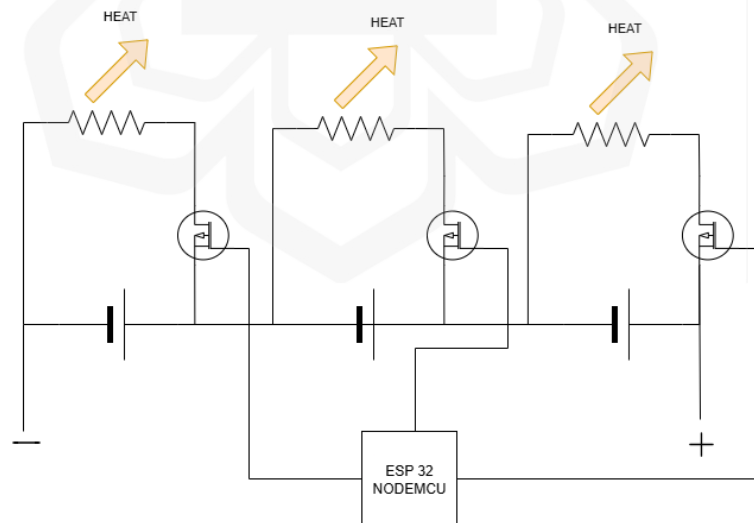


Figure 3.8 Balancing Portion of the BMS

### ***C. Protection***

It is important for the BMS to have key safety features that keep the battery safe and healthy for a longer time. One important way to protect a battery is to stop the flow of current when the voltage reaches certain levels while charging or discharging. To accomplish this, two main P-channel Metal-Oxide-Semiconductor (PMOS) transistors are used, one as the discharge MOSFET and the other as the charge MOSFET. As soon as the battery voltage exceeds the upper threshold set by the control algorithm, the charge MOSFET switches to interrupt the current flow. Thanks to this function, batteries are prevented from getting overcharged, which helps avoid permanent damage to their cells. During discharging, if the voltage of the battery drops below a certain value, the discharge MOSFET is turned on to stop the current, preventing the battery from becoming over-discharged and thus keeping it functioning for a long time. These relays are created by adding PMOS transistors at the cell level to specifically guard against too much current entering each battery. When a cell's voltage reaches a certain level, the intermediate relays turn on and control the charge and discharge MOSFET. As soon as the relay is activated, it separates the cell from the charger, letting it rest and keep its voltage at the current balance level. These relays help the BMS maintain safe current flow and battery voltage, ensuring battery reliability and durability.

#### **3.4.3 BMS Prototype Hardware Design**

System testing began through a breadboard prototype before transitioning to develop a reliable and compact BMS system using veroboard. The soldering process for the veroboard placed all components accurately to minimize signal interference while creating secure electrical connections between components. Using a veroboard allowed the BMS system to have a permanent setup which enhanced both reliability and system lifespan.

The necessary components of the BMS integrated seamlessly into the veroboard through soldering based on the proposed schematics as shown in Figure 3.9 and the finished prototype shown in Figure 3.10. The list of components used for Table 3.2 description for

addresses each component by its alphabetical designation as shown in the prototype illustration.

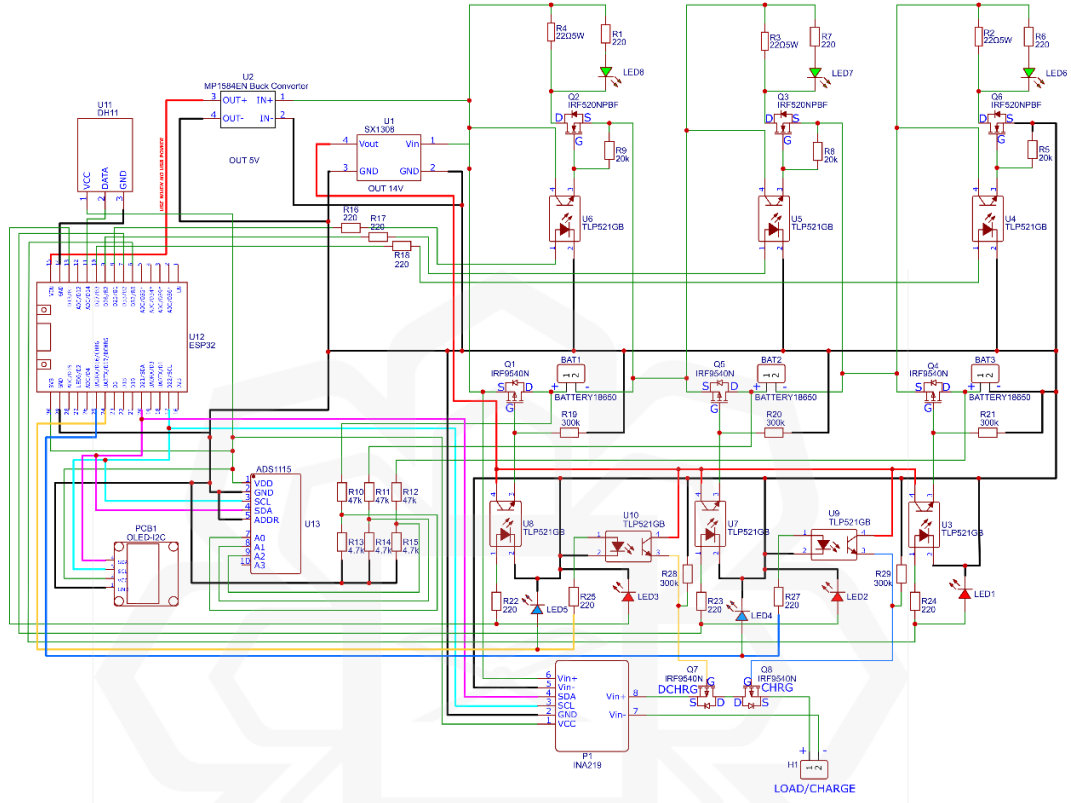


Figure 3.9 Prototype BMS Schematic Diagram

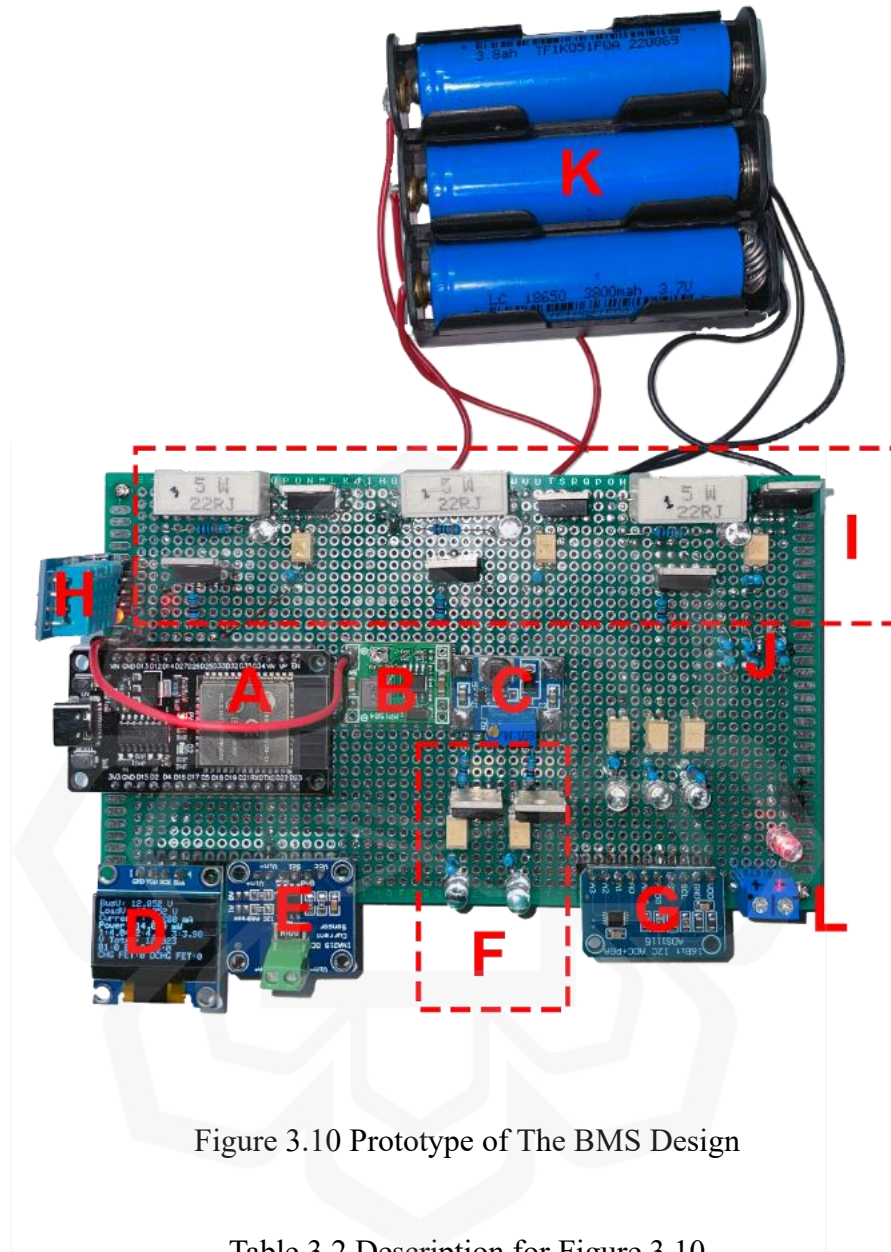


Figure 3.10 Prototype of The BMS Design

Table 3.2 Description for Figure 3.10

Component	Description	Component	Description
A	ESP32	G	ADS1115 ADC
B	Buck converter	H	DH11 Sensor
C	Boost converter	I	Cell balancer portion
D	OLED display	J	Voltage divider
E	INA219 current sensor	K	Li-ion battery
F	Cutoff MOSFET	L	Connect load/charger

## **3.5 THE INTEGRATION OF MACHINE LEARNING SOC ESTIMATION**

### **3.5.1 Machine Learning Model Training Workflow**

This section details the selection process of ML models focused on SOC estimation and explains why deep learning methods surpass traditional and conventional SOC estimation techniques. Modern battery behavior requires strong models because operational conditions lead to increased complexity and nonlinearity patterns. The deep learning models using Long Short-Term Memory (LSTM) and Convolutional Neural Networks (CNN) gain popularity for SoC estimation because they excel at detecting sequential relations and non-linear trends which is great for battery related data.

The workflow which the research implements is shown in Figure 3.11. The workflow starts by creating system requirements before performing data preparation functions which involve normalization while extracting features and segmenting the voltage and current together with temperature profiles from simulated and experimental datasets. The datasets underwent preprocessing methods that optimized their use in training the model after they were obtained through controlled charge-discharge operations. The selected ML models will be used to train the model followed by deploying compression techniques to enhance deployment efficiency. Model tuning is a crucial part in which measures its performance levels before integration into Simulink that later will be compared to OCV-based estimation method. The workflow for this stage will be discussed further in the other sections.

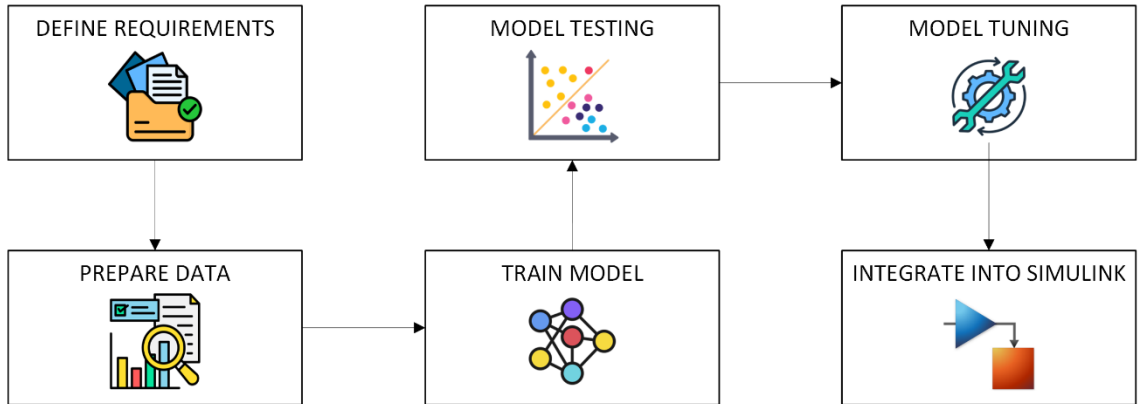


Figure 3.11 ML Training Workflow

### 3.5.2 Defining Model Requirements and Data Preparation

The development process of machine learning models for battery SOC estimation needs precise specifications that define data acquisition methods and neural network design as well as accuracy that targets the system integration rules and code implementation protocols. The entire framework encompasses multiple levels which guarantees both strong prediction capability and together with compatibility with real-world BMS operational requirements, computational needs and integration standards. Any machine learning model requires high-quality training data, which must be directly related to its application for successful model performance. When estimating SOC for batteries, it is necessary to work with data that correctly demonstrates battery performance across various operating conditions. Such data selection gives the model strong generalization abilities to deliver accurate predictions in real-life applications.

Several important features, including voltage, current and temperature should be measured and recorded over time when creating the training dataset. The behavior of the battery depends directly on these input data in which a wide range of temperature measurements from  $-10^{\circ}\text{C}$  to  $25^{\circ}\text{C}$  should be included in data collection because temperature strongly impacts battery performance and also SOC estimation. The dataset that has been used in this research was generated from a simulation using a variant of the

Simulink model in the Simscape Battery example such as shown in Figure 3.12 and its SOC (%) in Figure 3.13. This model simulates a battery charging and discharging over several hours. The data needs appropriate preparation before training because such preparation ensures the model learns efficiently. The first step involves normalization, in which it scales all input features to a standard range from 0 to 1 to prevent dominant features from affecting the learning process with their difference in magnitude. This step is crucial in maintaining model performance and improving accuracy of any model that would be trained, and it is illustrated in Figure 3.14 below. Later the dataset will be split into data chunks of 500-time steps shown in Figure 3.15 . The training process becomes more efficient when long data sequences are divided into shorter sections for computation and also ease the memory during training.

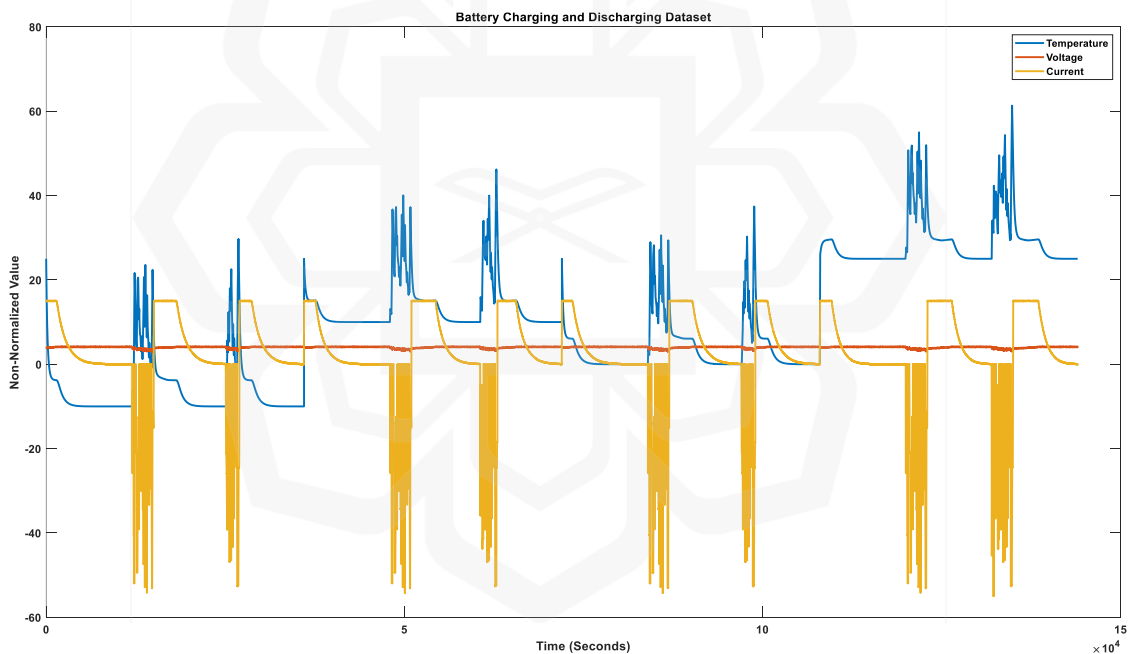


Figure 3.12 Non-Normalized Battery Data for Model Training

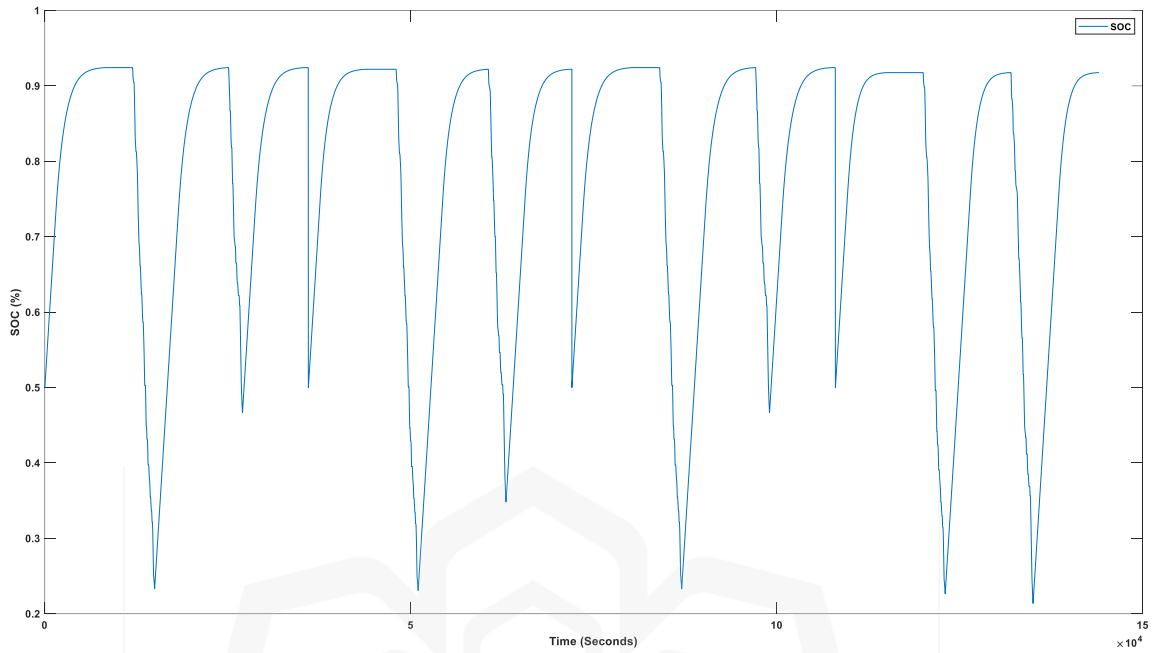


Figure 3.13 SOC (%) Data for Model Training

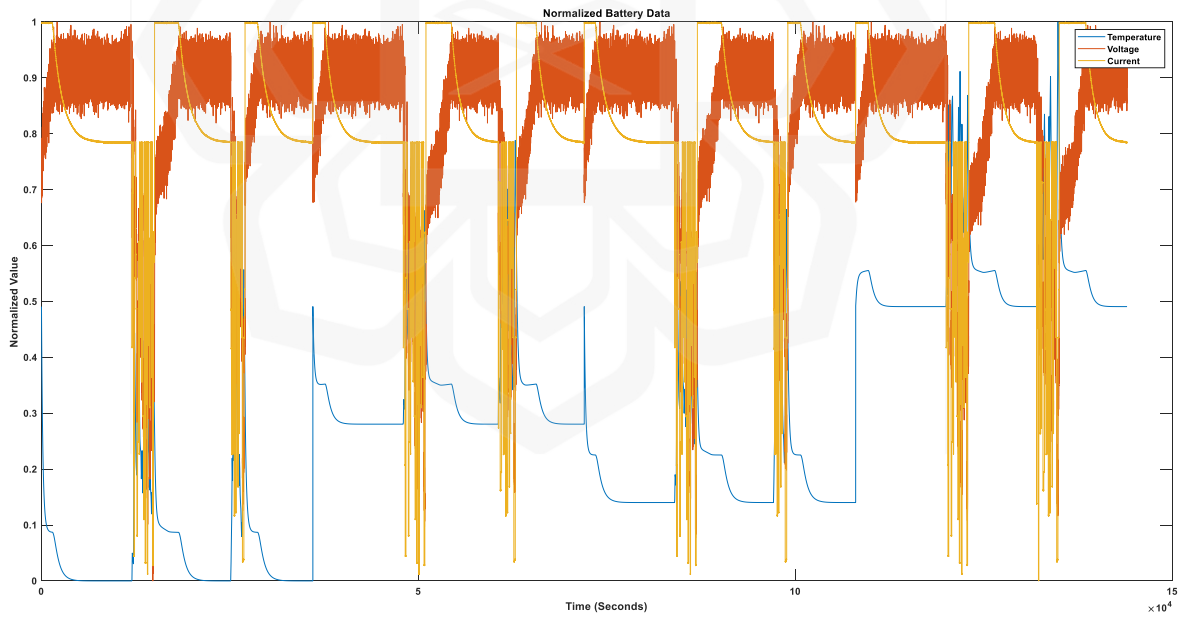


Figure 3.14 Normalized Battery Data for Model Training

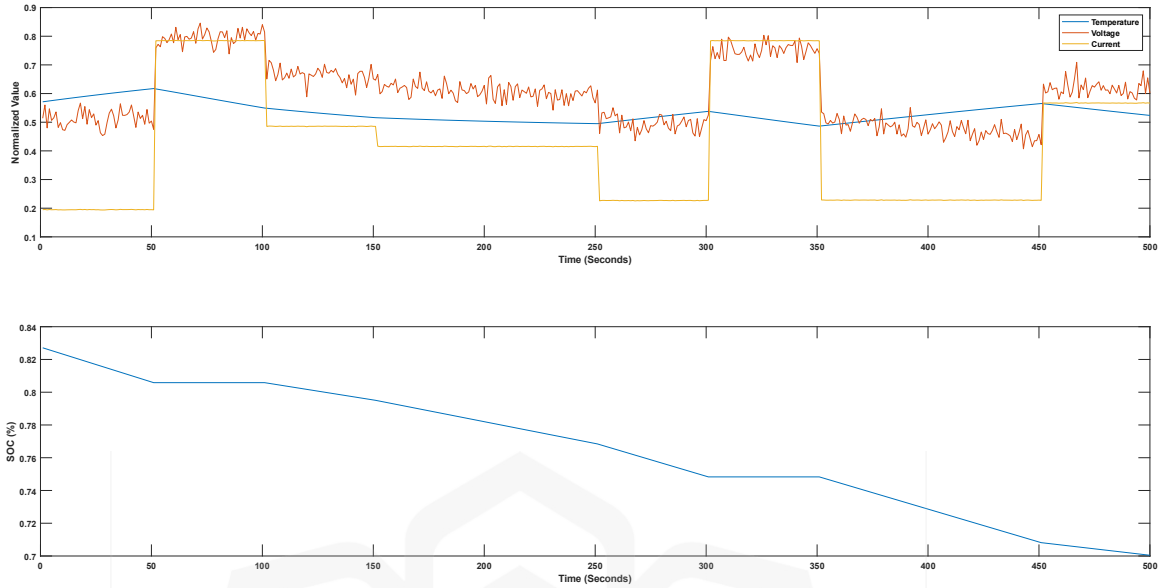


Figure 3.15 One Observation of One Dataset Chunk

### 3.5.3 Model Training and Model Testing

State of charge (SOC) represents battery charge level as a percentage of total capacity. Accurate SOC estimation is vital for BMS in electric vehicles and grid storage applications, enabling effective power management, predictive analytics, and system protection. Traditional methods combining open-circuit voltage with coulomb counting exhibit limited long-term accuracy due to error accumulation. In contrast, deep learning methods directly extract nonlinear SOC relationships from time-series measurement data, offering superior accuracy. Recurrent neural networks (RNNs) with Long Short-Term Memory (LSTM) layers predict SOC by processing sequential time-series data comprising temperature, voltage, and current measurements.

The machine learning model had been trained on a synthetically generated battery operation dataset generated using a combination of reference data, created with the help of the software packages, and not experiment measurements or public data repositories. The dataset was created using a variation of the Simscape Battery example model, which

implements a high-fidelity table-based model representation of a battery calibrated to Panasonic 18650 lithium-ion cell characteristics (2900 mAh nominal capacity, 3.7 V nominal voltage). The evaluated simulation model ran multiple charge-discharge cycles under different ambient temperatures (-10°C, 0°C, 10°C, and 25°C) to obtain the non-linear electrochemical behavior of the lithium-ion cells under different thermal environments. During each simulated cycle, time-series measurements of three critical parameters—whether they are battery terminal voltage (V), load current (A), and cell temperature (°C), the model recorded its ground truth state-of-charge (SOC) values computed internally-by the Simscape Battery block. The synthetic dataset consists of comprehensive operational profiles over several hours of charging and discharging operations in order to obtain a training corpus large enough to allow for deep learning model convergence.

The raw measurement data gets split into training sets and validation sets before commencing model training tasks. The input chunks of 500-time steps contain three features, which are stored in cell arrays *XTrain* and *XVal* as battery terminal voltage, current draw and cell temperature measurements. The SOC trajectories belonging to each data set are saved in *YTrain* and *YVal* respectively. The overall data has been divided into training and validation portions of 70% and 30%, making sure the performance evaluation of an untested model during training requires validation data to determine its effectiveness. The validation process stops overfitting and ensures the model can correctly predict new data points it has not encountered before.

The LSTM layers inside recurrent neural networks process sequential battery data through the network architecture as illustrated in Figure 3.16 below. A sequence input layer accepts three features, then two stacked LSTM layers with 256 and 128 hidden units produce full sequences as output. The LSTM blocks receive dropout layers with a 20% drop probability to reduce overfitting effects. The model calculates single SOC outputs at each time step through the fully connected regression layer, following which a sigmoid activation function enforces predictions between 0 and 1 values representing 0 to 100% SOC.

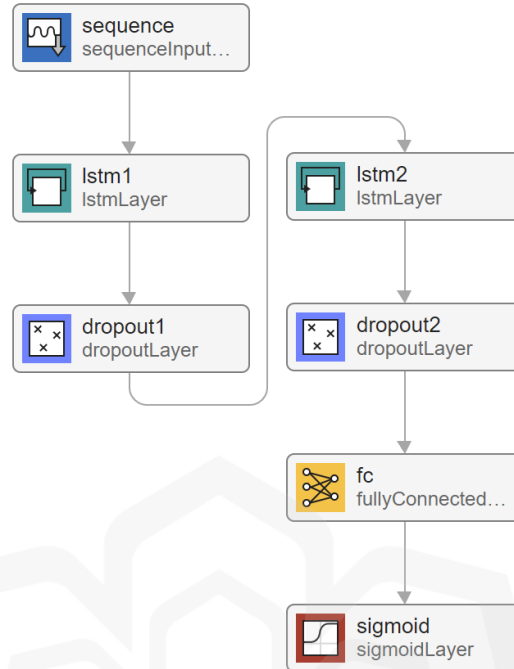


Figure 3.16 Illustration of The Model Network Architecture

MATLAB's *trainingOptions* function runs the training process with the Adam optimizer and mean-squared error loss to perform regression tasks. The algorithm achieves a suitable balance between speed of convergence and generalization through a learning rate of 0.01, 150 maximum epochs and a batch size of 32. Working in batches of 32 on each update sees enough examples to smooth out noisy gradients yet stays small enough to take full advantage of GPU speed and modest memory use. The data are shuffled during each epoch to avoid ordering biases, and validation tests are performed every 20 iterations on the held-out dataset so that it can catch any signs of overfitting early and adjust our learning rate or even stop training if needed. Finally, the root-mean-squared error (RMSE) throughout because squaring the errors means big misses hurt more, it ensures the model really focuses on avoiding large SOC prediction mistakes, and since RMSE is in the same as percentage-point deviations that can be easily understood. The training process conducts GPU-based training when GPU hardware becomes available; otherwise, it switches to CPU execution. Figure 3.17 below shows the training progress windows using LSTM to predict SOC measurement from the training dataset available.

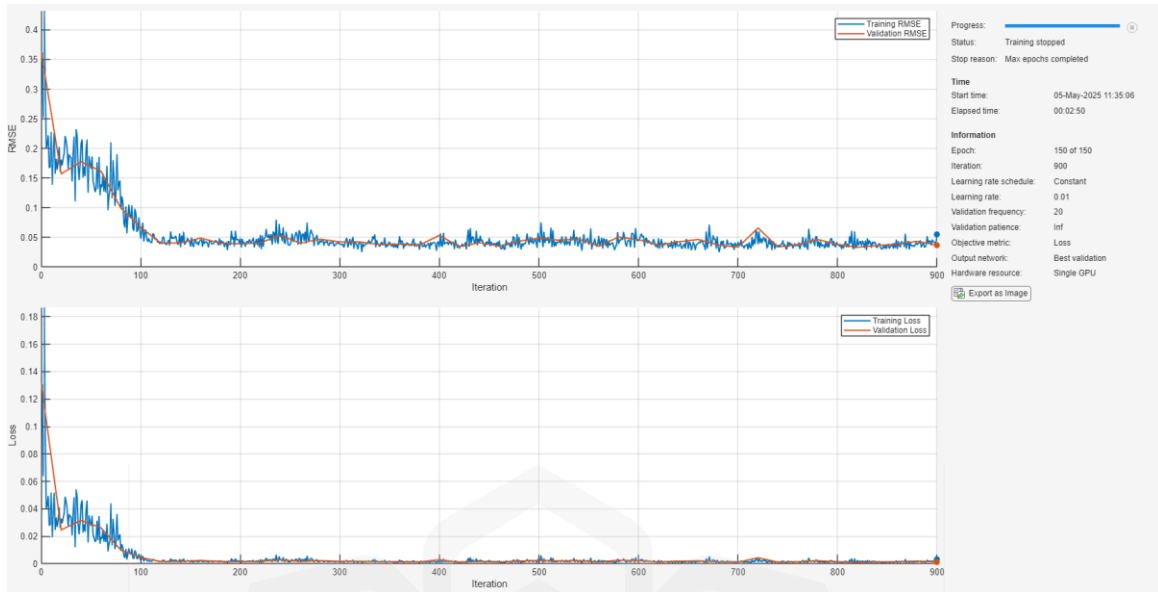


Figure 3.17 MATLAB Model Training Progress Window

Figure 3.17 illustrates the training progress of the LSTM model over the specified iterations. The top graph displays the Root Mean Square Error (RMSE) for both the training (blue) and validation (orange) datasets, indicating the model's increasing accuracy. The bottom graph represents the Loss function value, which quantifies the difference between the predicted and actual SOC. The convergence of both the training and validation curves towards zero demonstrates that the model is effectively learning the temporal dependencies in the data without overfitting. During the testing phase the LSTM network is tested for its capacity to extend its application beyond training data and identify situations where predictions become unreliable. The current step utilizes combined statistical diagnostics with test set data to determine the model's practical battery-management usage readiness. During the test phase of the LSTM-based SOC estimation, the main goal is to determine the extent of network generalization for previously unseen data inputs. The established test dataset collection which contains temperature, voltage and current measurement sequences measured across ( $-10^{\circ}\text{C}$ ,  $0^{\circ}\text{C}$ ,  $10^{\circ}\text{C}$  and  $25^{\circ}\text{C}$ ) ambient conditions. The test of the battery at the four different temperatures to ensure that the LSTM model can grasp the true electrochemical dynamics instead of retaining knowledge of only one operating condition

in which can be safely use the SOC estimator in real-world situations that experience temperature fluctuations throughout the testing scope. The test process loaded the pre-processed dataset to simulate the same training protocol used in the initial phase.

The model testing requires evaluation of its generalization potential through independent testing data in which that remained unused during the training phase. The evaluation process establishes the model's performance ability when dealing with new unseen data. The testing process requires prediction using test datasets, followed by label comparison with the true values of the datasets used. Performance metrics such as accuracy, RMSE, precision, and recall become computable after testing the trained model. Standard testing should be extended with abnormal data assessment to determine the model's robustness when processing data points that differ statistically from training data. Abnormal data detection serves as a procedure that reveals how well models recognize and correctly handle different forms of anomalous inputs.

The assessment of the test model performance requires evaluating its generalization ability through tests on data that was not used during training. The evaluation of the trained SOC estimation model takes place through systematic testing across the set temperature conditions. Temperature conditions in the environment play a fundamental role in affecting battery performance, so testing the predictive model across different temperatures reveals its operational stability across diverse environmental settings. The data sets are isolated by temperature condition to present X inputs which consist of voltage and current and temperature readings that match Y target SOC values. The test data needs normalization through minimum and maximum feature scaling parameters that come from the training dataset before prediction generation. The normalization process enables data consistency that matches test data to training conditions in order to maintain clear model interpretations and predictable results. The RMSE evaluation across different ambient temperatures provides essential information about how environmental conditions affect the predictive accuracy of SOC estimation model performance in which performance metric serves as a measurement tool to determine average error size and simultaneously detects both regular and systematic prediction inaccuracies. The predictive accuracy of SOC values increases

when RMSE decreases while higher RMSE indicates greater prediction errors. From the trained model a generated bar chart illustrates in Figure 3.18 displays the RMSE values of the results across test temperatures ranging from variation of temperature conditions. From the performance evaluation, noted that using the dataset for ambient temperature 10°C shows the lowest value of RMSE at 0.025, indicating good accuracy. The model generalization ability beyond training conditions is measured through RMSE variations observed between these different temperatures.

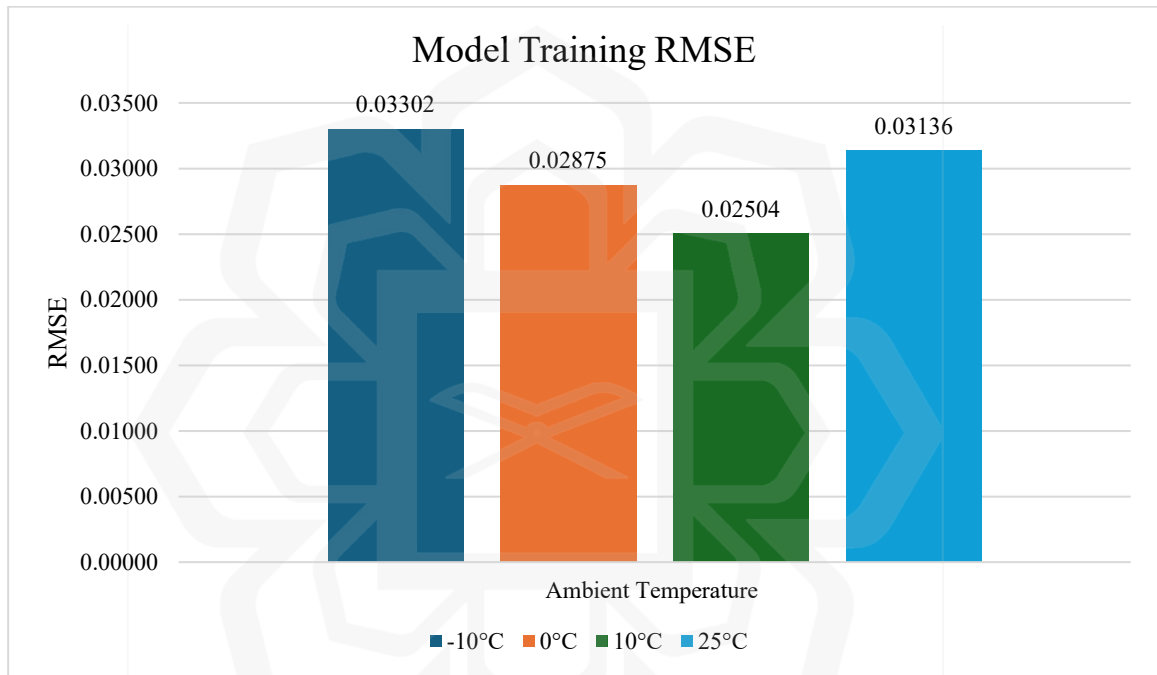


Figure 3.18 RMSE Values at Each Ambient Temperature Condition

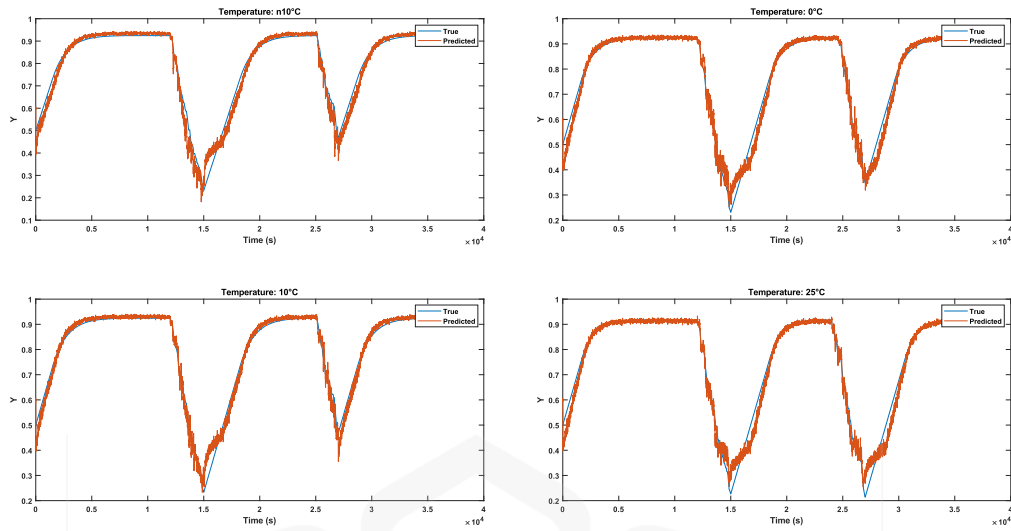


Figure 3.19 Plot of The Predicted and The Target SOC for Each Temperature Condition

Figure 3.19 presents a comparative plot of the predicted SOC versus the true (target) SOC across the four tested temperature conditions. In the simulation environment, these temperatures were rigorously controlled by adjusting the ambient temperature parameter within the Simscape Battery block. The close alignment between the predicted (red) and true (blue) trajectories confirms the model's high precision and its ability to maintain accuracy even when subjected to varying thermal parameters.

Furthermore, adding to the classic performance evaluation on test data, the robustness of the trained neural network model should be evaluated with abnormal data to ensure reliability and operational stability under real-world and different environments. Abnormal data is typically a set of input data that is very different from the training data, such as cases, sensor degradation, environmental changes or new operating conditions, etc.

In addition to standard performance evaluations, the robustness of the neural network was rigorously tested against abnormal data to ensure reliability under fault conditions. Abnormal data assessment was explicitly included in this research to simulate scenarios such as sensor degradation or signal drift. Using the MATLAB Deep Learning

Toolbox, specifically the *networkDistributionDiscriminator* function, the model was trained to distinguish between normal operating data and artificially induced noise or drift.

The model tested the ability to handle abnormal data cases by receiving artificial sensor drift signals from selected voltages in the validation set which simulated actual sensor breakdowns. As illustrated in Figure 3.20, artificially induced drift results in a major drop in the voltage readings compared to the stable baseline. The illustration graphically represents normal data voltage signals versus drifted abnormal data signals that simulate a sensor that was failing, which shows a stark contrast between the normal data and irregular data. The controlled drift mechanism enabled accurate evaluation of the discriminator while it successfully detected anomalous patterns in real-world environments for odd scenarios.

The discriminator demonstrated an effective ability to detect normal data (ND) versus drifted or abnormal data (AD) that have been created as noisy signal for 40 observations (1 observation = 500-time steps). Figure 3.21 confusion matrix shows the discriminator accuracy performance statistics in which the model demonstrated its effectiveness in abnormal pattern detection when it correctly identified all 40 instances of artificial drift abnormal data in the testing phase. The classifier performed successfully by correctly identifying most normal observations while misidentifying only seven of them as abnormal. The discriminator demonstrates its capability to detect standard data patterns together with its ability to detect irregular data patterns which fulfil requirements for integrating into Simulink models. Real-time simulation together with additional performance evaluations can be implemented through this stage for practical usage.

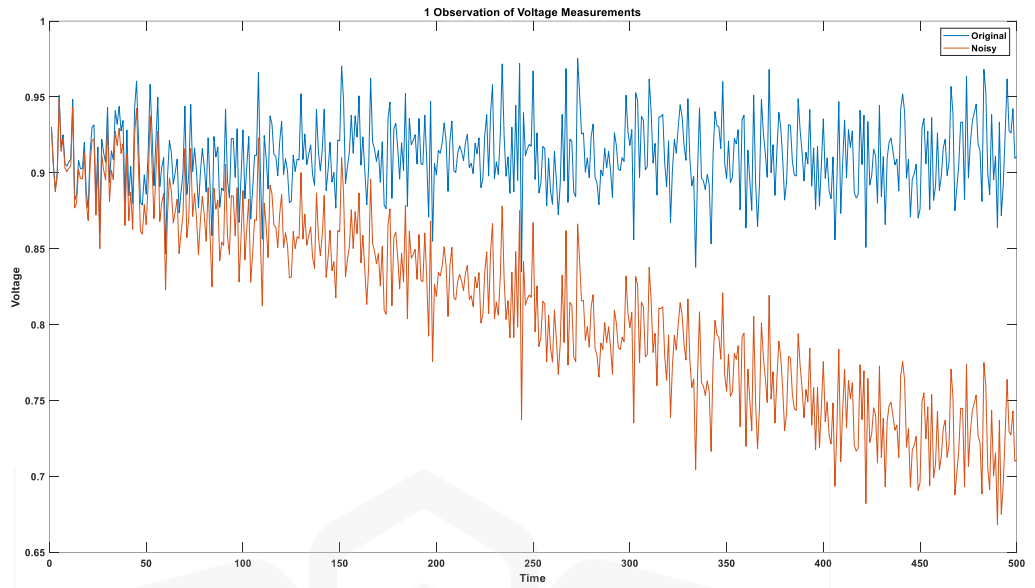


Figure 3.20 View of One Noisy Observation For The Battery Dataset

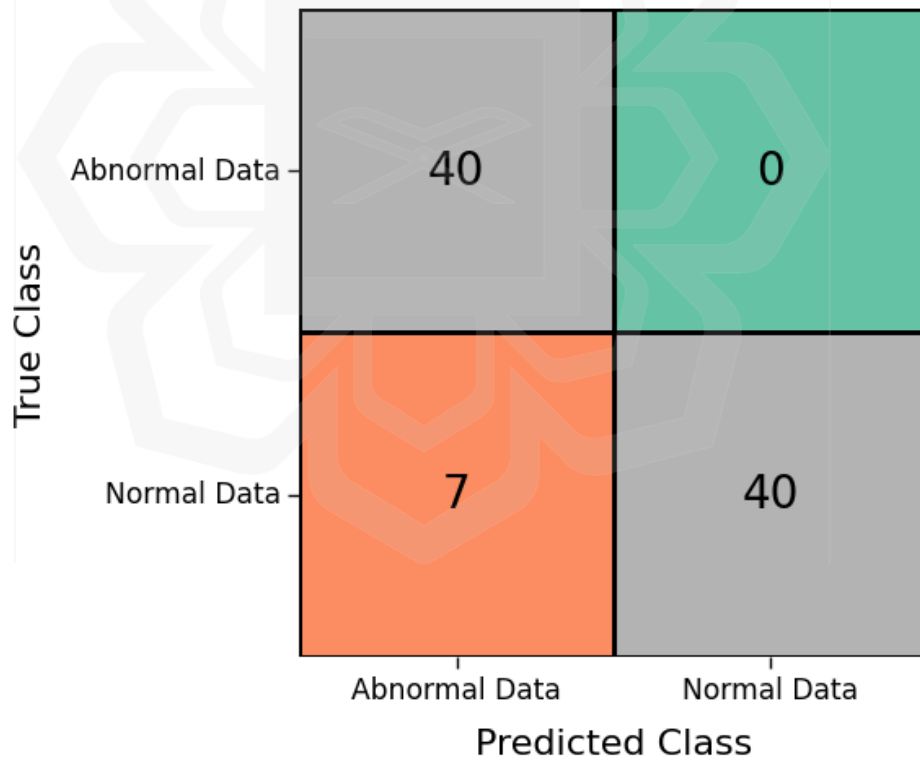


Figure 3.21 Confusion Matrix of Discriminator Accuracy

### 3.5.4 Model Tuning and Integration into MATLAB Simulink

After the training and validation phases, the fine-tuned machine learning model needs to be precisely tuned and integrated into a reliable simulation framework for practical use. This step ensures the network can predict real-world behavior under various operating conditions, particularly in BMS applications. The trained machine learning SOC estimation model takes three main inputs in which are battery temperature, voltage, and current. These important parameters are known to impact battery SOC accuracy that will be used to further enhance the balancing process from the BMS. The model has been pre-trained and pre-compressed, employs data collected in various ambient temperatures (-10°C, 0°C, 10°C, and 25°C) in which the variety of training data at these temperatures enables the model to generalize over a range of different conditions, essential for accurate SOC estimation.

To deploy the model into MATLAB Simulink simulation environment, it first will be loaded to the MATLAB workspace as the pretrained model. The trained network model requires exporting to Simulink for further simulation and real-time validation steps in which the *exportNetworkToSimulink* function in MATLAB exists for the purpose of facilitating this export process into Simulink block. The function creates a Simulink-compatible version of the neural network model, which separates it into distinct layer blocks. The structured format enables detailed analysis of network layers while providing enhanced model transparency and prediction interpretation.

To integrate the model into MATLAB Simulink, the simulation environment is configured with a fixed-step solver using a time step of 1 second, matching the temporal resolution of the training data. This ensures that the LSTM network receives appropriately sampled input sequences without temporal mismatch. The simulink model executes on a standard workstation (Intel Core i7 processor, 32 GB RAM) running MATLAB R2025, achieving model inference latency of less than 1 millisecond per prediction well within the 1-second simulation time step.

Figure 3.22 illustrates the input ports are configured to accept both dynamic and static inputs to handle operational data alongside historical battery measurement data. The model accepts essential battery data points, including temperature, voltage, and current data that directly impact battery performance and SOC prediction accuracy. A dedicated subsystem of layer blocks precisely displays the neural network structure inside the Simulink model such as shown in Figure 3.23. The network layers within this subsystem block use individual components to display all operations in a transparent and easily understandable way. Real-time estimations of battery SOC emerge from output ports embedded within the Simulink model in which the system generates outputs that simplify integration with various BMS and control systems. The model integration capabilities enable reliable SOC estimation while functioning as an optimized base for implementing battery management solutions to enhance operational efficiency and extend battery lifespan.

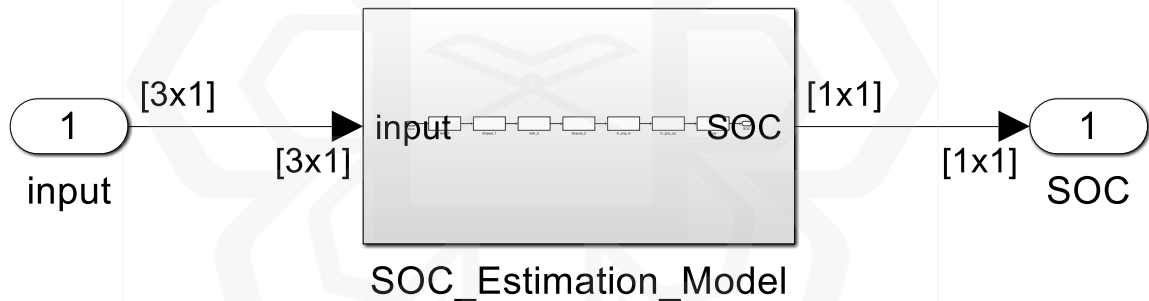


Figure 3.22 Exported SOC Estimation Model

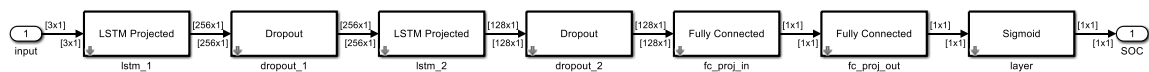


Figure 3.23 Subsystem of The Model Network

The exported model enables integration with the Simulink simulation model that previously conducted OCV-based initial simulations. Despite that, the model needed to be tested one last time with test data on one set of ambient temperature. For the sake of

simplicity, 10°C of ambient temperature has been chosen. Figure 3.24 illustrate a graph of predicted SOC and true SOC based on test data in which the results shows a good model fit and strong predictive ability. Furthermore, Figure 3.25 demonstrates how the SOC estimation model integrates successfully into the simulation environment which allows precise state of charge measurements under different testing conditions. The following chapter presents detailed examinations of simulation outcomes together with experimental verification protocols.

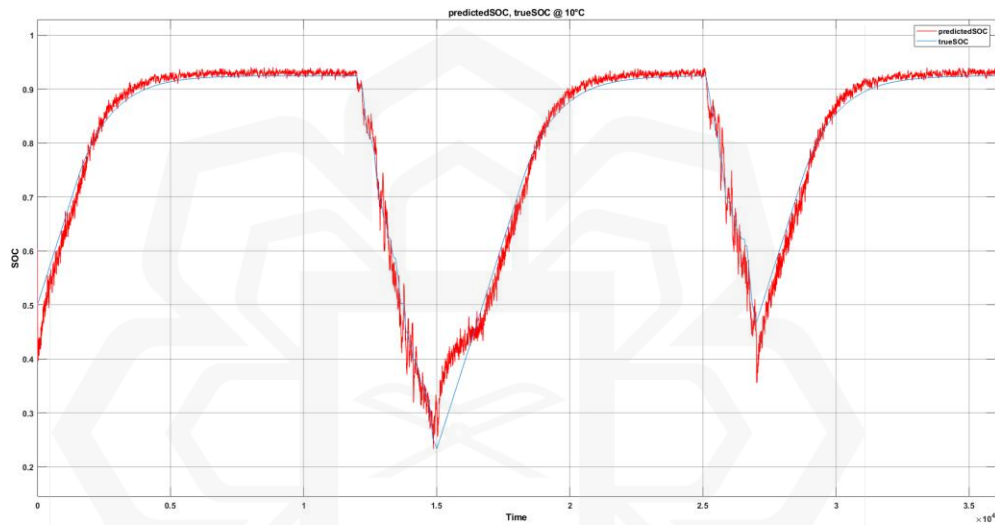


Figure 3.24 Plot of Predicted and True SOC Values at 10°C

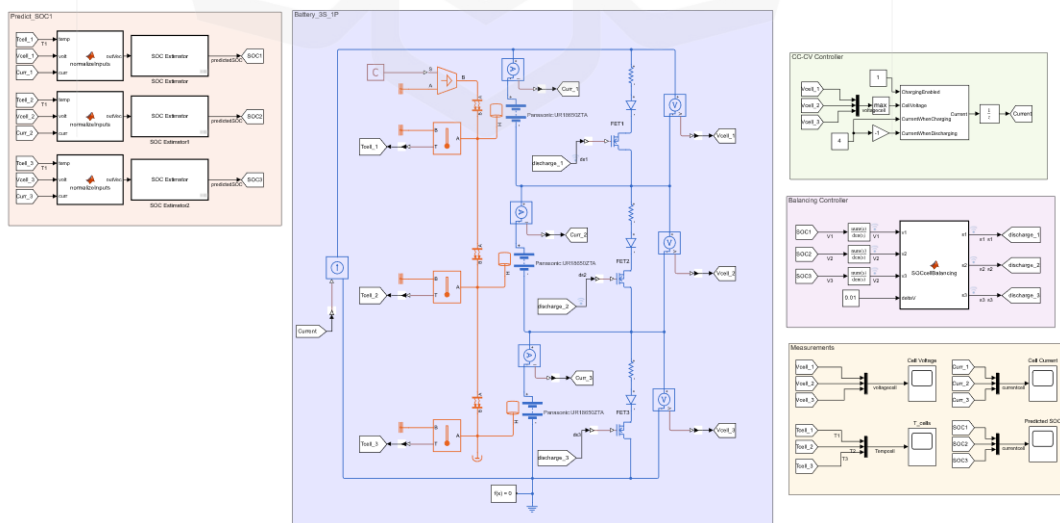


Figure 3.25 BMS Simulation Design in MATLAB Simulink With SOC Estimation Model

## CHAPTER FOUR

### RESULTS AND DISCUSSION

#### 4.1 OVERVIEW

This chapter discussed the findings of the simulation and experimental prototype test of the improved passive balancing system. A key point of attention is given to the comparison of the traditional OCV-based estimation framework and the new one based on the use of the Machine Learning (ML) framework. It is worth mentioning that the OCV-based approach that was adopted in this study is used to provide a standard baseline control. It employs a constant voltage threshold and standard hysteresis loop that is commonly used in commercial passive BMS to give a standard reference point in measuring the efficiency improvement, switching stability, and reduced stress of the new ML-driven approach. In the simulation environment, both estimation methods are checked under the same conditions, whereas the prototype experiments allow for understanding how they work in real conditions.

The prototype testing was also meant to prove that the BMS could perform other critical functions such as real-time monitoring and battery protection. This supports the fulfillment of a miscellaneous but very important goal: the creation of an efficient BMS that would not only improve balancing performance but also guarantee operational safety and system reliability. It should be noted, however, that despite the fact that this research is cast in the form of a comparative evaluation between ML-based and OCV-based SOC estimation techniques for passive balancing, the implementation of the ML algorithm could not be extended to the experimental prototype due to time constraints. As a result, only the OCV-based method was validated using hardware testing, while the ML-based method was evaluated in the simulation environment.

## 4.2 SIMULATION RESULTS

This section shows the results of the simulation of the BMS, where OCV and ML-based SOC estimation approaches were evaluated. The simulations were performed in a controlled environment to see how the passive balancing algorithm worked in terms of balancing efficiency, SOC estimation, and energy use. In this section, the results were discussed in order within each of the stages following the research methodology. These results gave more of a clear picture of how each estimation method acts under the same conditions, as well as provided a valuable opportunity to test the control logic before proceeding to the hardware testing in the real world.

### 4.2.1 Charging Simulation Results

#### *A. OCV Results*

Figure 4.1 shows how the cell voltage changes during the OCV charging simulation. The simulation results show that the voltage of each cell increases evenly, showing that the charging process is well-balanced during the balancing process that occurred. This means the algorithm is able to keep charging at a consistent rate until it reaches the upper limit it was given. At the beginning, the voltage between the cells was not the same, but as the system reacted, it stabilized due to the control algorithm sending signals to the balancing MOSFETS in which to direct energy to the bleeding resistor to prevent further imbalance. In this approach the use of passive balancing approach in which a voltage convergence is achieved which is very important for the health and lifespan of the batteries.

Furthermore, Figure 4.2 illustrates that passive balancing brings the cell voltages back to the needed level when all of them reach their upper limit. When there are controlled perturbations, the balancing resistor and switching MOSFET are turned on to equalize the

excess charges. It can be seen in Figure 4.3, Cell 3, that at the early stages of the control logic detects that the voltage is above the set limit of 3.95V and uses the balancing resistors to remove the extra charge. The set limit was predetermined following the battery data parameters in which approximately 3.95V was at 80% charged. Such unsteady changes during these phases prove that the system responds quickly to the current state of the cell. The balancing mechanism operates with pulses, turning on when the voltages are different and turning off within the hysteresis band set. By maintaining precise control, the voltage logic proves it is stable during charging which ensure the battery will not face any problems that might reduce its lifespan or endanger the user.

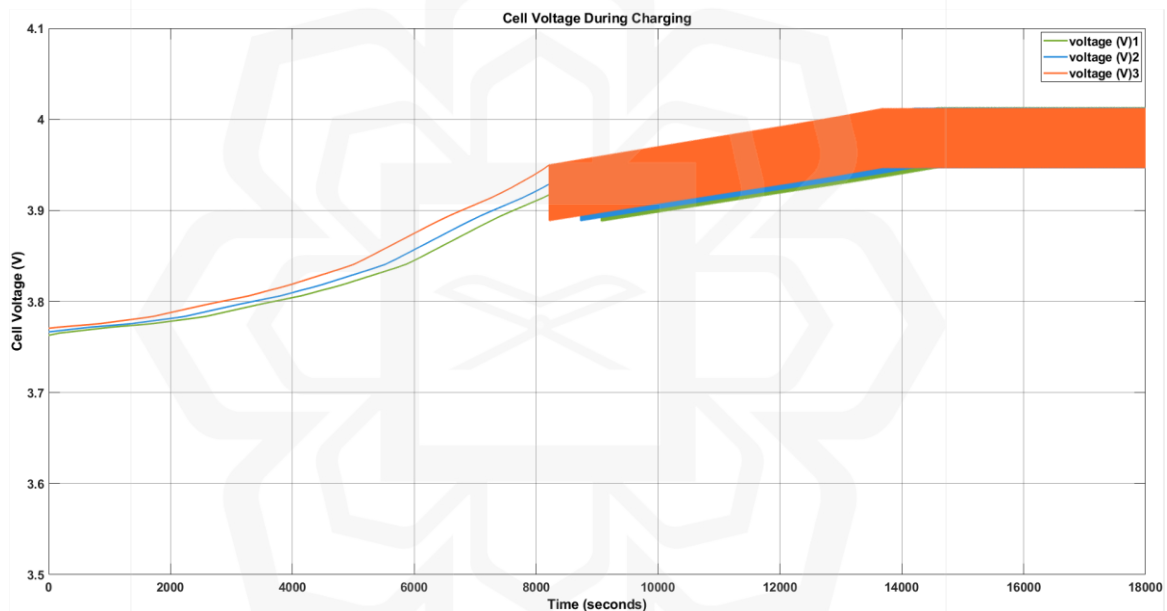


Figure 4.1 Cell Voltage During OCV Charging Simulation

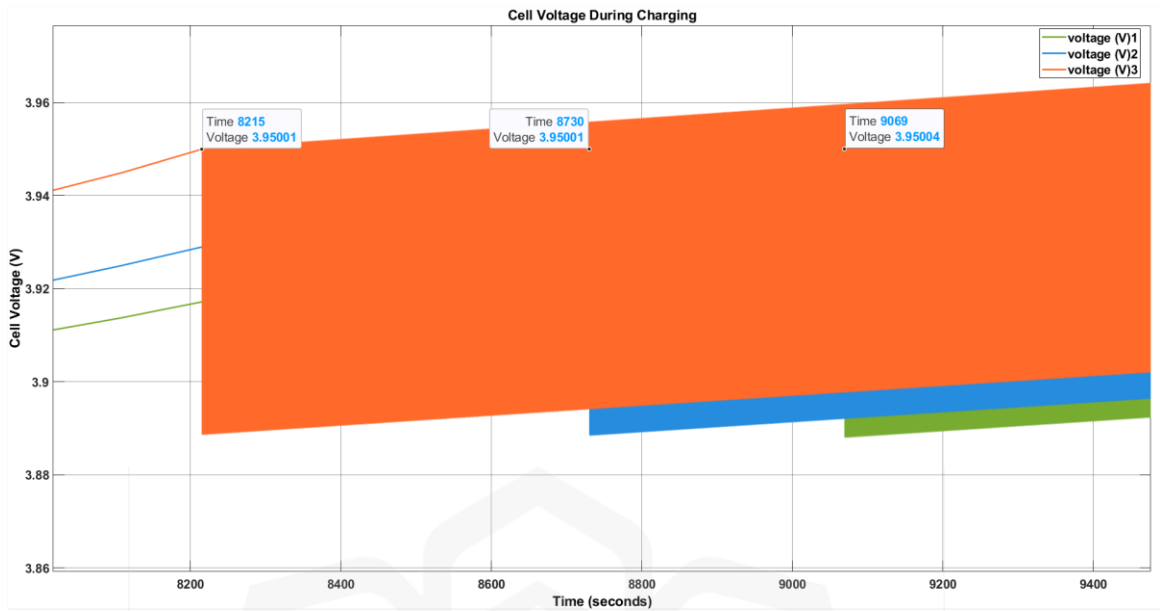


Figure 4.2 Voltage Fluctuation of Each Cell During Balancing Process

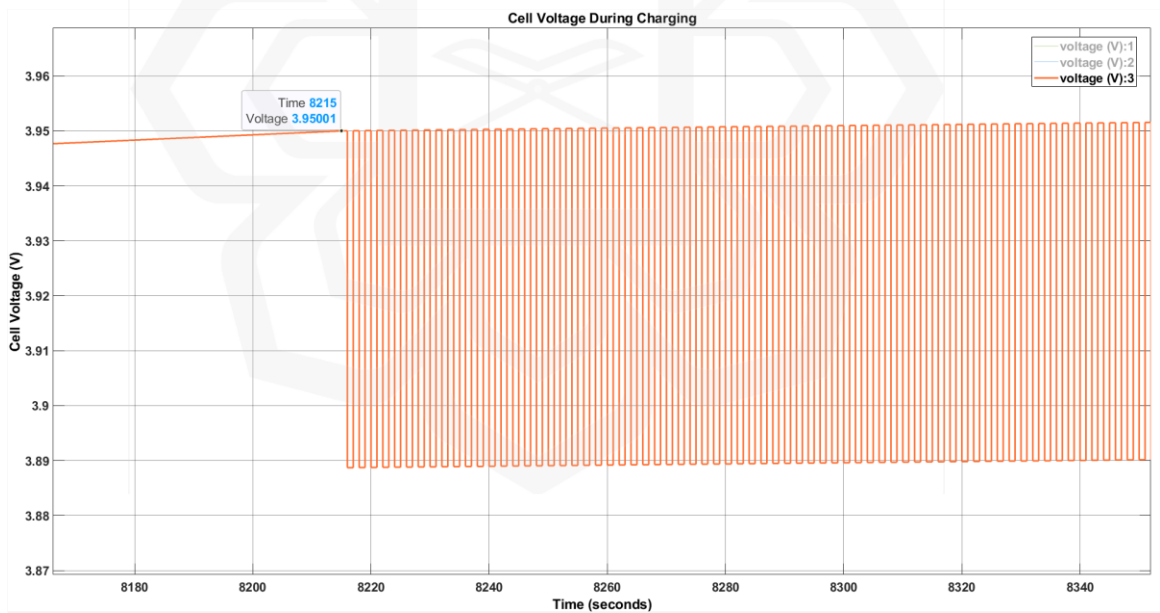


Figure 4.3 Close-up of Voltage Cell 3 During Balancing Process

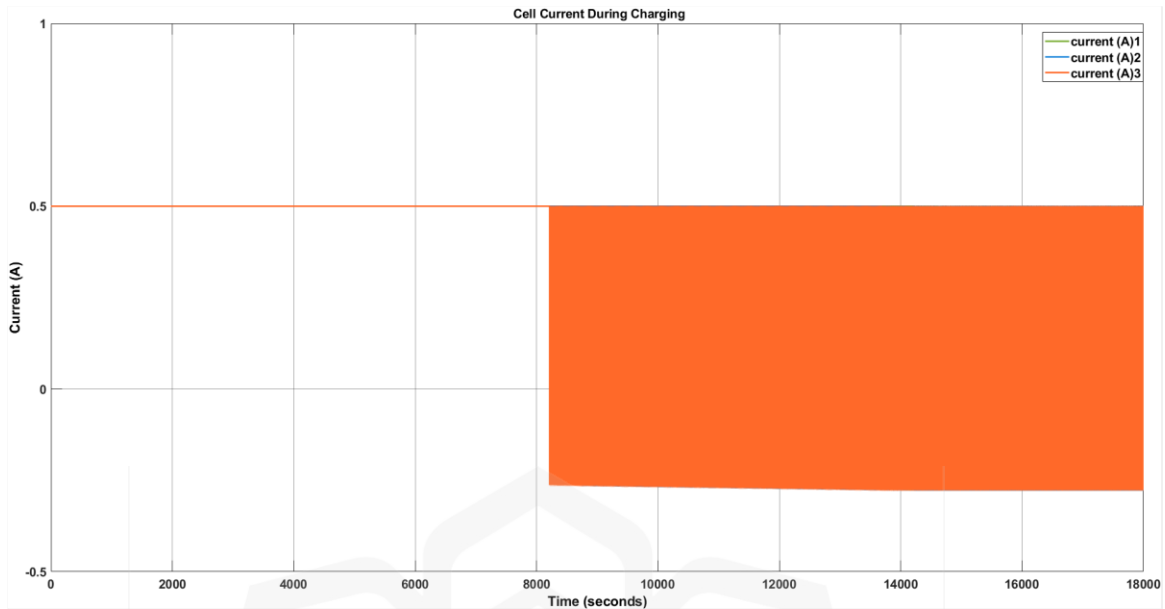


Figure 4.4 Cell Current During OCV Charging Simulation

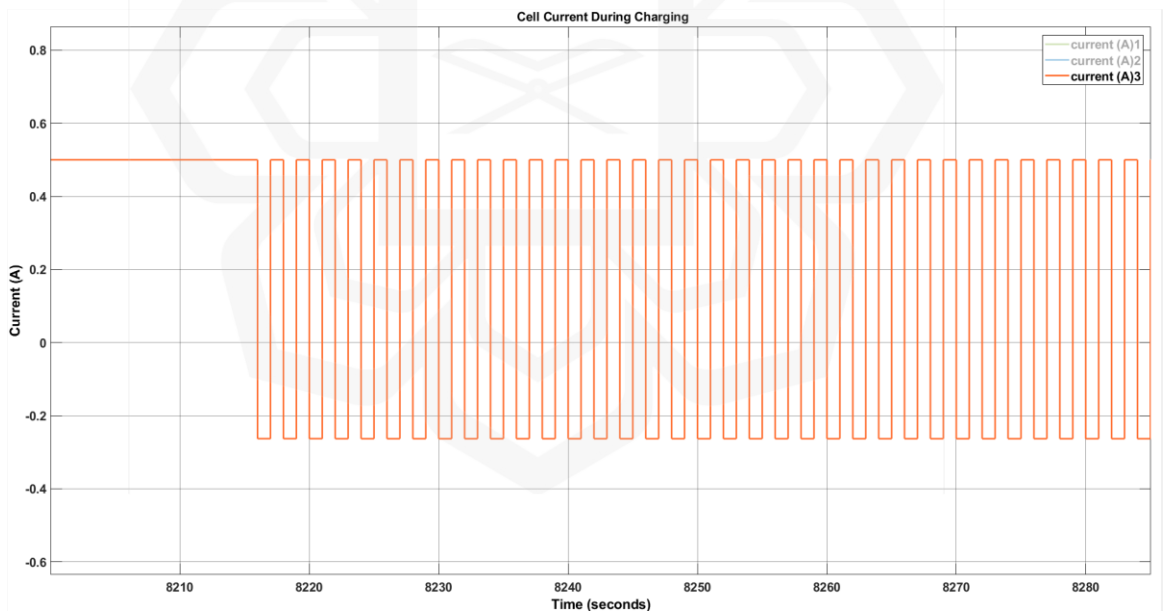


Figure 4.5 Close-up on Cell 3 Current During Balancing Process

The Figure 4.4 and Figure 4.5 above show the current profiles of the cells while they are being charged by OCV. The trend is one of steady current flow due to simplification of the simulation and when the OCV in one battery is higher than another,

the balancing circuits activate, and the current will drop to negative values indicate excess charge have been bleed out utilizing the resistors. Figure 4.5 highlights Cell 3, showing that there are drops in current every time the balancing resistor is used, in which shows that the balancing algorithm works to remove excess energy from the battery cell. The algorithm remains strong and reliable as long as the current flow is consistent.

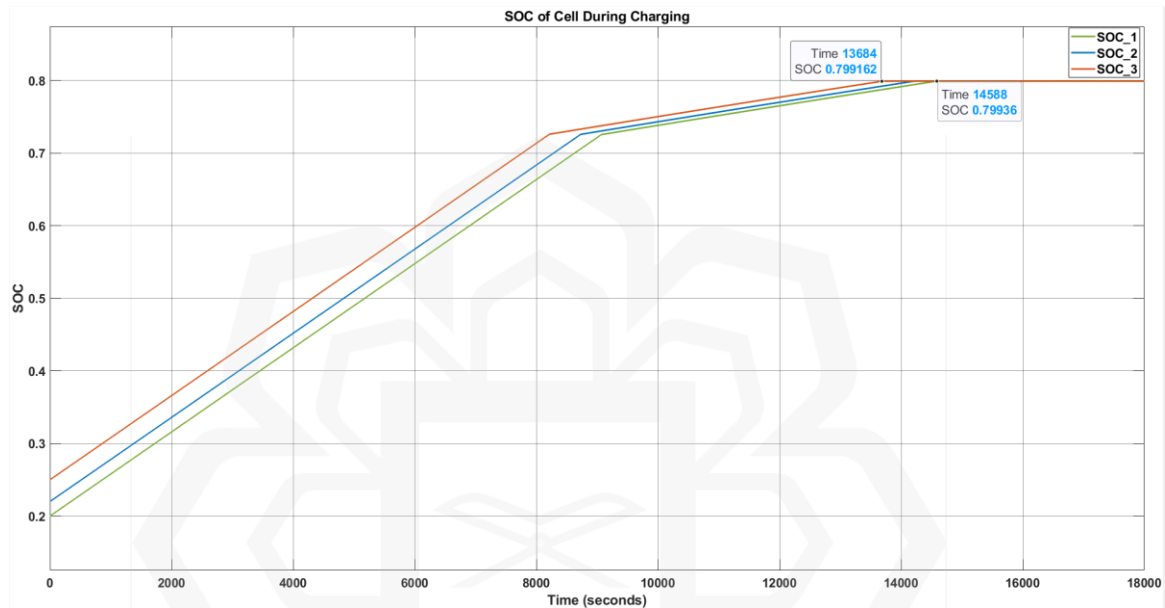


Figure 4.6 SOC of Each Cell for OCV Charging Simulation

The SOC value during charging is shown in Figure 4.6 and Figure 4.7. The SOC results were achieved by using the built-in feature of the MATLAB Simulink battery block that allows the direct extraction of SOC values based on the battery's internal settings. The findings of utilizing OCV estimation led to consistent SOC monitoring for all cells during its charging process while maintaining the SOC level to be around 79% to 80% of the safe range. Cell 3 was the first to reach approximately 0.8 SOC level at 13684 seconds (3.8 hours) and later then all the battery cells were fully charged around the 14588 seconds (4.05 hours). This observation is also crucial in comparing these two approaches in balancing the cells during the charging process. Moreover, we can see in Figure 4.7, the close-up figure demonstrates that the SOC have a high switching frequency corresponding to each event of the balancing act that occurred during the charging process. In Figure 4.8, the switching

frequency reached the point of 333.768 mHz during the balancing process, which will be the benchmark to be compared to the ML-SOC estimation results in further sections. Although the frequent changes in voltage help stabilize the battery, it may result in less efficient use of the battery and problems with long-term batteries and component longevity.

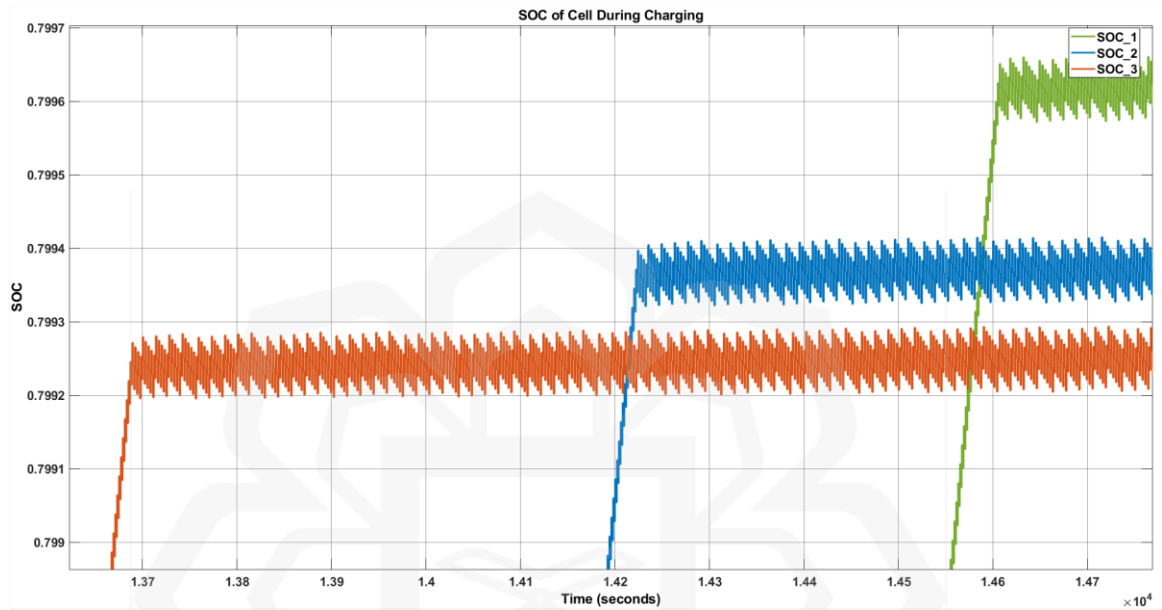


Figure 4.7 Close-up SOC of Each Cell During Charging

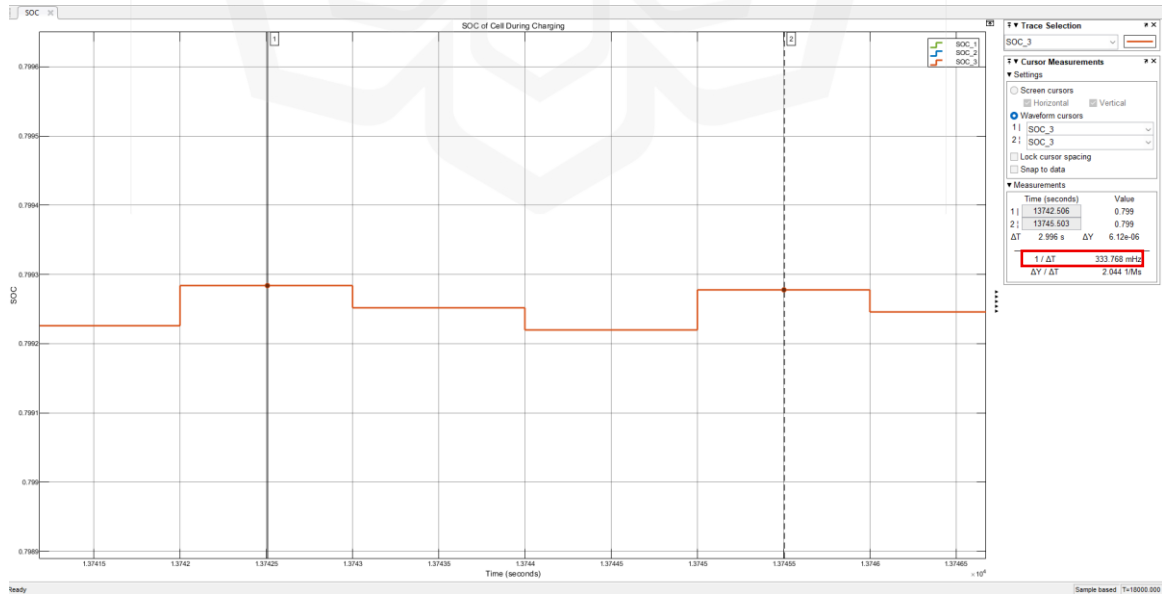


Figure 4.8 Measurement of Switching Frequency During OCV Balancing Process

Figure 4.9 illustrates the switching state signals during the OCV charging balancing process. The balancing algorithm will act as the controller which is able to switch on the MOSFET and making sure that the excess energy from the charging process. Switching devices often helps keep the battery balanced and almost equal but may increase losses in power and create more heat cycles for the switches. Therefore, the overall performance and usefulness of the BMS might be reduced in the long run. From Figure 4.10 provides a zoomed view of Switch 3's switching state during the active balancing phase, showing the rectangular pulse patterns that correspond to activation events. Both figures demonstrate the hysteresis-based control logic maintaining balance. A comparison between the OCV balancing approach and the ML-SOC balancing approach will be discussed in detail.

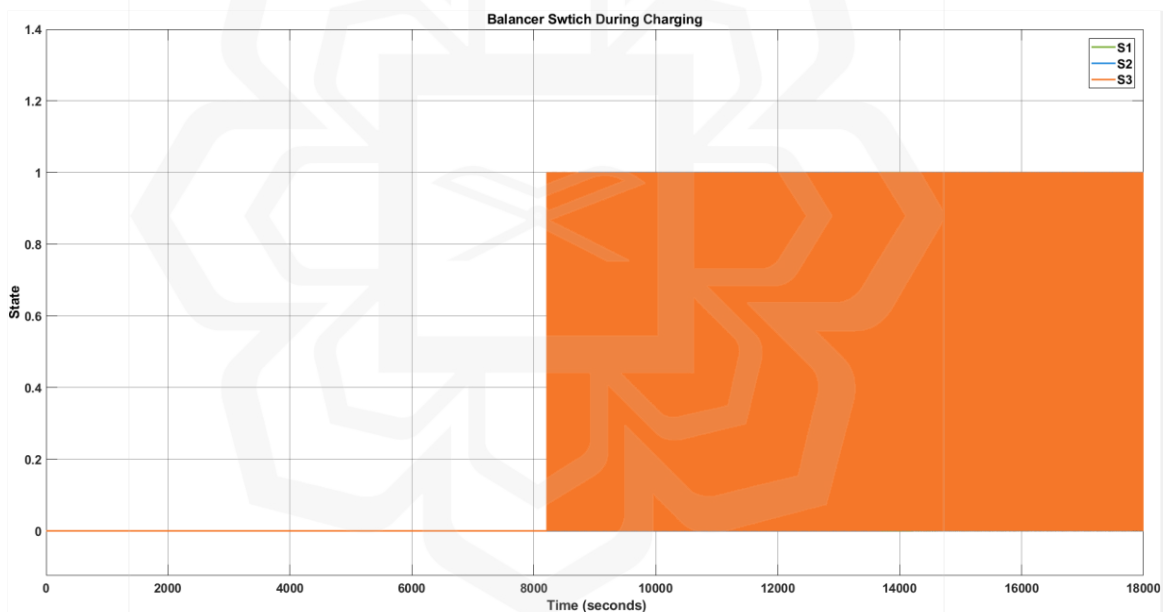


Figure 4.9 Switching State During Balancing Process

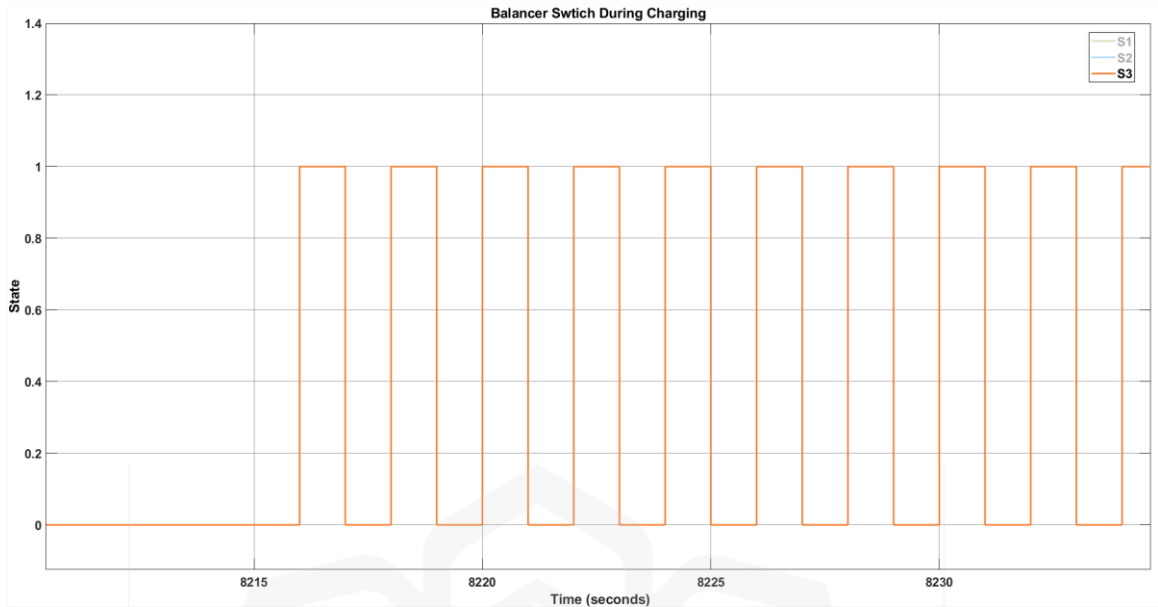


Figure 4.10 Close-up of Switch 3 Switching State During Balancing Process

Figure 4.11 and Figure 4.12 shows the power dissipated in the three balancing resistors (R1, R2 and R3) while the battery is charging. The waveform of the power profiles shows that the passive balancing circuitry is engaged only occasionally. Every resistor's peak dissipation is above 2W, and the switching happens together with the logic's control actions. Since waveforms are triangular, there are fast cycles where energy is dissipated to keep all cells at a balance voltage level. It confirms that balancing is active and reveals the speed and effect of the passive strategy on both time and temperature. Table 4.1 below shows the total average power loss for each key component that make up the balancing part of the BMS. The total power loss was around 2.22W which later was compared to the ML-SOC based simulation. The amount of power loss was calculated from the start of charging and at the point approximately when all the battery cells have been fully charged or at 80% of the cell SOC's.

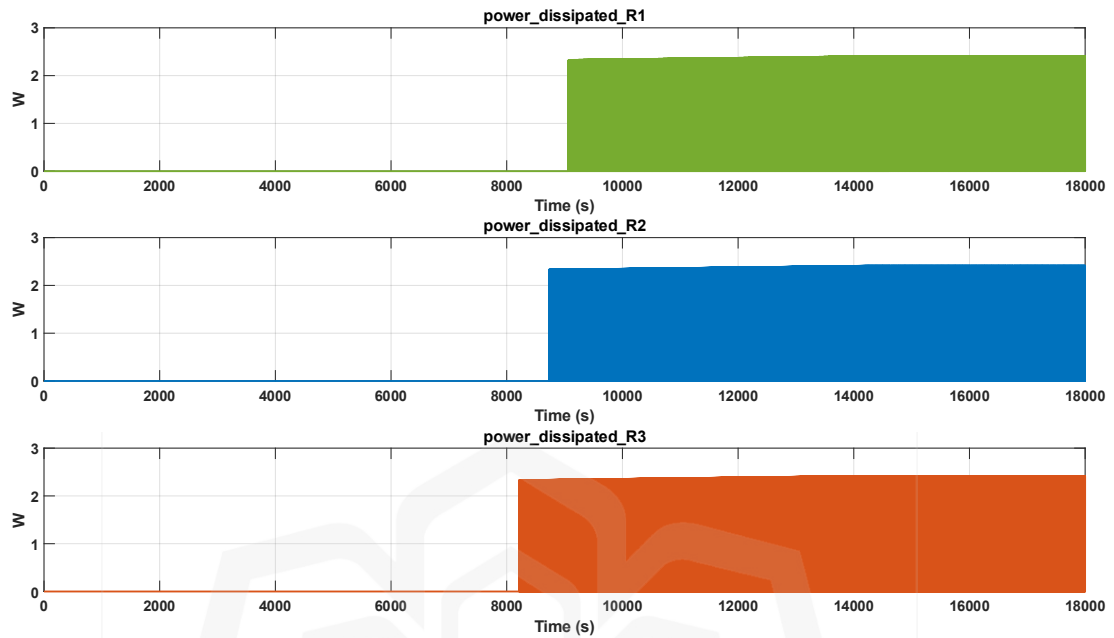


Figure 4.11 Power Dissipation of Balancing Resistors During Charging

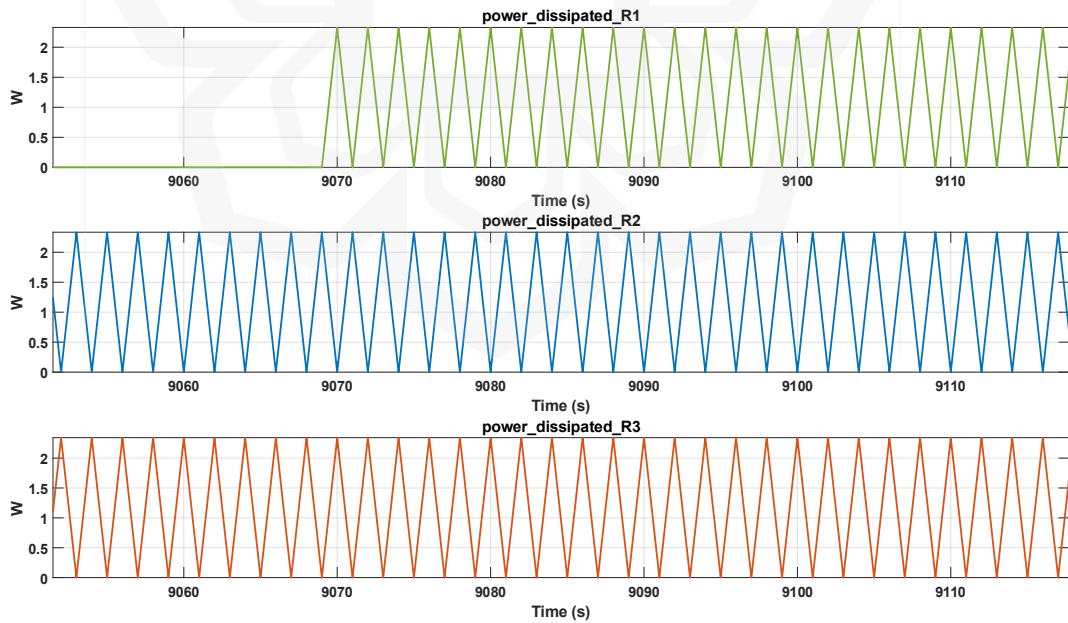


Figure 4.12 Close-up of Power Dissipation of Balancing Resistors During Charging

Table 4.1 Total Average Power Loss During OCV Charging

<b>Node</b>	<b>Average Power Loss (Watt)</b>
R1	0.54533
R2	0.56903
R3	0.62977
D1	0.14696
D2	0.16054
D3	0.16595
FET1	0.0014541
FET2	0.0015787
FET3	0.0016617
<b>TOTAL</b>	<b>2.22W</b>

Figure 4.13 represents the temperature changes of T1, T2 and T3 over the course of OCV charging. When the battery starts at 25°C, the temperature inside each cell slowly rises as a result of heating from the cells and energy dissipation from charging and balancing. Among the three, T3 shows the highest temperature of close to 28°C, while T2 and T1 reach slightly lower values. Changes in the thermal behavior of the cells are linked to individual cell impedance, the frequency of the current and the rate at which energy is lost. At the point of balancing has started, the temperatures remain high and gradually decrease, showing that heat is being controlled and the system is relying on proper heat dissipation and heat transfer between each cell. The temperature measurements indicate that the BMS helps the battery not to exceed safe temperatures, proving that the passive balancing strategy can meet thermal safety requirements during controlled charging.

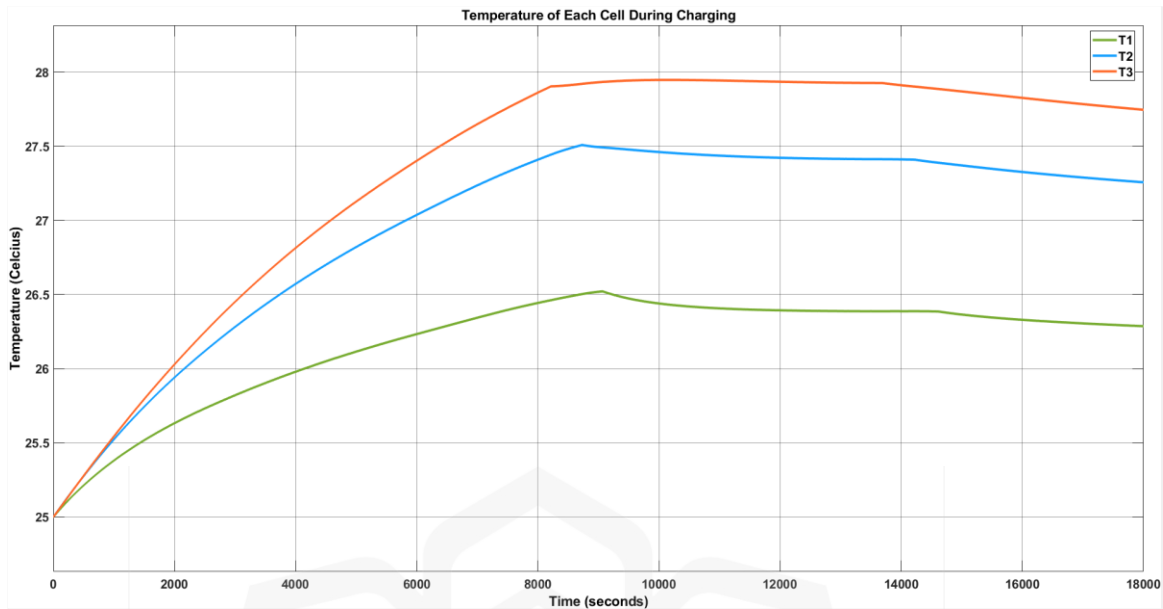


Figure 4.13 Temperature of Cell During OCV Charging

### ***B. Prototype Results***

In this test, a hardware prototype has been developed and tested using the same algorithm as the first OCV simulation test. The prototype was initially to evaluate that the simulation reflects real world applications such as a passive balancing BMS such as the developed prototype. Results shown in this subchapter observed the main functionality of the designed prototype in the important aspect of battery balancing during charging and also a protection test that prevents any overcharging to occur with the battery used in this experimental prototype testing.

The behavior of balancing during the charging phase is thoroughly examined in Figure 4.14, Figure 4.15 and Figure 4.16. The initial charging voltages for the cells were 3.88 V for Cell 1, 3.79 V for Cell 2 and 3.31 V for Cell 3. Figure 4.15 shows that Cell 1 reaches 4.1 V at 4579 seconds (1.27 hours) and Balancer 1 is then activated, putting it in the HIGH (ON) state. Red arrows in Figure 4.16 displays the protection monitoring interface showing the balancer activation status during the charging test. After that,

Balancer 2 takes action at 4.1 V when Cell 2 reaches 8859 seconds (2.46 hours). During this period, the system helps keep cell voltages similar by releasing excess energy as heat through special resistors in the BMS. It was confirmed that these resistors were working by feeling heat on contact when the balancers were in the HIGH (ON) state. The control mechanism stops charging when all balancers have reached their maximum voltage limits. The signal in Figure 4.16 clearly demonstrates that the CHARGMOSFET stops current from flowing to the battery, starting the deactivation of the charging circuit.

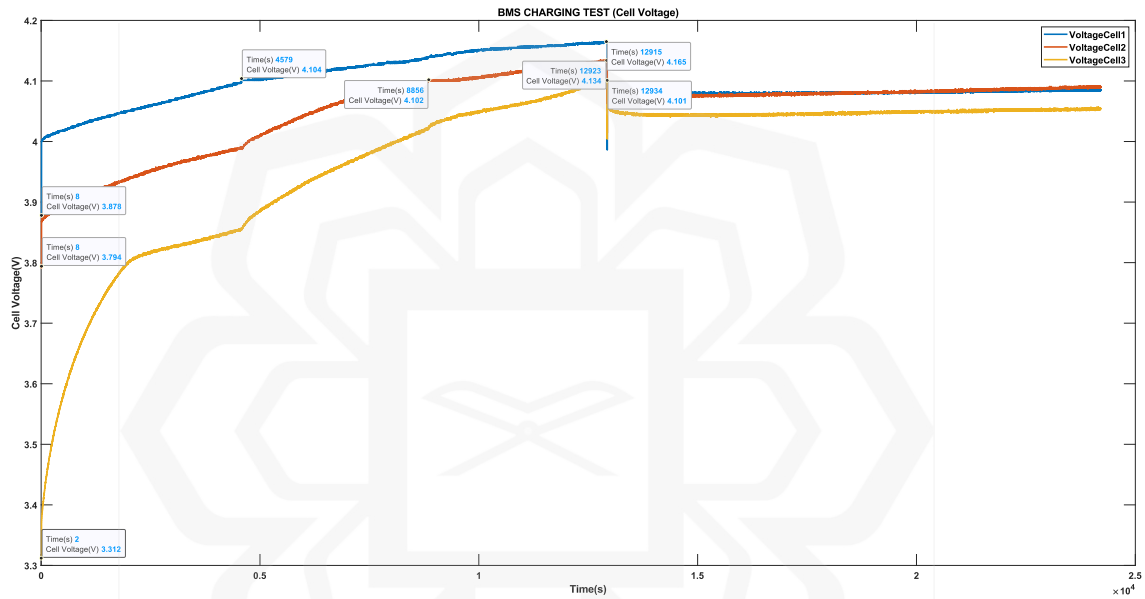


Figure 4.14 Monitoring of Cells Voltage During BMS Charging Test

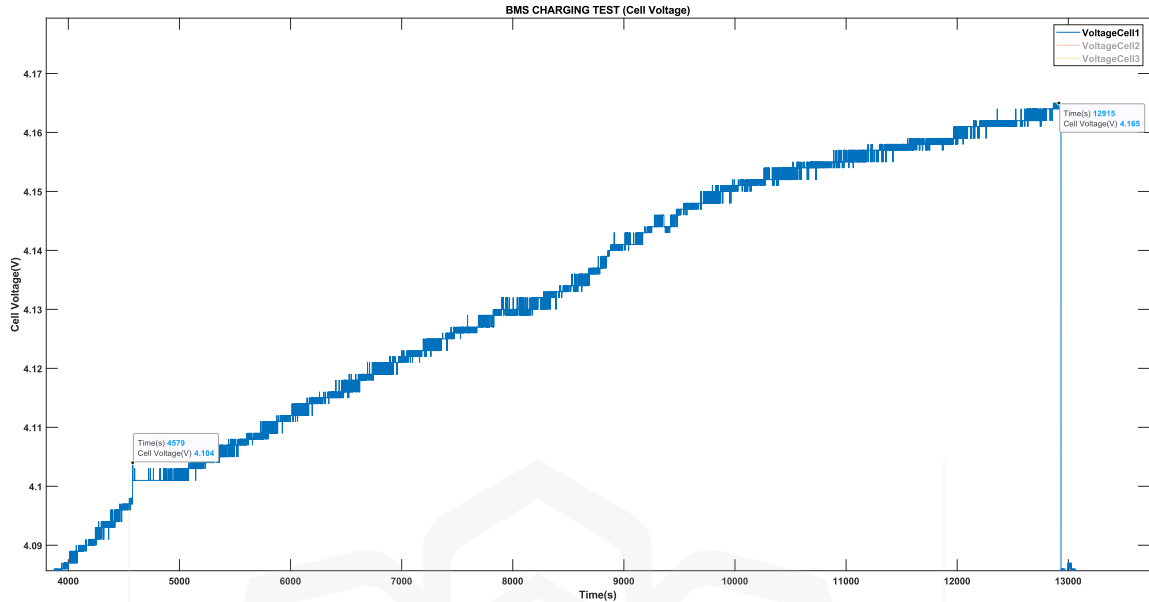


Figure 4.15 Close-up of Cell Voltage 1 During BMS Charging Test

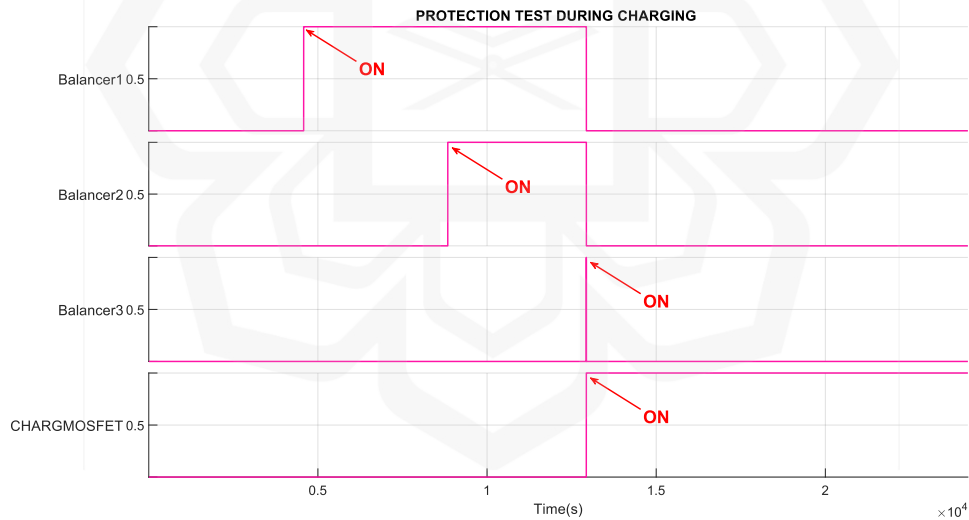


Figure 4.16 Protection Monitoring of Balancer Condition During Charging

The BMS prototype shown in Figure 4.17 includes indicator LEDs mounted on the balancing circuit board. The three green indicator LEDs correspond to the three balancing channels (one per cell); when an LED illuminates, it indicates that the MOSFET gate for that channel is receiving an activation signal, meaning the corresponding balancing resistor

is actively dissipating excess charge from that cell. The red LED indicates the charging status in which it remains illuminated during active charging and extinguishes when the charging process is complete. When multiple green LEDs are lit simultaneously, it shows that multiple cells are being balanced in parallel. These visual indicators provide real-time feedback confirming that the BMS control algorithm is functioning correctly and responding to voltage imbalances as designed. This helps to keep the battery safe, protected, and stay reliable for a longer period.

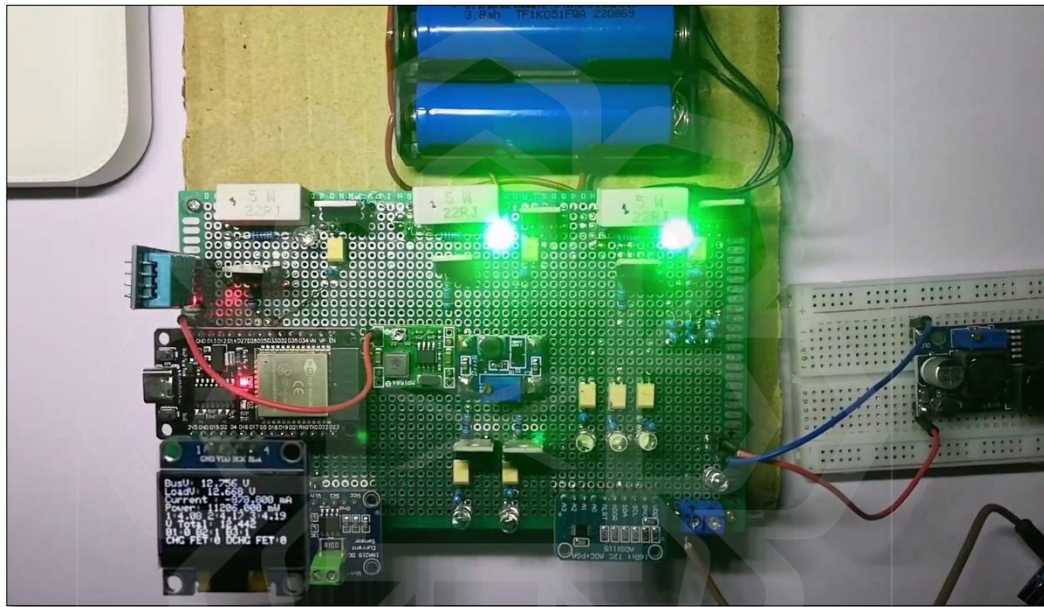


Figure 4.17 BMS Prototype Balancer Light Activate During Charge Balancing Process

### ***C. ML – SOC Estimation Results***

Moving on to the simulation results from the ML-based approach of estimating SOC for the battery cells. The model uses a trained machine learning network to estimate SOC and then uses that data to control balancing rather than depending on a direct voltage-SOC relationship, as in OCV simulation. The test is meant to check how well the ML-driven SOC estimation in which can help balancing strategy performs, responds and remains stable during charging in a controlled environment. Voltage stability, convergence behavior and

the real-time balancing effects are studied in a simulation environment if it can be used in future embedded BMS systems. The testing of ML-based SOC estimation with real prototype hardware was out of scope for this research due to limitations of time and resources.

In Figure 4.18 clearly shows the voltage of the cells over the whole charging process. At the beginning, all three voltages increase gradually as the battery is charged, although their levels can differ slightly due to differences in charge. Yet, when the cells get close to 4.01V, which is the maximum voltage set for 80% charged, active balancing events start to happen because of the ML-estimated SOC. The voltage response can be seen more clearly in Figure 4.19. When cells release power, the battery's voltage drops and then it is quickly brought back up by the others. This is because for this simulation, the balancing limit was not set according to its OCV value, but it is set to a limit that follows the estimated SOC predicted by the ML model. Because of this strategy, the system responds to predicted SOC in real time and prevents any cell from getting too high a voltage level, in which the results demonstrate that the new method supports the balancing strategy and also leads to better voltage control and safety.

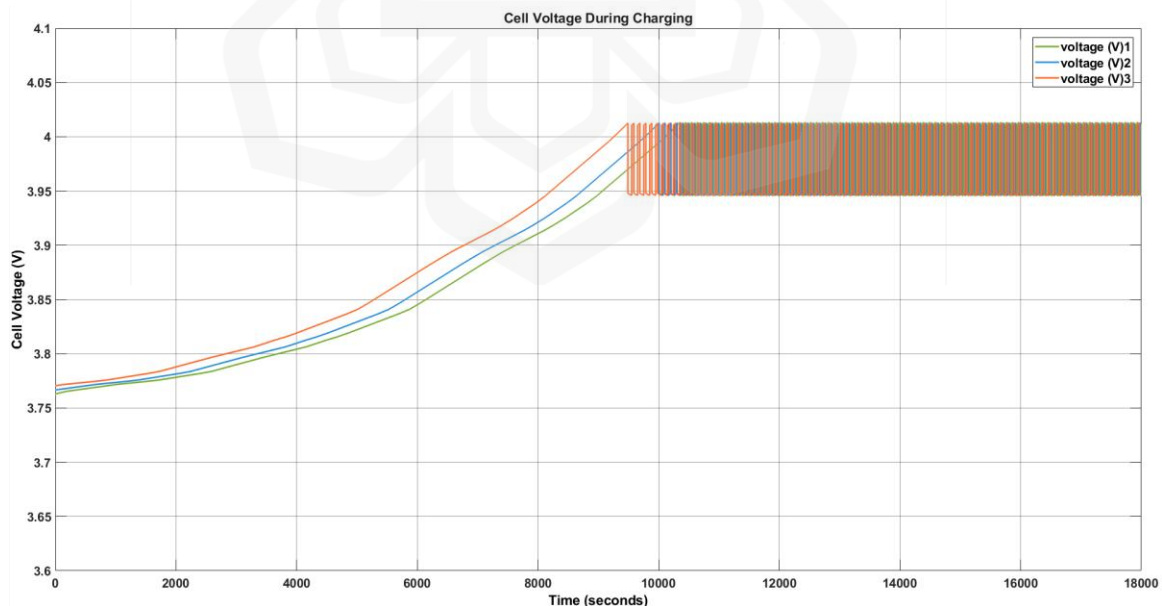


Figure 4.18 Cell Voltage During Charging for ML-SOC Simulation

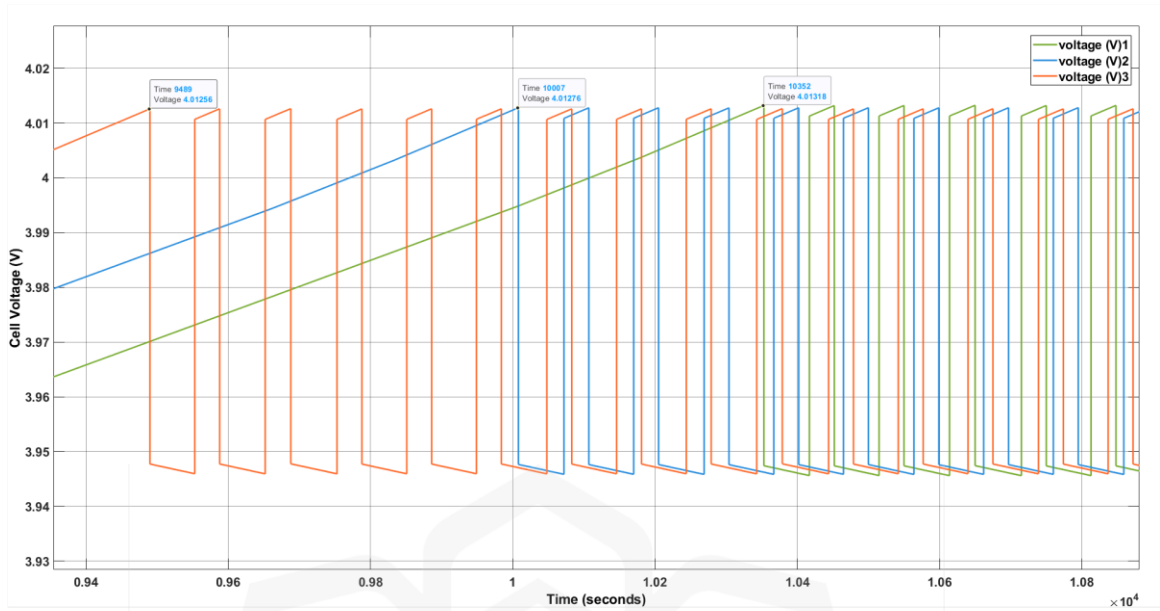


Figure 4.19 Close-up of Cell Voltage During Charging for ML-SOC Simulation

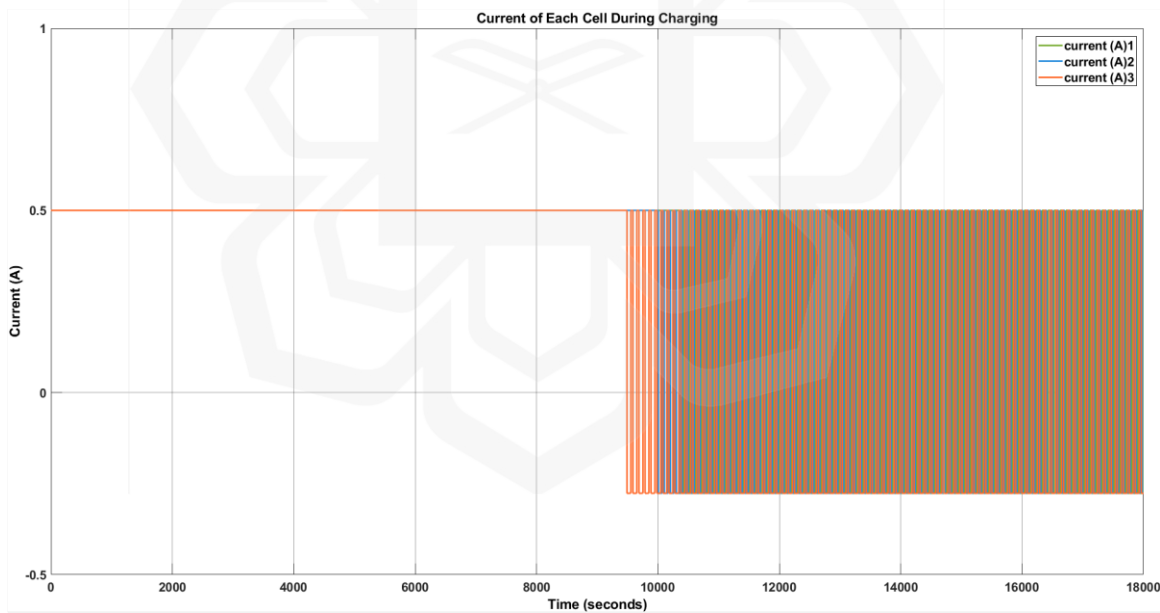


Figure 4.20 Cell Current During ML-SOC Charging

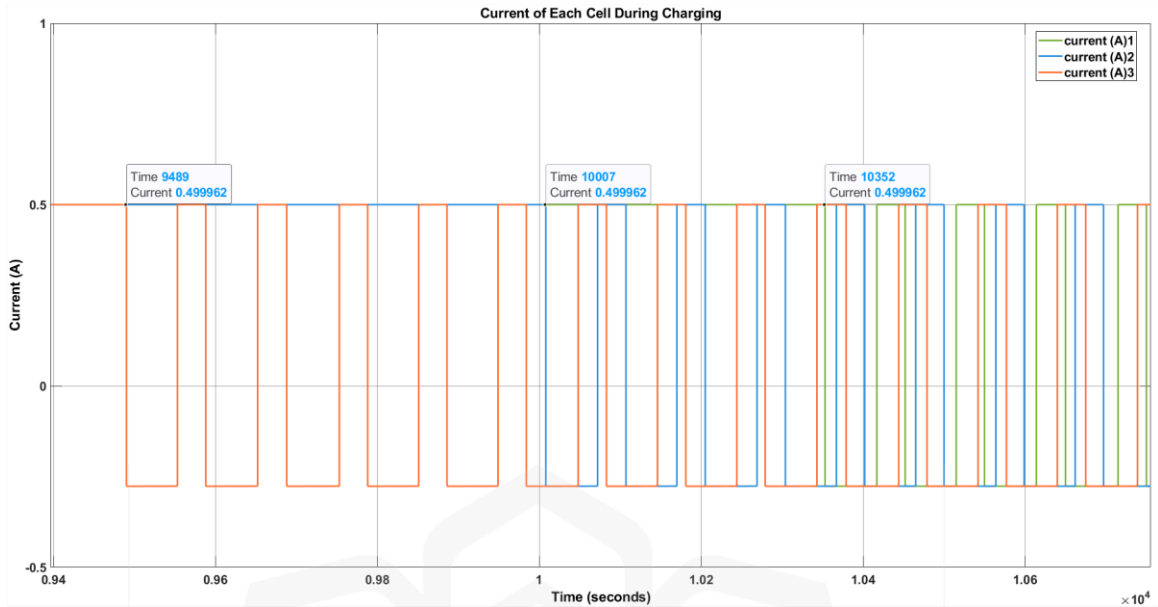


Figure 4.21 Close-up of Cell Current During ML-SOC Charging

Next, the current for each cell during charging can be illustrated in Figure 4.20 and Figure 4.21. The waveform shown are the same as the OCV simulation in which the battery was charged with 0.5A of current for approximately 18000 seconds (5 hours). However, a notable observation of the waveform is it exhibit more spaced out and with a noticeably higher duty cycle because the balancing process were trigger with a lower frequency. This proves that under the ML-SOC approach, balancing actions take place less often which increase the time between balancing events.

Furthermore, in Figure 4.22, Figure 4.23 and Figure 4.24, the observation of each cell's SOC during the ML-SOC charging simulation. All three cells in Figure 4.22 have their SOC increase linearly in the first charging phase and reach around 0.8 before starting the balancing process. The observation can be compared to the OCV simulation results in Figure 4.6 which for this simulation test, the cell reached the optimal charge level faster than the OCV approach. As illustrated in Figure 4.22 and Figure 4.25, the first cell reach 80% charge at time 9489 second and all the battery cells were fully charged at time 10352 second, hence beating the time needed to fully charge the battery cell compared to the OCV balancing approach by 29.0% of improvement . The fact that the method indicates that the

ML-based estimation method reliably tracks the SOC across all the battery cells. Once the cells get close to being fully charged, the balancing logic activates to prevent them from charging further and being overcharged. Figure 4.23 gives a closer look at the balancing phase of the SOC in which it be seen typical triangular oscillations in the waveform. When these fluctuations occur, it shows that the balancing circuits are being turned on and off from the ML predictions of the battery’s SOC in which follow the set hysteresis band. It is worth noting that SOC of all cells remain near 0.8, showing that the ML algorithm keeps all the cells charged at a similar level. Figure 4.24 shows the switching frequency during the process of balancing the battery’s state of charge. The frequency based on the interval between SOC peaks and troughs is approximately 10.208 mHz which the lower frequency of switching means the power system is balanced and gentler to the balancing components, thus reducing wear on the switch. It is likely that the ML model values steady and stable performance over quick convergence during balancing in which ML-SOC based approach achieves roughly a 97 % lower switching frequency compared to the OCV-based method.

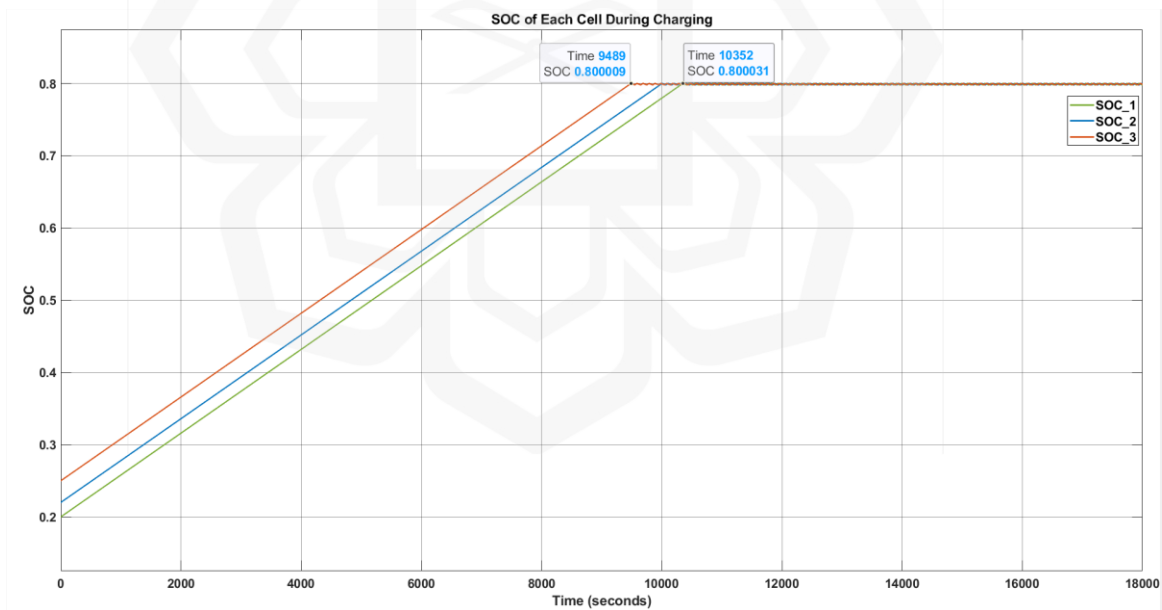


Figure 4.22 SOC of Each Cell During ML-SOC Charging

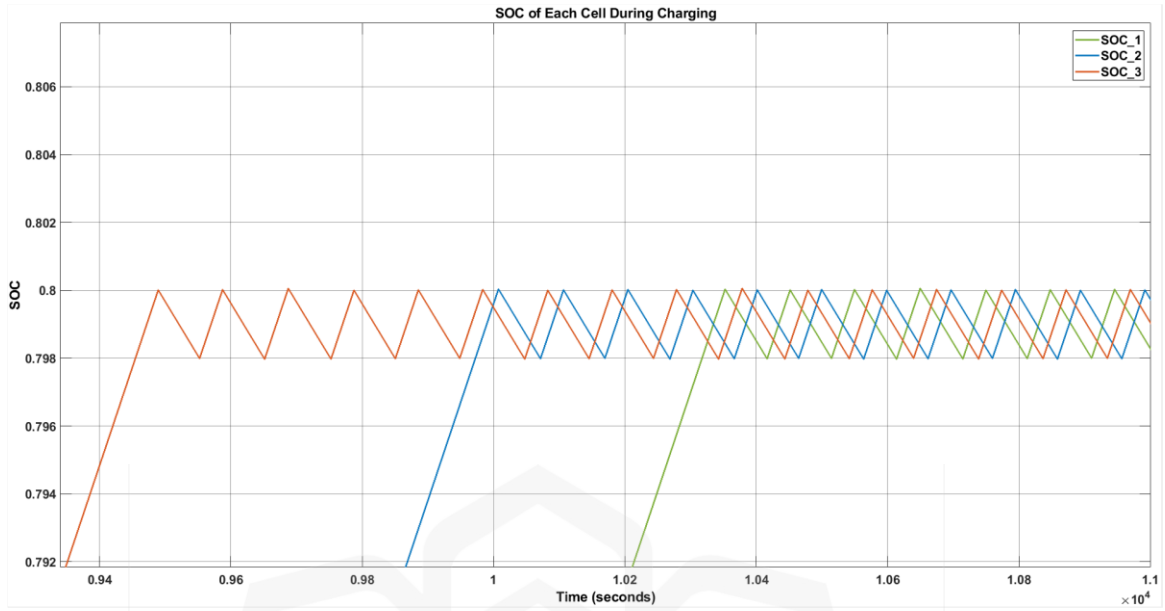


Figure 4.23 Close-up of SOC of Each Cell During ML-SOC Charging

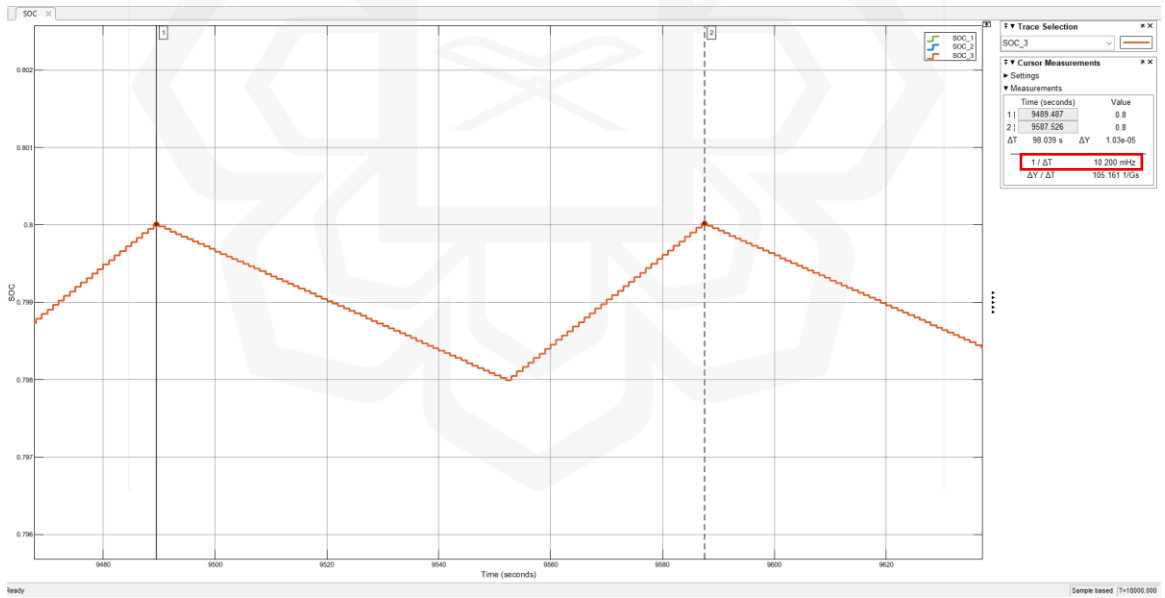


Figure 4.24 Measurement of Switching Frequency During ML-SOC Balancing Process

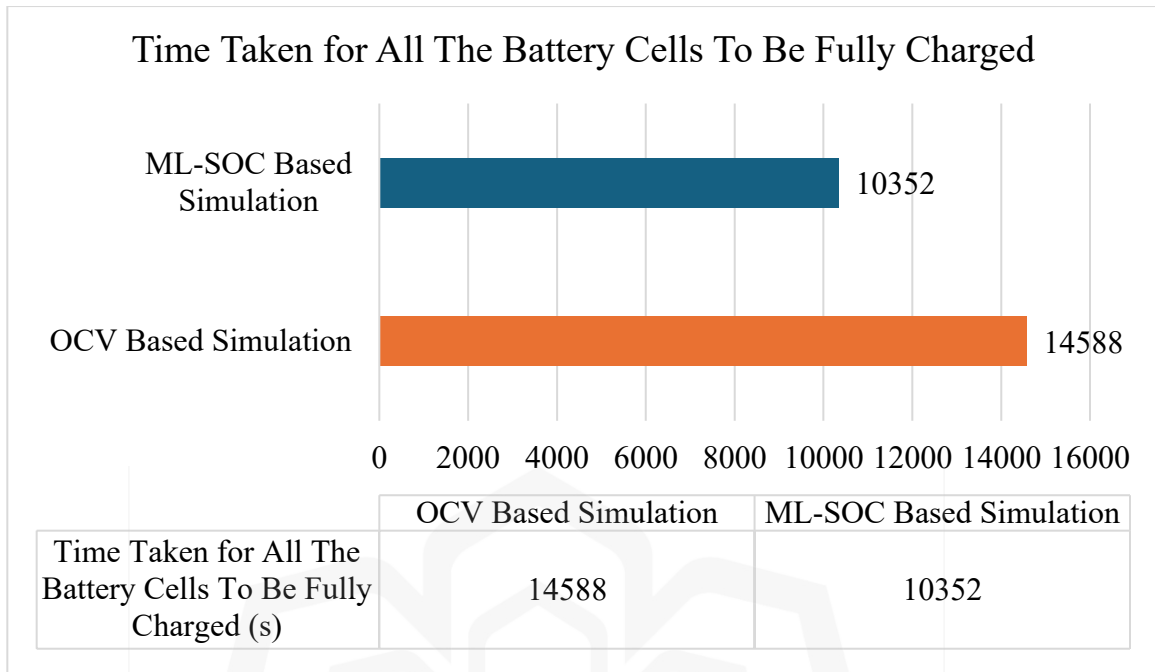


Figure 4.25 Comparison of Time Needed to Fully Charge the Battery Cells

The graph in Figure 4.26 demonstrates the difference in switching frequency when charging with the OCV approach versus the ML-SOC approach. In the OCV simulation, the switching frequency was 333.768 mHz which is much higher than the 10.208 mHz that is found in the ML-SOC simulation, demonstrating the main difference between the two approaches. Because of this method, the system regulate and balance each cell to maintain a more consistent voltage and SOC within the upper limit set during the charging process. Therefore, ML-SOC is preferred because the switches does not activate at high frequency compared to the OCV simulation test, in which this may help to save energy and ensures all parts are not overworked. As a result, it is evident that better performance overtime can be achieved with a lower switching frequency in BMS MOSFETs that can have a high impact on the long-term system performance which can lead to overheating and gradual degradation of the switches' reliability in the long run (Morel & Morel, 2025).

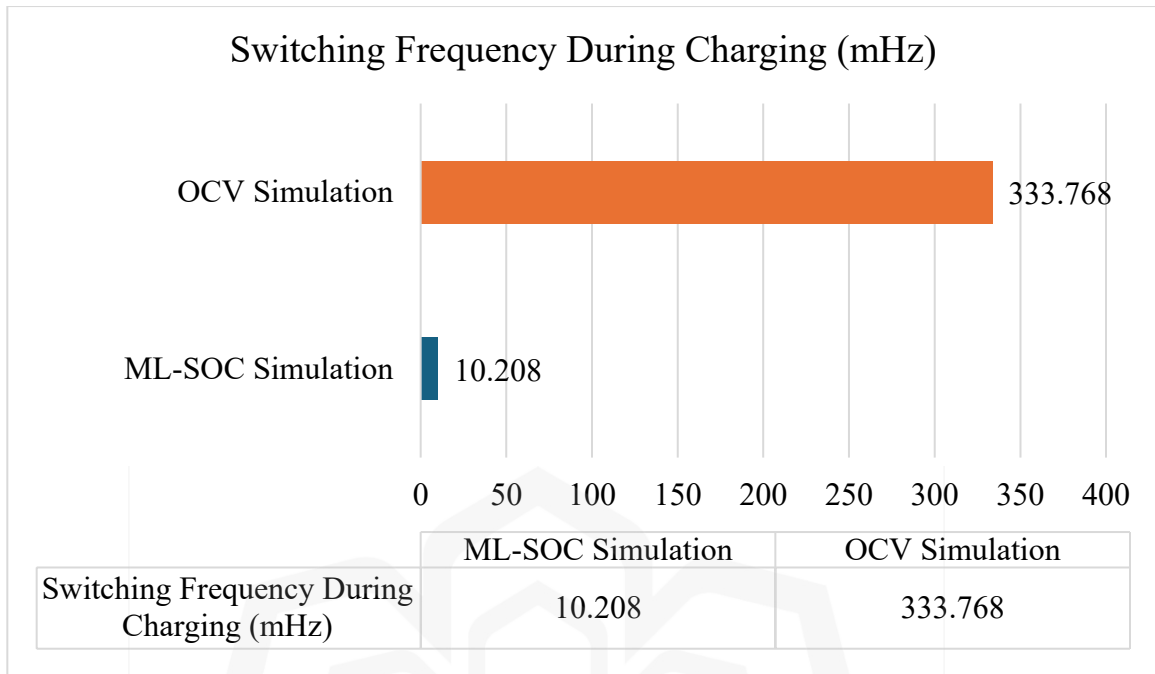


Figure 4.26 Frequency Comparison Between the OCV vs ML-SOC During Charging Simulation

Additionally, it can be observed in Figure 4.27 and Figure 4.28 that the switching state for each balancing MOSFETs occurs around the 9500 seconds (2.638 hours) mark for S3 and followed by the other switch S2 and S1. The switching simulation exhibits a lower switching frequency than the first OCV simulation which can also be reflected in the power dissipation by the bleeder resistors results in Figure 4.29 and Figure 4.30.

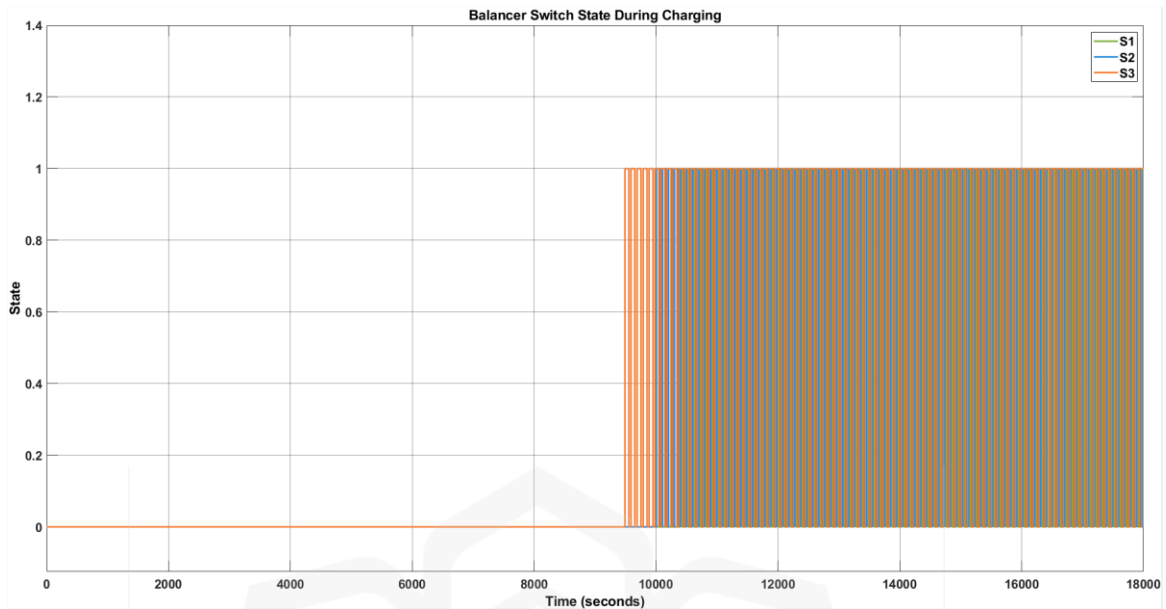


Figure 4.27 Switching State During Balancing Process of ML-SOC Simulation

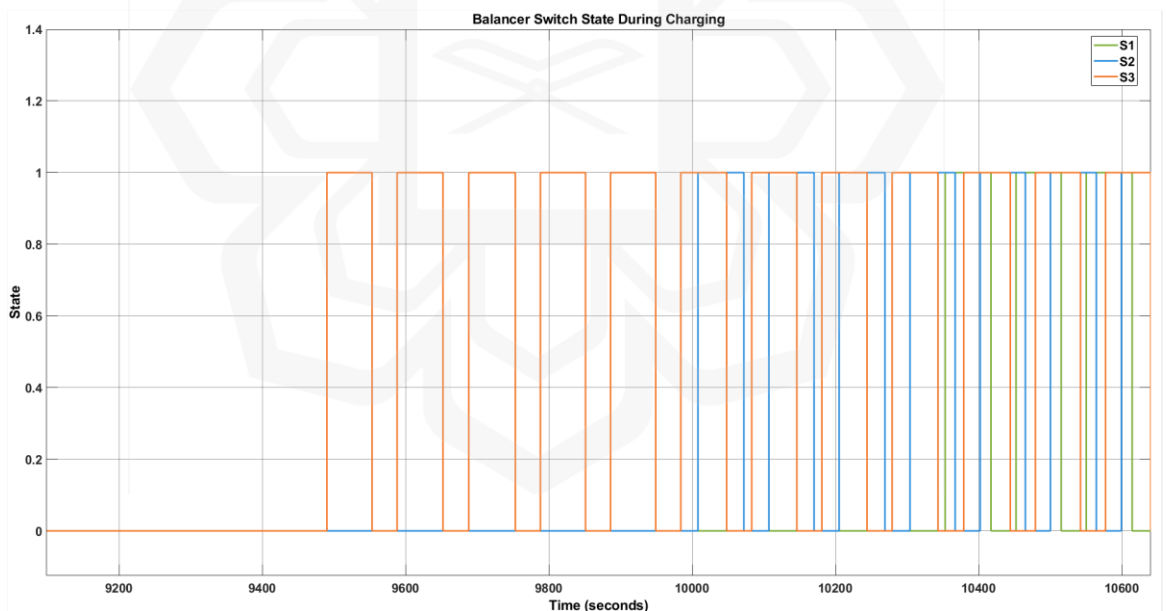


Figure 4.28 Close-up of Switching State During Balancing Process of ML-SOC Simulation

Notably, the frequency at which the battery is switched on and off is slower in the ML-SOC method than it was in the earlier OCV-based simulation results. This implies that the ML-based SOC estimation helps the system recognize only major imbalances which

prevents frequent and unnecessary switch operations that will have more power loss. Therefore, the switching behavior is not as active and jumpy which can have a direct effect on the system's performance and temperature. Figure 4.29 and Figure 4.30 make it clear that the power dissipated by R1, R2 and R3 tracks the expected switching events and has a square-wave shape. The square-waves prove that the resistors are in action only during the pulses rather than continuous non-stop pulses. As a result, components work more efficiently for a longer period and the balancing circuit uses less energy in which fewer switches per second helps reduce the pressure and overload on the MOSFETs and their power losses.

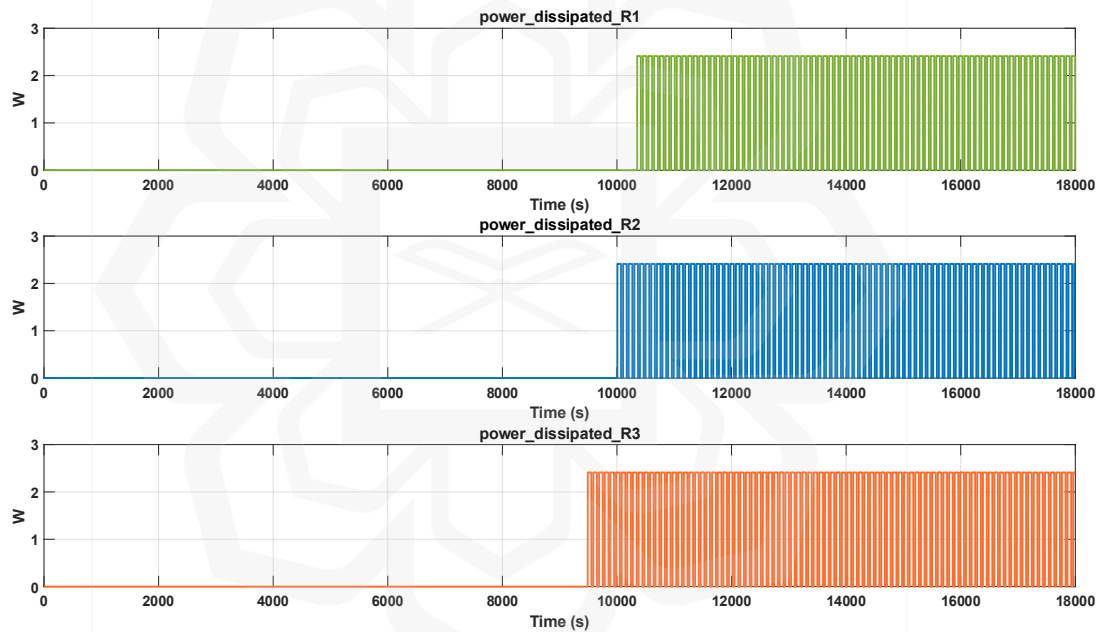


Figure 4.29 Power Dissipation of Balancing Resistors During ML-SOC Charging

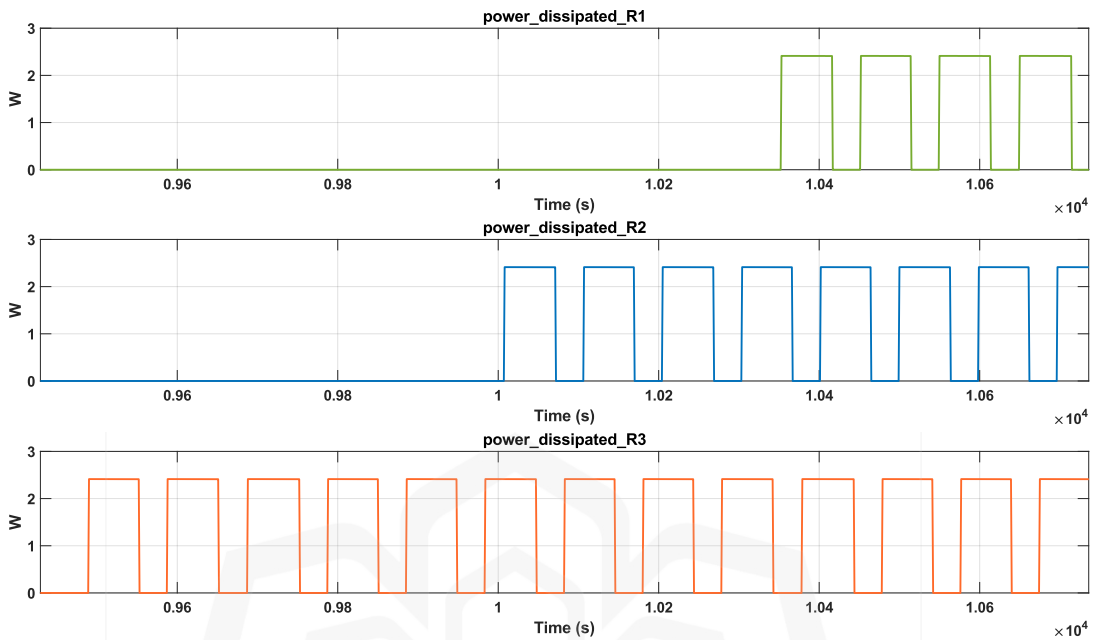


Figure 4.30 Close-up of Power Dissipation of Balancing Resistors During ML-SOC Charging

Table 4.2 shows the average amount of power lost during the ML-SOC based charging simulation. For the balancing process, the losses are shared by different nodes, but most of them are found in the resistive elements in which the bleeding resistors are noted by R3, R2 and R1. The diodes D1, D2 and D3 lose between 0.027309 W and 0.069507 W, while the MOSFETs do not lose much power which is all below 0.0005 W. All the components in the circuit together lose an average of 0.4218 W during ML-SOC charging process. The OCV-based simulation had much higher losses at similar nodes compared to the measured values in which the OCV situation, the system loses about 2.7383 W, meaning that the main cause is the constant balancing taking place at a higher frequency compared to the ML-SOC based approach. The increased power dissipation happens because the OCV-based approach is less adaptable and relies on fixed voltage thresholds to trigger the balancing algorithm, without considering the changes in battery states. Unlike the first method, the ML-SOC approach uses a variety of inputs to determine the SOC of the cell, resulting in less energy being lost through the balancing resistors. In addition, the drop in losses at the diode and MOSFET levels implies that the circuit operates

more efficiently and produces less heat when using ML-SOC. In other words, the ML-SOC balancing strategy cuts the overall power dissipation by roughly 81% compared to the OCV-based method. It makes better use of energy and supports the long-term operation of the battery's components, as well as better heat management.

Table 4.2 Total Average Power Loss During ML-SOC Charging

<b>Node</b>	<b>Average Power Loss (Watt)</b>
R1	0.025839
R2	0.10176
R3	0.15127
D1	0.069507
D2	0.027309
D3	0.045085
FET1	0.00017948
FET2	0.000366211
FET3	0.00048784
<b>TOTAL</b>	<b>0.4218W</b>

Figure 4.31 illustrates the temperature variations of three cells as they charge with the ML-SOC balancing strategy. All three cells begin at 25 °C ambient temperature and as time progresses, the temperatures differ depending on how much bleed and the internal resistance changes from the balancing process. So, since the battery is fully charged, the heat stops increasing and the system cools down any remaining heat which causes the temperature to drop by approximately 0.3 – 0.5 °C in all cells during the last section of the charging process in which the ML-SOC approach reduces thermal stress and helps to keep all the cells at the same temperature and enhancing its lifespan.

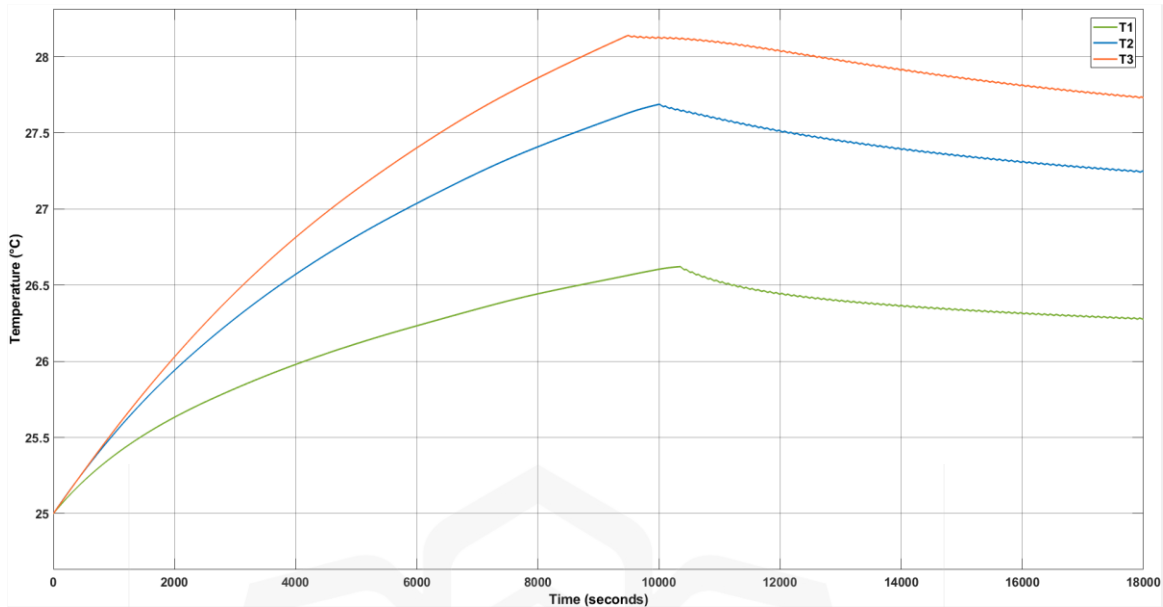


Figure 4.31 Cell Temperature During Charging

## 4.2.2 Discharging Results

In this subsection, a detail the discharging simulation performed on the three-cell battery stack under a constant-current draw, serving primarily to validate the BMS’s cutoff functionality and to establish a baseline and SOC behavior prior to balancing analysis. The MATLAB/Simulink model applies a uniform 0.5 A discharge current to each cell and monitors terminal voltage, cell current, and state of charge until the most depleted cell reaches the prescribed cutoff of 0.20 SOC. The result will be later discussed in the next section for each of the tests from the simulation test and also from the experimental prototype test. It is noted the prototype test will focus on how the BMS protect the battery in preventing overdischarging.

### A. Simulation Results

The discharging simulation is an important part of a BMS, but this simulation were tested to observed the cutoff limit and to obtain a reference response from all cells during constant

current flow in order to protect the cell from overdischarging. In the discharge simulation, each cell is supplied with a constant current of 0.5 A, leading to an even decrease in both cell voltage and state of charge. As seen in Figure 4.32, all the cell voltages drop from their starting levels ( $\approx 3.91$  V, 3.88 V, 3.91 V) to about 3.67 V by the end, due to the equal current being introduced to each of the cells. Figure 4.33 demonstrates that the current in each cell is always -0.5 A (with overlapping plots), suggesting that the discharge current is constant throughout the simulation. As a result, Figure 4.34 shows how the SOC decreases linearly from 0.80, 0.78 and 0.75 to 0.20, at which point the BMS stops discharge to keep the battery from overdischarging that could damage the cells if it is not prevented. The BMS algorithm have been set to be able to cut off the discharging while ensuring the battery does not run too low, avoiding any cell damage.

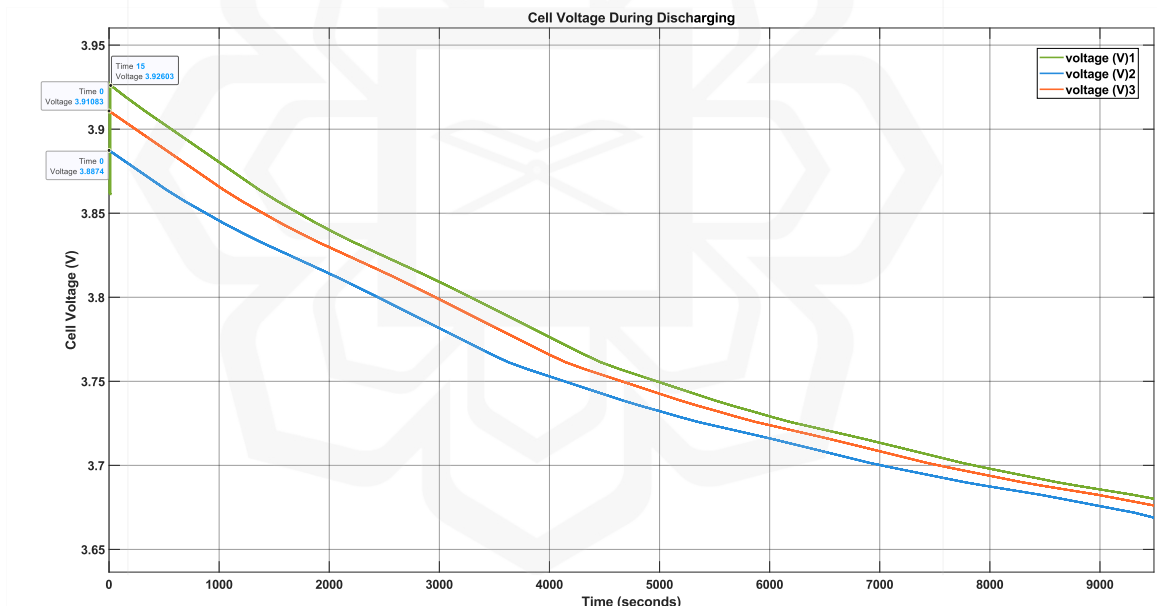


Figure 4.32 Cell Voltage During Discharging Simulation

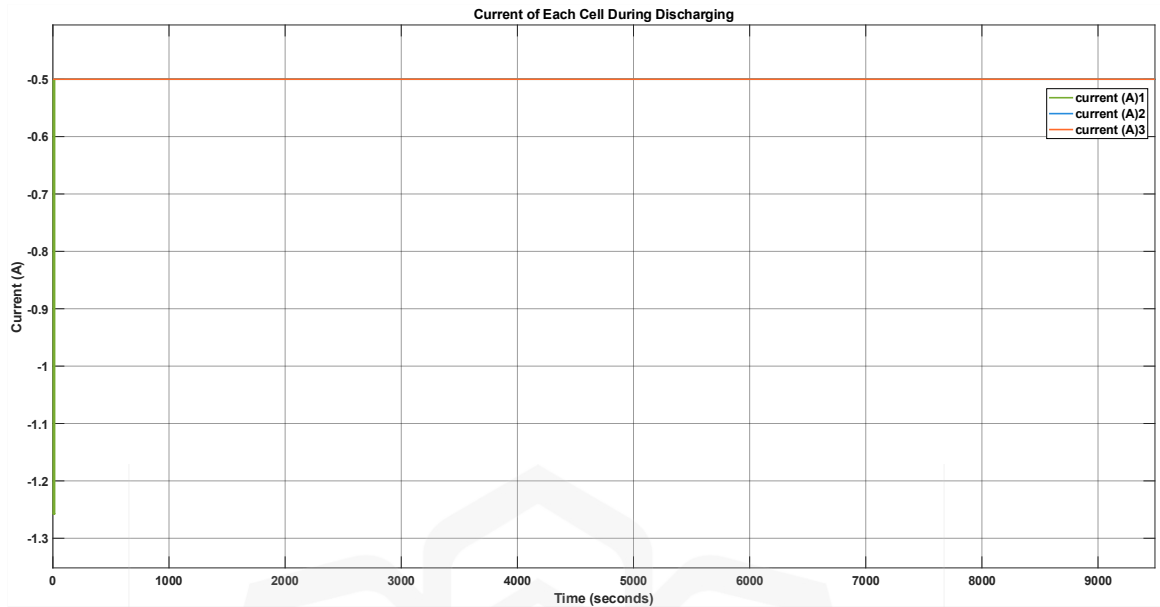


Figure 4.33 Cell Current During Discharging Simulation

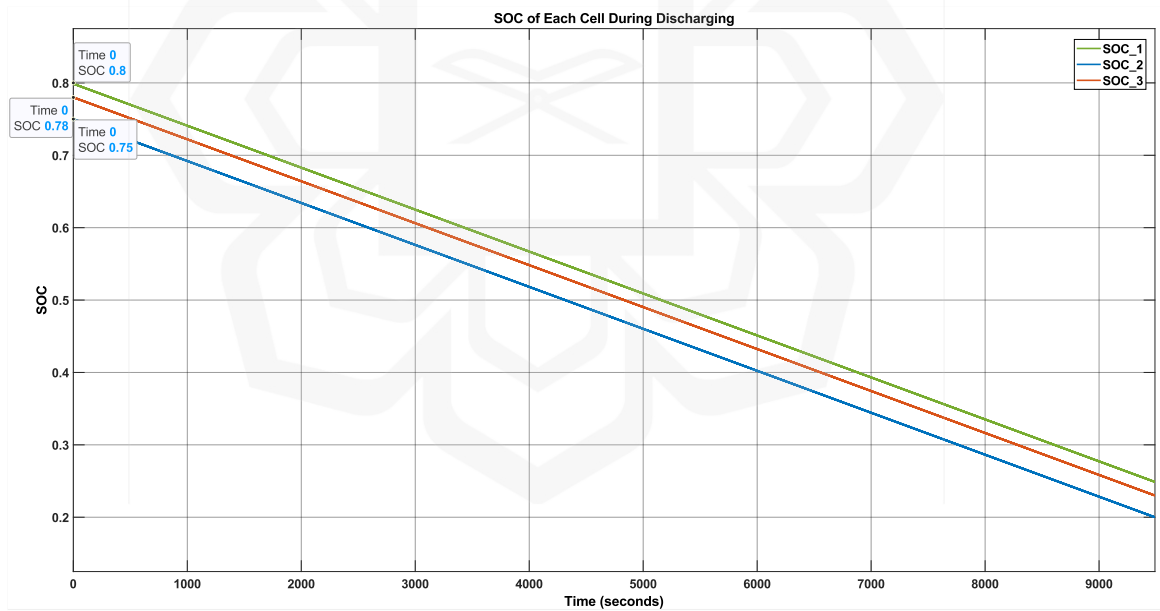


Figure 4.34 SOC of Each Cell During Discharging Simulation

## B. Experimental Prototype Results

This section explains the results and analysis of the monitoring test carried out as the battery was discharging. The experimental test was done to find out if the BMS was able to monitor the voltage of each cell correctly and offer a stable supply of electricity to the connected load. As shown in Figure 4.35, the cells were discharged using initial voltages of 4.00 V, 3.96 V and 3.86 V for Cells 1, 2 and 3, respectively. It took about 30 minutes for the entire discharge sequence and Figure 4.35 and Figure 4.36 illustrate the voltage of the cells and the overall performance of the system during the discharging process.

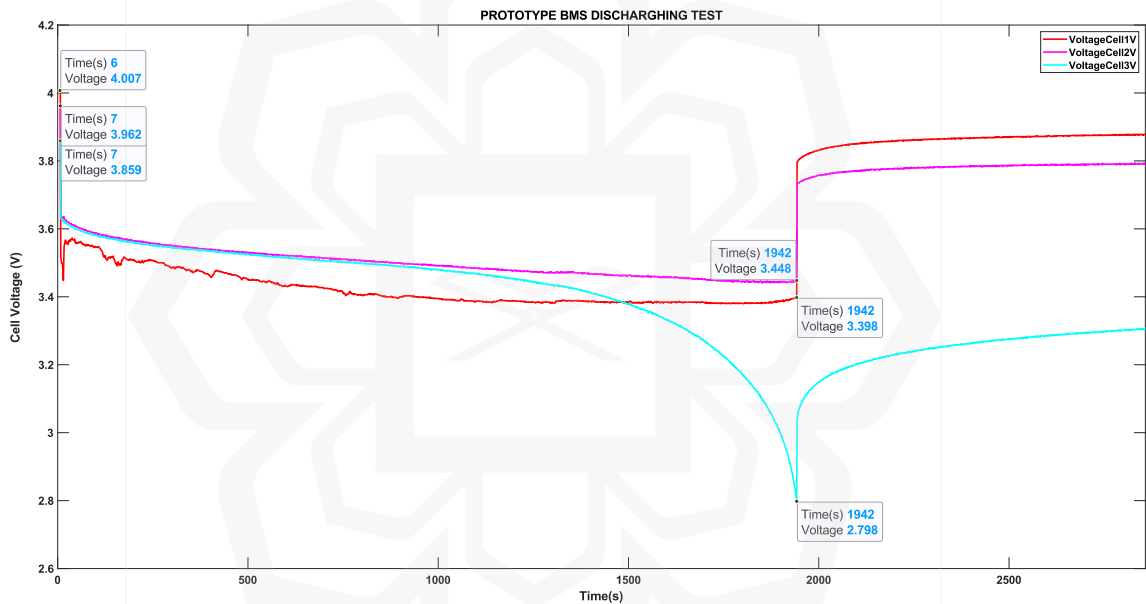


Figure 4.35 Cells Voltage During Experimental BMS Discharging Test

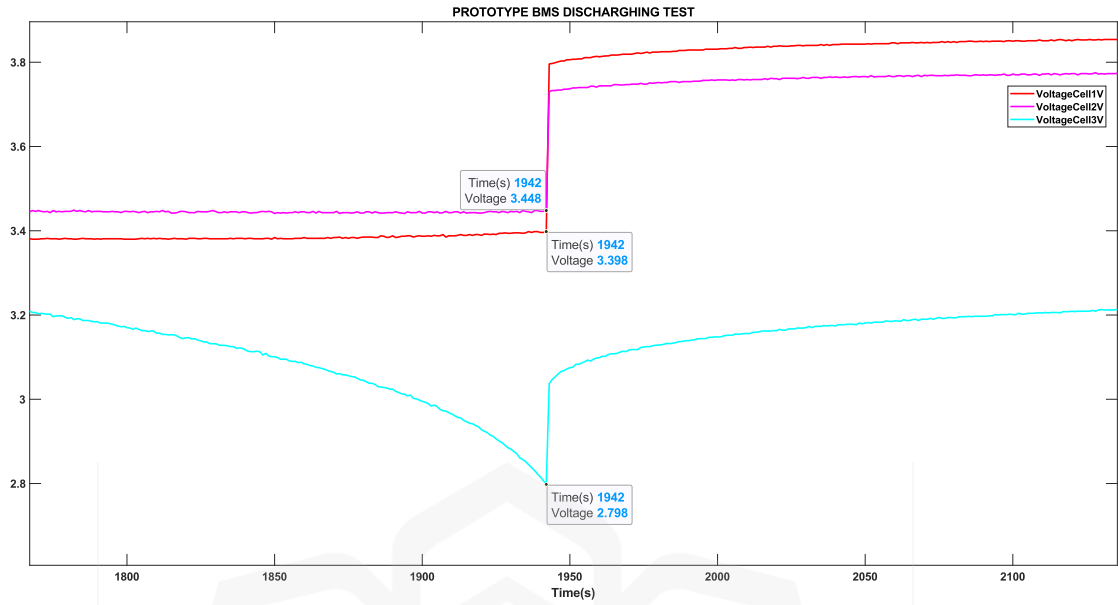


Figure 4.36 Close-up of Cell Voltage During BMS Discharging Test

Next, the results and analysis of the protection test conducted during the discharging process of the battery are presented below in Figure 4.37 and Figure 4.38. The main objective of this test was to assess the effectiveness of the BMS in protecting the battery against potential hazards, such as overvoltage. The test involved subjecting the batteries to a 10W load that would drain the batteries during the test. As can be seen in Figure 4.37, the batteries have been discharged with a current measurement of 1011.9mA and with the power that measured 10682mW on the initial discharge. The discharging phase took about 1942 seconds or 32.36 minutes, which triggered the auto protection system of BMS. As the graph above shows, both current and power consumption dropped to zero.

In addition to that, the auto cut-off from overdischarging can be shown in detail in Figure 4.38. The graph shows that the DISCHARGMOSFET has been triggered to turn OFF the outgoing flow of current and supply to the load as soon as the condition of any one of the cells reaches below 2.80V, and as depicted in the figure below, the DISCHARGMOSFET cuts off the supply when the voltage of cell3 reached 2.798V during discharging. Thus, it is proven that the overdischarge protection system was working as intended.

The next section explains the results and analysis of the protection test done during the battery's discharge phase which are shown in Figure 4.37 and Figure 4.38. The main reason for this evaluation was to determine if the BMS could protect the battery against damage, especially overdischarge. A 10W load was applied to the battery pack during the test to start the controlled discharge of energy. As shown in Figure 4.37, the first discharge had a current of about 1011.9 mA and an output power of 10,682 mW. After the discharge took 1942 seconds (32.36 minutes), the BMS activated its protection mechanism and both current and power fell to zero.

More evidence of the overdischarge protection feature is provided in Figure 4.38. The system responds to protect the battery when the voltage of any cell drops below 2.80 V. The voltage in Cell 3 was 2.798 V which made the DISCHARGMOSFET stop the current from going to the load. The result proves that the overcharge protection logic in the system is reliable and effective at avoiding overcharging the battery under a continuous load.

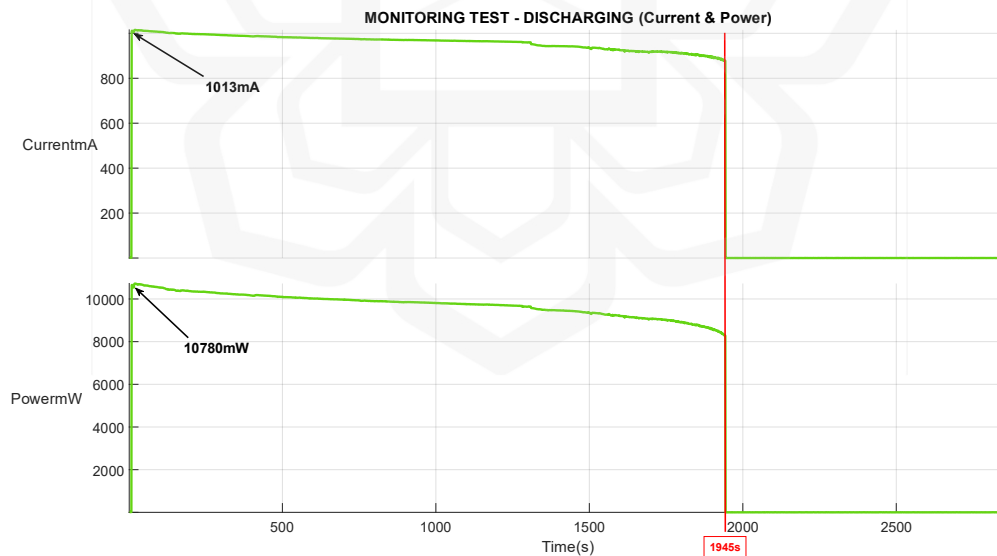


Figure 4.37 BMS Monitoring of Current and Power Used During BMS Discharging Test

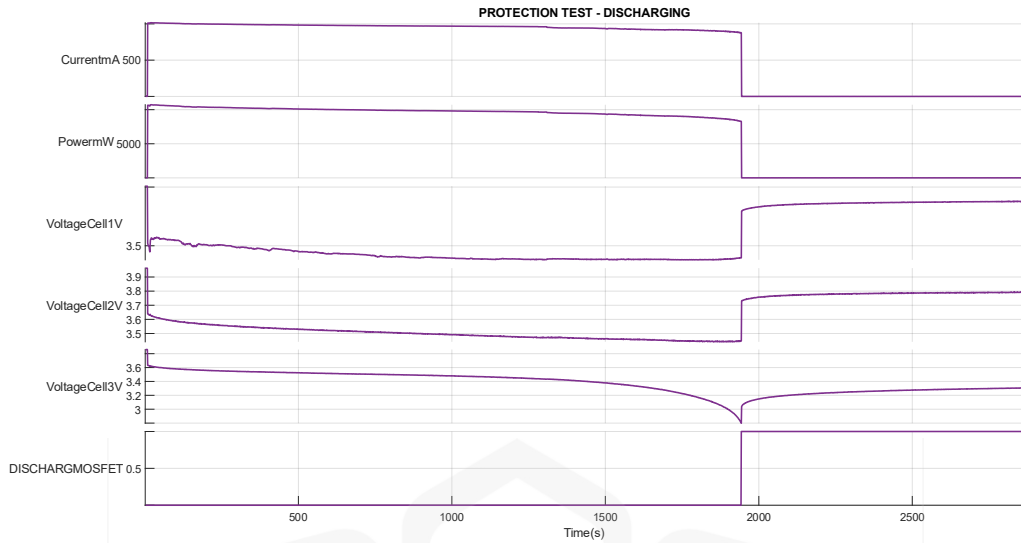


Figure 4.38 Cell Voltages and Discharge MOSFET Gate Signal Status During Discharging Test

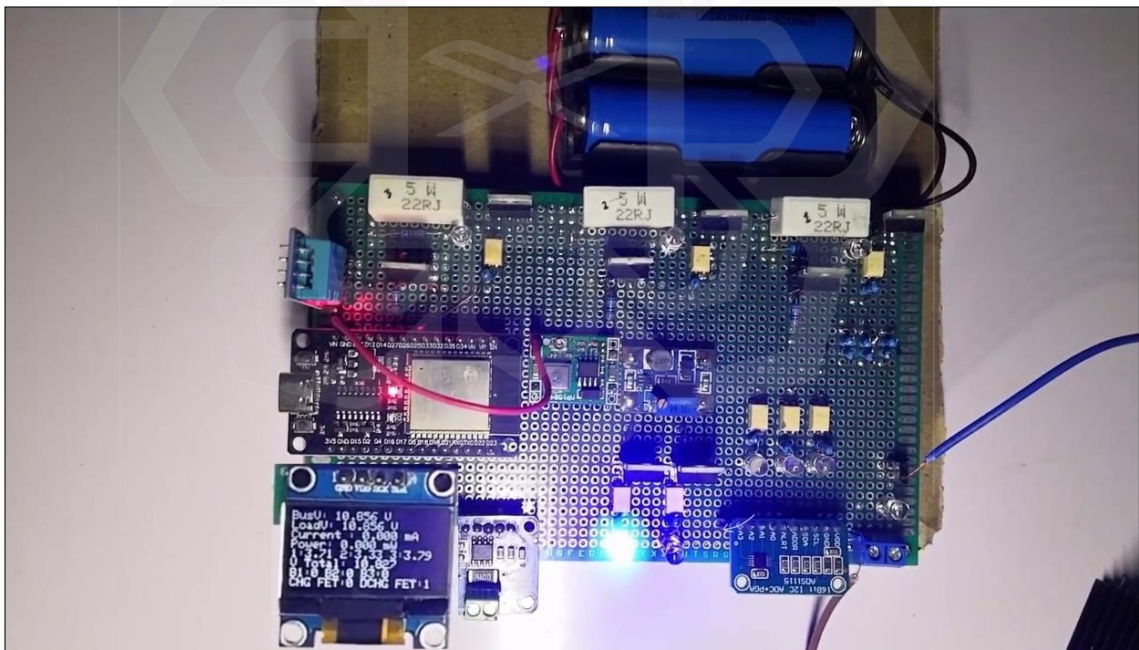


Figure 4.39 BMS Prototype Discharging Light Activated at End of Discharging Process

Figure 4.39 shows the setup for the BMS prototype when the discharge process is stopped. The discharge protection system functions as follows: During normal discharge

operation, the blue LED remains OFF and the discharge MOSFET is ON (signal = 1), allowing current to flow to the load. Real-time monitoring tracks each cell's voltage and calculates SOC. When the lowest-voltage cell approaches the cutoff threshold (2.8V per cell, equivalent to SOC = 0.20), the protection algorithm triggers and immediately sets the discharge MOSFET gate signal to 0 (OFF), disconnecting the load and halting discharge. Simultaneously, the blue LED illuminates, providing visual confirmation that over-discharge protection has been activated. This prevents damage to the cells from excessive discharge, which would cause irreversible capacity loss and safety risks.

### 4.3 SUMMARY

In this chapter a detailed comparison was made between two passive cell-balancing approaches used in BMS which is the commonly used OCV and using enhancements such as an ML-SOC estimator. Both approaches were tested using MATLAB/Simulink simulations under the same charge and discharge situations and their performance is measured by looking at balancing efficiency, switching frequency, energy losses, temperature rise and the overall charging time of the batteries. Moreover, a hardware prototype was developed in order to evaluate the OCV simulation method and see how it works in a real-world environment. Nonetheless, because of certain project limitations, the ML-SOC method could not be implemented into the prototype, which highlights a significant limitation and opportunity for future experimental work.

Table 4.3 Summary of OVC SOC Estimation and ML SOC Estimation Results

<b>Metric</b>	<b>OCV-Based</b>	<b>ML-SOC</b>	<b>Improvement</b>
Charging Time (To 80%)	14,588 sec	10,352 sec	29% faster
Switching Frequency	333.8 mHz	10.2 mHz	97% reduction
Total Power Loss	2.22 W	0.4218 W	81% reduction
Max Temperature	~28°C	~25.3-25.5°C	2.7°C cooler
Thermal Behavior	Continuous rise	0.3-0.5°C cooling	Thermal stability

Table 4.3 provides a comprehensive summary comparing key performance metrics between the OCV-based and ML-SOC estimation methods during the charging simulation. The OCV-based balancing achieved stable voltage curves and battery levels, but it required a high switching rate of 333.8 mHz on average to maintain the predefined hysteresis band. Because of frequent switching in the MOSFET, the passive energy loss was approximately 2.22 W, in which most was from resistors and extended the device's full charging cycle took 14588 seconds (4.05 hours). Furthermore, the maximum cell temperature measured was nearly 28 °C, suggesting that under these temperatures rise might lead to faster ageing and a shorter battery life. Yet, the prototype implementation showed that the findings were accurate, providing correct voltage protection and cutoff logic, supporting the conclusions drawn from the simulations.

On the other hand, ML-SOC, which relies on algorithms to estimate its SOC, did better than the OCV-based approach on all metrics measured. First, by reducing the switching frequency by 97% to 10.2 mHz and the average power loss during balancing also decreased to a low 0.422 W that improved its charging efficiency by 81%. The Charging process for the ML-SOC based simulation was completed in 10352 seconds (2.87 hours), about 29% faster than the OCV method and the cells' temperatures stayed within 0.3–0.5 °C of ambient after the balancing period which means they performed well thermally. The results confirm that balancing with adaptive, ML-SOC estimation leads to less energy wastage and effective SOC convergence. Although hardware tests are still needed, the simulation findings clearly show that the ML-SOC method is a better and more stable option than standard voltage-threshold balancing, helping to achieve the thesis goal of improving battery life and safety.

## CHAPTER FIVE

### CONCLUSION AND FUTURE WORKS

#### 5.1 CONCLUSION

This research has achieved its goal by introducing and testing an improved approach to passive balancing in BMS, which uses machine learning for SOC estimation in which enhancing the ability of the BMS to passively balance the battery during charging. The first research objective was met by thoroughly reviewing the most recent literature on passive balancing and machine learning for SOC estimation. The limitations of using OCV-based method to estimate SOC were the ability to handle flat voltage levels and differences in cell performance. It pointed out that ML algorithms can help SOC prediction adjust to its data input which can make balancing strategies both more precise and quicker. These findings guided and gave motivation for the research direction chosen in the study.

The development of a BMS framework integrating enhanced passive balancing with ML-based SOC estimation was realized through a two-tiered development process. A MATLAB/Simulink simulation model was constructed, incorporating an ML-trained SOC estimator into a passive balancing control algorithm. This simulation environment enabled the testing of dynamic cell balancing behavior under controlled conditions in which simultaneously developing a hardware prototype to implement and validate the conventional OCV-based passive balancing method. While real-time deployment of the ML-based algorithm on the hardware platform could not be completed within the project timeline, the design architecture was established to facilitate future integration in to a prototype BMS. This dual approach ensured a robust comparison between traditional and intelligent balancing strategies across both simulated and physical domains.

On top of that, the performance of the proposed ML-SOC balancing approach relative to conventional OCV-based methods was addressed through a detailed comparative analysis shown in the results chapters above. The simulation results demonstrated that the ML-SOC estimation approach has substantially outperformed the OCV-based approach in every key metric, such as reducing the switching frequency by 97%, decreasing balancing energy losses by over 80%, and shortening charge balancing duration by approximately 29% until all the battery was fully charged. Additionally, it maintained thermal stability, minimizing temperature rise and thereby reducing the risk of thermal degradation. These results empirically validate the thesis hypothesis that integrating ML with passive balancing enhances energy efficiency, operational safety, and system longevity. Although hardware testing of the ML-SOC method remains a task for future work, this study provides compelling simulation-based evidence and a practical design pathway for intelligent BMS development. In conclusion, the research not only fulfills its stated objectives but also compares existing methods with the proposed enhanced method.

## **5.2 FUTURE WORKS**

While this study succeeds in demonstrating the feasibility of the ML-enhanced passive balancing approach through extensive simulation and validation by the prototype, several limitations should be recognized to provide context for the results that might be useful in the future in terms of informing the research direction. The OCV-based balancing method was tested using hardware prototype testing, the ML-SOC approach was only tested in simulation because of time and resource constraints. This gap makes it impossible for direct experimental comparison between the OCV and ML-SOC estimation performances under real-world conditions where includes noisy data, sensor errors and microcontroller latency. However, the results obtained in the simulation gives a strong proof of the superiority of ML-SOC over the hardware results that still remains crucial in order to prove these advantages were transformed into physical systems running under realistic environments.

The testing was also limited to moderate temperature range of  $-10^{\circ}\text{C}$  to  $25^{\circ}\text{C}$ , excluding extreme conditions encountered in harsh environments because of the simulation environment. High-temperature operation such as  $40\text{-}60^{\circ}\text{C}$  in tropical climates or confined enclosures and severe cold conditions such as  $-20^{\circ}\text{C}$  to  $-30^{\circ}\text{C}$  in arctic regions or winter EV operation still present challenges for both battery electrochemistry and ML model robustness. Expanding validation to these temperature extremes would ensure the ML-SOC approach maintains reliability across global environment scenarios. Despite these limitations, the research provides compelling evidence that ML-based SOC estimation fundamentally improves passive balancing efficiency, establishing a strong foundation for future work addressing these constraints through expanded datasets, aging models, hardware prototyping, and extended operating condition validation.

### **5.2.1 Real-Time Hardware Implementation and Embedded ML Deployment**

Transitioning from through-hole components to a Surface-Mount Technology (SMT) design on the present prototype is a very important step toward industrial feasibility which has two main goals which is to lower the PCB footprint by 50-70% and simultaneously impact the signal integrity and thermal management of the PCB. This steps will require the use of excellent grade components, such as AEC-Q100 qualified MOSFETs and ADCs, to address the very high reliability requirements to meet the standards for electric vehicle as well as grid storage applications thus, limiting parasitic inductance with optimized trace routing, and facilitating automated assembly, the redesigned hardware will be suitable for the kind of scalability and robustness needed for mass manufacturing.

Concurrently, future work should leverage the ability of the ESP32 microcontroller for its own connectivity, in order to develop an IoT-enabled ecosystem that enables a shift from reactive to predictive BMS maintenance. The presence of power microcontroller can make use MQTT protocols to provide real-time telemetry streaming to the cloud platforms to support each battery anomaly detection and pack level health monitoring. Furthermore,

the implementation of Over-the-Air (OTA) update will enable the continuous improvement of the algorithms and the remote tests to implement a closed-loop system for the continuous improvement of the model inference accuracy throughout the life operation of the battery.



## REFERENCES

- Ahwiadi, M., & Wang, W. (2025). Battery Health Monitoring and Remaining Useful Life Prediction Techniques: A Review of Technologies. *Batteries*, *11*(1), 31.
- Alwabli, A. (2024). From data to durability: Evaluating conventional and optimized machine learning techniques for battery health assessment. *Results in Engineering*, *23*, 102445.
- Anapolsky, A., Aung, K., Bhargava, A., Chang, B., Chen, F., Forker, T., Gordon, M., Shibusawa, T., & Tieskoetter, B. (2024). (Invited) Physics Informed Data Driven Manufacturing for Li-ion Batteries. *ECS Meeting Abstracts*, *MA2024-02*(3), 368–368.
- Anurudha Gedam, Kiran M. Kimmatkar, & Manjeet Sakhare. (2024). Comparative Analysis of Active and Passive Cell Balancing Strategies in Battery Management Systems. *International Journal of Advanced Research in Science, Communication and Technology*, 634–649.
- Ashraf, A., Ali, B., Alsunjury, M. S. A., & Tricoli, P. (2024). Adaptive Controller Design and Power Loss Analysis of Resistive and Inductive Cell Balancing During Static, Charging, and Discharging Mode. *2024 IEEE International Conference on Electrical Systems for Aircraft, Railway, Ship Propulsion and Road Vehicles & International Transportation Electrification Conference (ESARS-ITEC)*, 1–5.
- Aswini, A., Siva Kumar, P., Kaleeswari, M., & Agadeesh, V. J. (2024a). Unobtrusive Optimization: Passive Cell Balancing for Enhanced Battery Efficiency. *2024 IEEE Third International Conference on Power Electronics, Intelligent Control and Energy Systems (ICPEICES)*, 951–956.
- Aswini, A., Siva Kumar, P., Kaleeswari, M., & Agadeesh, V. J. (2024b). Unobtrusive Optimization: Passive Cell Balancing for Enhanced Battery Efficiency. *2024 IEEE*

*Third International Conference on Power Electronics, Intelligent Control and Energy Systems (ICPEICES)*, 951–956.

B., D. B., CH., N., B., C. M., & B., D. (2024). REMAINING USEFUL LIFE PREDICTOR FOR EV BATTERIES USING MACHINE LEARNING. *Turkish Journal of Computer and Mathematics Education (TURCOMAT)*, 15(3), 413–418.

Bairwa, B., & R, S. (2024). Mathematical Modeling and Analysis of Electric Vehicle Battery. *2024 1st International Conference on Innovative Sustainable Technologies for Energy, Mechatronics, and Smart Systems (ISTEMS)*, 1–6.

Balaji, S., M.S., V., H.B., M. R., H, J., & T., M. (2024). Data-Driven Estimation of Lithium-Ion Battery State-of-Health Prediction Approach Using Machine Learning Algorithm for Enhanced Battery Management Systems. *Nanotechnology Perceptions*, 20(S7).

Bashir, H., Yaqoob, A., Kousar, F., Khalid, W., Akhtar, S., & Sultan, W. (2022). A Comprehensive Review of Li-ion Battery Cell Balancing Techniques & Implementation of Adaptive Passive Cell Balancing. *2022 International Conference on Electrical Engineering and Sustainable Technologies (ICEEST)*, 1–6.

Bihn, S., Rinner, J., Witzenhausen, H., Krause, F., Ringbeck, F., & Sauer, D. U. (2024). Physics-Based Equivalent Circuit Model Motivated by the Doyle–Fuller–Newman Model. *Batteries*, 10(9), 314.

Cabrera García, J., Zepeda-Hernández, J. A., López-Pérez, M. de J., & Domínguez Zenteno, J. E. (2024). SOH Estimation of Lithium-Ion Batteries Based on ANNs and Synthetic Data. *Memorias Del Congreso Nacional de Control Automático*, 7(1), 536–541.

Cao, Y., Li, K., & Lu, M. (2021). Balancing Method Based on Flyback Converter for Series-Connected Cells. *IEEE Access*, 9, 52393–52403.

Castro-Gutiérrez, J., Celzard, A., & Fierro, V. (2020). Energy Storage in Supercapacitors: Focus on Tannin-Derived Carbon Electrodes. *Frontiers in Materials*, 7, 217.

- Chandana, P., & Chavan, A. (2024). Machine Learning Applications in Battery Management System. In *How Machine Learning is Innovating Today's World* (pp. 173–200). Wiley.
- Dai, S., Zhang, F., & Zhao, X. (2021). Series-connected battery equalization system: A systematic review on variables, topologies, and modular methods. *International Journal of Energy Research*, 45(14), 19709–19728
- Devi B, A., & N, A. (2021). Automatic Cell Balancing with Switched Capacitor for Multi Cell Connectivity. *2021 Fourth International Conference on Electrical, Computer and Communication Technologies (ICECCT)*, 1–7.
- Duraisamy, T., & Kaliyaperumal, D. (2021). Machine Learning-Based Optimal Cell Balancing Mechanism for Electric Vehicle Battery Management System. *IEEE Access*, 9, 132846–132861.
- El-Sayed, E. I., ElSayed, S. K., & Alsharif, M. (2024a). Data-Driven Approaches for State-of-Charge Estimation in Battery Electric Vehicles Using Machine and Deep Learning Techniques. *Sustainability*, 16(21), 9301.
- El-Sayed, E. I., ElSayed, S. K., & Alsharif, M. (2024b). Data-Driven Approaches for State-of-Charge Estimation in Battery Electric Vehicles Using Machine and Deep Learning Techniques. *Sustainability*, 16(21), 9301.
- El-Sayed, E. I., ElSayed, S. K., & Alsharif, M. (2024c). Data-Driven Approaches for State-of-Charge Estimation in Battery Electric Vehicles Using Machine and Deep Learning Techniques. *Sustainability*, 16(21), 9301.
- Erdoğan, B., Savrun, M. M., Köroğlu, T., Cuma, M. U., & Tümay, M. (2021). An improved and fast balancing algorithm for electric heavy commercial vehicles. *Journal of Energy Storage*, 38, 102522.
- Eyasu Tenawerk, Y., Xia, L., Fu, J., Wu, W., Quan, Z., & Zhen, W. (2024a). An Ensemble Learning Method for SOC Estimation of Lithium-Ion Batteries Using Machine Learning. *Journal of Electronic Research and Application*, 8(6), 136–144.

- Eyasu Tenawerk, Y., Xia, L., Fu, J., Wu, W., Quan, Z., & Zhen, W. (2024b). An Ensemble Learning Method for SOC Estimation of Lithium-Ion Batteries Using Machine Learning. *Journal of Electronic Research and Application*, 8(6), 136–144.
- Fu, J., Wu, C., Wang, J., Haque, M. M., Geng, L., & Meng, J. (2024). Lithium-ion battery SOH prediction based on VMD-PE and improved DBO optimized temporal convolutional network model. *Journal of Energy Storage*, 87, 111392.
- Gabbar, H. A., Othman, A. M., & Abdussami, M. R. (2021). Review of Battery Management Systems (BMS) Development and Industrial Standards. *Technologies*, 9(2).
- Ganapati Chikkalkar, S., Naveen Kumar, M., & Chidanandappa, R. (2022). Online State of Charge(SOC) estimation of Lithium-Ion battery using Improved Extended Kalman Filter. *2022 IEEE 2nd Mysore Sub Section International Conference (MysuruCon)*, 1–7.
- Gao, Y., Nguyen, T., & Onori, S. (2024). Model-Based State-of-Charge Estimation of 28 V LiFePO<sub>4</sub> Aircraft Battery. *SAE International Journal of Electrified Vehicles*, 14(1), 14-14-01–0003.
- Garche, J. (2025). *Encyclopedia of electrochemical power sources*. Elsevier.
- Gole, A. C., Aher, P. K., & Patil, S. L. (2023a). SOC Estimation of a Li-ion Battery using Deep Learning Method: A comparative Study of LSTM and GRU Architecture. *2023 11th National Power Electronics Conference (NPEC)*, 1–6.
- Gole, A. C., Aher, P. K., & Patil, S. L. (2023b). SOC Estimation of a Li-ion Battery using Deep Learning Method: A comparative Study of LSTM and GRU Architecture. *2023 11th National Power Electronics Conference (NPEC)*, 1–6.
- Grebtsov, D. K., Kubasov, M. K., Bernatskii, E. R., Beliauski, P. A., Kokorenko, A. A., Isokjanov, S. Sh., Kazikov, S. P., Kashin, A. M., Itkis, D. M., & Morozova, S. M. (2024). Electric Vehicle Battery Technologies: Chemistry, Architectures, Safety, and Management Systems. *World Electric Vehicle Journal*, 15(12), 568.

- Hariprasad, A., Priyanka, I., Sandeep, R., & Ravi, O. (2020). Battery Management System in Electric Vehicles. *International Journal of Engineering Research And*, *V9*.
- Hernández, E., Prieur, C., & Cerpa, E. (2022). A tracking problem for the state of charge in an electrochemical Li-ion battery model. *Mathematical Control and Related Fields*, *12*(3), 709.
- Hosseinzadeh, E., Arias, S., Krishna, M., Worwood, D., Barai, A., Widanalage, D., & Marco, J. (2021). Quantifying cell-to-cell variations of a parallel battery module for different pack configurations. *Applied Energy*, *282*, 115859.
- Hosseinzadeh, E., Odio, M. X., Marco, J., & Jennings, P. (2019). Unballanced Performance of Parallel Connected Large Format Lithium Ion Batteries for Electric Vehicle Application. *2019 International Conference on Smart Energy Systems and Technologies (SEST)*, 1–6.
- How, D. N. T., Hannan, M. A., Lipu, M. S. H., Ker, P. J., Mansor, M., Sahari, K. S. M., & Muttaqi, K. M. (2022a). SOC Estimation Using Deep Bidirectional Gated Recurrent Units With Tree Parzen Estimator Hyperparameter Optimization. *IEEE Transactions on Industry Applications*, *58*(5), 6629–6638.
- How, D. N. T., Hannan, M. A., Lipu, M. S. H., Ker, P. J., Mansor, M., Sahari, K. S. M., & Muttaqi, K. M. (2022b). SOC Estimation Using Deep Bidirectional Gated Recurrent Units With Tree Parzen Estimator Hyperparameter Optimization. *IEEE Transactions on Industry Applications*, *58*(5), 6629–6638.
- How, D. N. T., Hannan, M. A., Lipu, M. S. H., Ker, P. J., Mansor, M., Sahari, K. S. M., & Muttaqi, K. M. (2022c). SOC Estimation Using Deep Bidirectional Gated Recurrent Units With Tree Parzen Estimator Hyperparameter Optimization. *IEEE Transactions on Industry Applications*, *58*(5), 6629–6638.
- Hussain, S. O., Khan, H., & Hameed, M. Z. (2025). Intelligent Battery Management Systems. *International Journal For Multidisciplinary Research*, *7*(1).

- Imran, S. A., Ali Kazmi, S. N., Sakandar, H., Ulasyar, A., & Khalid, A. (2024). A Distributive Hybrid Cell Balancing Technique for Series-Connected Lithium-Ion Cells. *2024 3rd International Conference on Emerging Trends in Electrical, Control, and Telecommunication Engineering (ETECTE)*, 1–5.
- International Electrotechnical Commission. (2010). *IEC 61508 - Functional safety of electrical/electronic/programmable electronic safety-related systems* (2nd ed.). IEC.
- Itagi, A. R., Kallimani, R., Pai, K., Iyer, S., & Lopez, O. L. A. (2024). *Cell Balancing for the Transportation Sector: Techniques, Challenges, and Future Research Directions*.
- Kallimani, R., Pai, K., & Patil, P. (2024). *Comparative Analysis of State-of-Health Estimation Techniques* (pp. 53–69).
- Karmakar, S., Bera, T. K., & Bohre, A. K. (2023). Novel PI Controller and ANN Controllers-Based Passive Cell Balancing for Battery Management System. *IEEE Transactions on Industry Applications*, *59*(6), 7623–7634.
- Karmakar, S., Bohre, A. K., & Bera, T. K. (2023). Novel PID Controller-Based Passive Cell Balancing for BMS. *2023 IEEE 3rd International Conference on Smart Technologies for Power, Energy and Control (STPEC)*, 1–4.
- Kim, T., Song, W., Son, D. Y., Ono, L. K., & Qi, Y. (2019). Lithium-ion batteries: outlook on present, future, and hybridized technologies. *Journal of Materials Chemistry A*, *7*(7), 2942–2964.
- Koriker, M., Drif, M., Saigaa, D., & Loukriz, A. (2024). Experimental validation of an advanced electrical model for lead-acid batteries. *STUDIES IN ENGINEERING AND EXACT SCIENCES*, *5*(3), e12711.
- Krishna, G., Singh, R., Gehlot, A., Almogren, A., Altameem, A., Ur Rehman, A., & Hussen, S. (2024). Advanced battery management system enhancement using IoT and ML for predicting remaining useful life in Li-ion batteries. *Scientific Reports*, *14*(1), 30394.

- Kumar, S., Rao, S. K., Singh, A. R., & Naidoo, R. (2023). Switched-Resistor Passive Balancing of Li-Ion Battery Pack and Estimation of Power Limits for Battery Management System. *International Journal of Energy Research*, 2023, 1–21.
- Kurpiel, W., Deja, P., Polnik, B., Skóra, M., Miedziński, B., Habrych, M., Debita, G., Zamłyńska, M., & Falkowski-Gilski, P. (2021). Performance of Passive and Active Balancing Systems of Lithium Batteries in Onerous Mine Environment. *Energies*, 14(22).
- Lakshmi, M., kishore, Dr. G. I., Dharani, P., Roshini, N., & Rambabu, M. (2024). A Review on Towards Long Lifetime Battery: AI Based Manufacturing and Management. *INTERANTIONAL JOURNAL OF SCIENTIFIC RESEARCH IN ENGINEERING AND MANAGEMENT*, 08(12), 1–6.
- Lee, H., Park, J., & Kim, J. (2019). Incremental Capacity Curve Peak Points-Based Regression Analysis for the State-of-Health Prediction of a Retired LiNiCoAlO<sub>2</sub> Series/Parallel Configured Battery Pack. *Electronics*, 8(10).
- Lee Pan. (2025, June 19). *Passive Balancing vs Active Balancing in Lithium Batteries Explained*. Large Power.
- Li, C., Cui, N., Wang, C., & Zhang, C. (2021). Reduced-order electrochemical model for lithium-ion battery with domain decomposition and polynomial approximation methods. *Energy*, 221, 119662.
- Li, H., Li, X., Xiong, L., & You, L. (2024). SOC Balance Control Strategy Based on High Voltage Cascaded Power Conversion System. *2024 3rd International Conference on Energy and Electrical Power Systems (ICEEPS)*, 1341–1344.
- Li, H., Zhuo, S., Zhu, R., Zhang, Y., Peng, H., Ren, W., & Zhang, R. (2024). A Digital Twin-Based Distributed Method for the SOC Estimation of Li-Ion Battery Pack. *2024 IEEE International Conference on Systems, Man, and Cybernetics (SMC)*, 3350–3355.

- Li, Y., Qi, H., Shi, X., Jian, Q., Lan, F., & Chen, J. (2024). A Physics-Based Equivalent Circuit Model and State of Charge Estimation for Lithium-Ion Batteries. *Energies*, *17*(15), 3782.
- Liang, Z., & Cheng, G. (2024). SOH probability prediction for lithium-ion batteries based on improved DeepAR. In Y. Wang & C. P. Chioncel (Eds.), *Tenth International Conference on Energy Materials and Electrical Engineering (ICEMEE 2024)* (p. 37). SPIE.
- Lim, J.-H., Heo, G. W., Lim, J.-Y., Kim, D. H., Jun, B., & Lee, B. K. (2024). State of Charge Estimation Based on Thermal Modeling Compensation Considering Capacity Variation by Internal Temperature Effects of LiFePO<sub>4</sub> Battery. *2024 IEEE Applied Power Electronics Conference and Exposition (APEC)*, 1800–1804.
- Lu, M., Fan, Y., & Chong, B. (2020). A Novel Comprehensive SOC-Voltage Control Scheme for Lithium-ion Battery Equalization. *2020 International Conference on Power, Instrumentation, Control and Computing (PICC)*, 1–6.
- M, R. R., Siddeshkumar, C., Sekhar, N., Boddapati, V., Naik, R. S., & S, N. (2024). Advanced Optimized Active Cell Balancing with Efficient Power Electronics Algorithms for Superior Battery Performance in Electric Vehicle. *2024 6th International Symposium on Advanced Electrical and Communication Technologies (ISAECT)*, 1–6
- Maddireddy, S. R. R. (2024). Exploring Pack-level Current-Split Strategies for Optimized Energy Distribution in Li-ion Battery Systems. *Journal of Energy Research and Reviews*, *16*(7), 47–63.
- Maksimovna Vakhrusheva, D., & Xu, J. (2024). Model-Driven Manufacturing of High-Energy-Density Batteries: A Review. *Batteries & Supercaps*.
- Malik, G., & Saini, M. K. (2025). A Real-Time Adaptive Machine Learning Charging and Neural Network Balancing Mechanism of Lithium-Ion Battery Pack. *Energy Storage*, *7*(1).

- Mirela, O., Pereuş, D., & Simionuş, A. (2024). Comparative Analysis of Active Balancing Types for Lithium-Ion Cells. *2024 IEEE 30th International Symposium for Design and Technology in Electronic Packaging (SIITME)*, 352–357.
- Morel, C., & Morel, J.-Y. (2025). Chaos Anticontrol and Switching Frequency Impact on MOSFET Junction Temperature and Lifetime. *Actuators*, 14(5), 203.
- Mostafa, A., Gaafar, M. A., Abdel-Rahim, O., & Orabi, M. (2023). Comparative Study of the State of Charge (SoC) Balancing Techniques for Battery Power Module Configurations. *2023 IEEE Conference on Power Electronics and Renewable Energy (CPERE)*, 1–5.
- Nam, E., Lee, S., & Kwon, Y. (2023). Buck-Boost Active Cell Balancing Based on SOC Estimation for Battery Pack in Electric Vehicles. *Journal of the Korea Academia-Industrial Cooperation Society*, 24(2), 32–41.
- Olugbade, E., & Park, J. (2024). Boosting predictive accuracy of single particle models for lithium-ion batteries using machine learning. *Applied Physics Letters*, 125(14).
- Omi, T., & Hatakeyama, T. (2024). State-of-Charge Balancing Control Utilizing the Circulating Current for Battery Energy Storage System. *2024 13th International Conference on Renewable Energy Research and Applications (ICRERA)*, 375–380.
- Paraschiv, C.-L., Tufeanu, L. M., & Vochin, M.-C. (2024). Enhancing Battery Management Systems with Machine Learning and 5G Connectivity beyond Maritime Transport Software Architectures. *2024 15th International Conference on Communications (COMM)*, 1–6.
- Paudyal, B., Timilsina, A., Khanal, A., & Ghimire, S. (2019). *Comparative Analysis of Cell Balancing Topologies in Battery Management System*.
- Pujari, P., Gnanasambanthan, L. R., Sharma, P., & P, Sriramalakshmi. (2024). Data-Driven Battery Health Optimization in Electric Vehicles: A Machine Learning Approach. *2024 IEEE 4th International Conference on Sustainable Energy and Future Electric Transportation (SEFET)*, 1–6.

- Qin, L., Sun, T., Sun, X.-M., & Xia, W. (2025). Managing Battery Performance Degradation Using Physics-Informed Learning Scheme for Multiple Health Indicators. *IEEE Transactions on Transportation Electrification*, 1–1.
- Rahnama, M., Tashakor, N., Hashemi-Zadeh, A., Panchal, S., & Goetz, S. (2024). A Novel Technique for Battery Parameter Estimation Using Equivalent Circuit Models. *2024 Energy Conversion Congress & Expo Europe (ECCE Europe)*, 1–7.
- Rehman, A. (2024). Review Paper for SOC Estimation Techniques: Challenges and Future Areas for Improvement. *Power System Technology*, 48(3), 1006–1047.
- Sabarimuthu, M., Sabarish, P., Raj, G. G., Juhair, P. M., Johitha, B., & Kaviya, S. (2023). State of Charge Detection in Electric Two Wheeler. *2023 9th International Conference on Electrical Energy Systems (ICEES)*, 201–205.
- Schwenzer, M., Ay, M., Bergs, T., & Abel, D. (2021). Review on model predictive control: an engineering perspective. *The International Journal of Advanced Manufacturing Technology*, 117(5–6), 1327–1349.
- Shakir, T., Naz, H., Jamil, M., & Kirmani, S. (2024). A Comparative Analysis of Deep Learning Algorithms Based SoH Prediction of Li-Ion Batteries. *2024 International Conference on Computer, Electronics, Electrical Engineering & Their Applications (IC2E3)*, 1–5.
- Sharma, A. K., Letha, S. S., Syal, P., Rathee, S., & Kumar, A. (2025). State Estimation and Cell Balancing for Lithium-Ion Batteries Powering Electrical Vehicles. In *Smart Electric and Hybrid Vehicles* (pp. 1–53). Wiley.
- Sharma, M., & Geda, S. R. (2021). An Overview of SOC estimation in Li-ion batteries with Direct Measurement methods. *SGS - Engineering & Sciences*, 1(01).  
<https://spast.org/techrep/article/view/1950>
- Singh, S. V. P., & Agnihotri, P. (2022). ANN Based Modelling of Optimal Passive Cell Balancing. *2022 22nd National Power Systems Conference (NPSC)*, 326–331.

- Sitompul, S., Hatakeyama, T., & Nakatani, M. (2024). Simplified Equivalent Circuit Model for Battery Energy Storage System Used for Grid Frequency Response. *2024 13th International Conference on Renewable Energy Research and Applications (ICRERA)*, 432–437.
- Sultan, Y. A., Eladl, A. A., Hassan, M. A., & Gamel, S. A. (2025). Enhancing electric vehicle battery lifespan: integrating active balancing and machine learning for precise RUL estimation. *Scientific Reports*, *15*(1), 777.
- Thakkar, R. R., Rao, Y. Srinivasa., & R.Sawant, R. (2020). Performance Analysis of Electrical Equivalent Circuit Models of Lithium-ion Battery. *2020 IEEE Pune Section International Conference (PuneCon)*, 103–107.
- Turksoy, A., Teke, A., & Alkaya, A. (2020a). A comprehensive overview of the dc-dc converter-based battery charge balancing methods in electric vehicles. *Renewable and Sustainable Energy Reviews*, *133*, 110274.
- Turksoy, A., Teke, A., & Alkaya, A. (2020b). A comprehensive overview of the dc-dc converter-based battery charge balancing methods in electric vehicles. *Renewable and Sustainable Energy Reviews*, *133*, 110274.
- Wang, J., Zhou, S., & Mao, J. (2024). Research on Fast SOC Balance Control of Modular Battery Energy Storage System. *Energies*, *17*(23), 5907.
- Wang, Q., Gao, T., & Li, X. (2022). SOC Estimation of Lithium-Ion Battery Based on Equivalent Circuit Model with Variable Parameters. *Energies*, *15*(16), 5829.
- Weng, Y., & Ababei, C. (2024). AI-assisted reconfiguration of battery packs for cell balancing to extend driving runtime. *Journal of Energy Storage*, *84*, 110853.
- Wu, H., Zhao, H., Qin, D., Yang, J., & Chen, J. (2024). Multi-Cell-to-Multi-Cell active equalization method based on k-means clustering and battery pack SOC estimation. *International Journal of Electrochemical Science*, *19*(6), 100588.

- Wu, T., Ji, F., Liao, L., & Chang, C. (2019). Voltage-SOC balancing control scheme for series-connected lithium-ion battery packs. *Journal of Energy Storage*, 25, 100895.
- Xia, B., Li, Y., Zhang, G., Cheng, Q., & Ding, F. (2024). A double-layer ring-structured equalizer for series-connected lithium-ion battery pack based on model predictive control. *Journal of Energy Storage*, 78, 110047.
- Xiong, Z., Chen, A., Zhou, Y., Wang, J., & Ci, S. (2025). SOC balancing strategy for parallel-connected power conversion system based on PQ decoupling control. *IET Conference Proceedings*, 2024(6), 1253–1257.
- Yağcı, M., & Orbeyi, Ö. (2024). Programmable logic controlled lithium-ion battery management system using passive balancing method. *Journal of Radiation Research and Applied Sciences*, 17(2), 100927.
- Yang, R., & Yang, F. (2024). An Adaptive Droop Control Method for SOC Balancing in DC Microgrids with Photovoltaic and Energy Storage Systems. *2024 IEEE Transportation Electrification Conference and Expo, Asia-Pacific (ITEC Asia-Pacific)*, 1010–1015.
- Yang, X., Xi, L., Gao, Z., Li, Y., & Wen, J. (2020). Analysis and Design of a Voltage Equalizer Based on Boost Full-Bridge Inverter and Symmetrical Voltage Multiplier for Series-Connected Batteries. *IEEE Transactions on Vehicular Technology*, 69(4), 3828–3840.
- Yi, B., Zhang, J., & Song, Z. (2024). Bias-Compensated State Estimation Algorithm for Lithium Iron Phosphate Batteries with Flat OCV-SOC Curves. *2024 American Control Conference (ACC)*, 1423–1428.
- Yildirim, B., Elgendy, M., Smith, A., & Pickert, V. (2019). Evaluation and Comparison of Battery Cell Balancing Methods. *2019 IEEE PES Innovative Smart Grid Technologies Europe (ISGT-Europe)*, 1–5.
- Zhou, W., Zheng, Y., Pan, Z., & Lu, Q. (2021). Review on the Battery Model and SOC Estimation Method. *Processes*, 9(9), 1685

Zilberman, I., Schmitt, J., Ludwig, S., Naumann, M., & Jossen, A. (2020). Simulation of voltage imbalance in large lithium-ion battery packs influenced by cell-to-cell variations and balancing systems. *Journal of Energy Storage*, 32, 101828.



## LIST OF PUBLICATIONS

### Journal Papers:

1. M. A. M. M. Fahmi, S. H. Yusoff, T. S. Gunawan, S. A. Zabidi, and M. S. Abu Hanifah, “Battery management system employing passive control method,” *International Journal of Power Electronics and Drive Systems (IJPEDS)*, vol. 16, no. 1, p. 35, Mar. 2025.

### Conference Papers:

1. N. Rosli, S. H. Yusoff, H. Mansor, S. N. M. Sapihie, and M. A. M. M. Fahmi, “Using Model Predictive Control in Renewable Energy Sources,” in *2023 IEEE 9th International Conference on Smart Instrumentation, Measurement and Applications (ICSIMA)*, IEEE, Oct. 2023, pp. 263–268. doi: 10.1109/ICSIMA59853.2023.10373520.
2. S. A. Z. Abidin, S. H. Yusoff, H. Mansor, S. N. M. Sapihie, and M. A. M. M. Fahmi, “Scheduling of the Battery for Peak Shaving Using Model Predictive Control (MPC),” in *2023 IEEE 9th International Conference on Smart Instrumentation, Measurement and Applications (ICSIMA)*, IEEE, Oct. 2023, pp. 269–273.
3. M. H. A. Kadir, M. A. Zakaria, M. A. M. M. Fahmi, N. S. Midi, S. H. Yusoff, and M. S. A. Hanifah, “Energy Performance Indicator (EnPI) Prediction of a Compressed Air System in a Can Manufacturing Factory,” in *2023 IEEE 8th International Conference on Recent Advances and Innovations in Engineering (ICRAIE)*, IEEE, Dec. 2023, pp. 1–5.